NIST

MSEL

FY 2001 PROGRAMS AND ACCOMPLISHMENTS

National Institute of Standards and Technology
Technology Administration
U.S. Department of Commerce
NISTIR 6780
September 2001

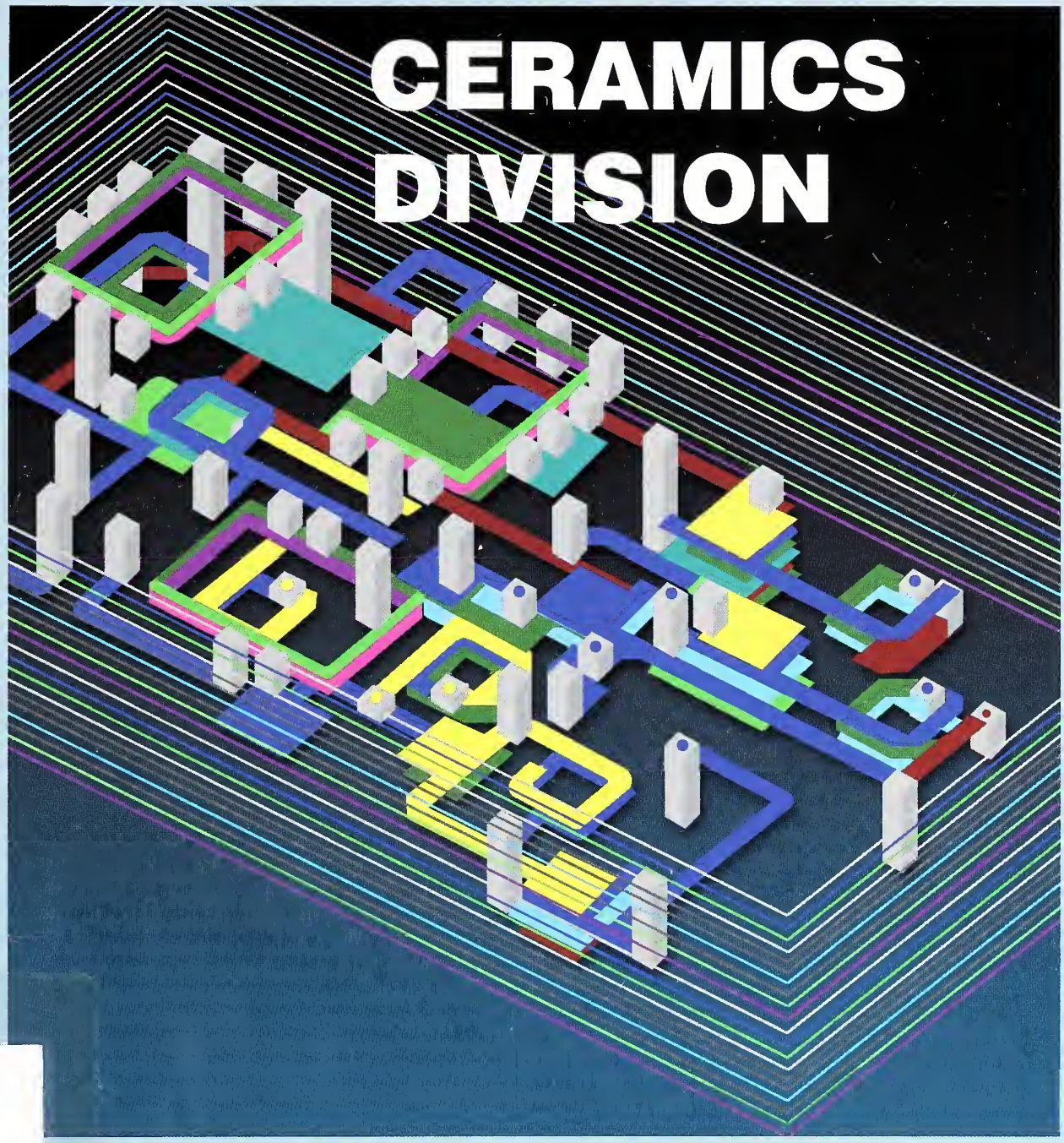

Low temperature co-fired ceramic (LTCC) integrated passives used to support a Motorola tri-band direct conversion receiver module are shown. A direct conversion IC, three SAW filters, a band select switch, balun, matching networks and DC blocking capacitors are integrated into a 328 mil X 586 mil, 19 layer Multi-layer Ceramic Integrated Circuit (MCIC) design. The LTCC module contains 24 embedded passives and 15 surface mount components (not shown). The National Imagery and Mapping Agency(NIMA), the executive agent for the National Technology Alliance(NTA), is providing funds for the development of the RF module by Motorola Labs in Tempe, AZ, and Schaumburg, IL.

National Institute of Standards and Technology
Karen H. Brown,
Acting Director

Technology Administration

U.S. Department of Commerce
Donald L. Evans,
Secretary

MATERIALS SCIENCE AND ENGINEERING LABORATORY

FY 2001 PROGRAMS AND ACCOMPLISHMENTS

CERAMICS DIVISION

Stephen W. Freiman, Chief

Stanley J. Dapkunas, Deputy

NISTIR 6780

September 2001

Table of Contents

Disclaimer
Certain commercial equipment, instruments, software, or materials are identified in this report to specify adequately experimental procedures, methods of analysis, or material substrates. Such identification does not imply recommendation or endorsement by the National Institute of Standards and Technology, nor does it imply that the equipment, instruments, software, or materials identified are necessarily the best available for the purposes.

Executive Summary

The mission of the Ceramics Division is:

Work with industry, standards bodies, academia, and other government agencies in providing the leadership for the Nation's measurements and standards infrastructure for ceramic materials.

The range of materials on which we work is broad, ranging from nitrides for structural applications, complex oxides used in wireless devices and high T_c superconductors, to semiconducting and optoelectronic materials, pertinent to a wide spectrum of important applications. Ceramics in the broadest sense are crucial to many modern technologies including wireless communication, photonics, and biomaterials. Ceramics are used in components, not just as monolithic parts, but, as films, coatings, or single crystals. Throughout this range of materials, there are common measurement issues, e.g., phase identification, the role of microstructure on properties, brittle material design, and many others.

We continue to look for new and unique ways to provide services to our customers, i.e. the engineers and scientists in both companies and universities who use the measurement tools that we are developing. For example, we are expanding our search for topics which can be published as NIST Recommended Practice Guides. The first such Practice Guide on "*Particle Size Characterization*," authored by Ajit Jillavenkatesa, Sandy Dapkunas, and Lin Lum, was published this Spring. This document has been enthusiastically received; over 1800 copies have been distributed as a result of requests. Another Practice Guide authored by Vince Hackley, on "*The Use of Nomenclature in Dispersion Science and Technology*" is in-press. The draft of a Practice Guide addressing mechanical reliability issues for brittle materials has been completed, as has one addressing X-ray topography using synchrotron radiation.

Workshops continue to be an important way for us to identify industrial measurement needs. During this past year we held workshops related to measurement needs for Low Temperature Co-fired Ceramics (LTCC) for wireless applications, Contact Damage on Engine Components, and Accuracy in Powder Diffraction III. Workshops were also held to guide programs in the markup language for exchange of materials information (MatML) and object oriented finite element analysis (OOF).

We also rely on visits to individual companies to assess their measurement needs. This year a group led by Sandy Dapkunas visited the major engine manufacturers who are involved with thermal barrier coatings. We expect these visits will lead to enhanced collaborative activities between our program and theirs.

During the past year, we divided our Ceramic Manufacturing Program into two Programs, Powder Measurements and Advanced Engine Materials. This change was made in order to better focus the broad range of activities being carried out on the specific needs of two different customer groups. Work in the Advanced Engine Material Program addresses reliability issues with respect to coatings (previously part of the Ceramic Coatings Program) as well as contact damage on bulk materials. Our level of effort associated with the Materials for Magnetic Data Storage Program was increased to better address the tribological measurement needs of this community.

Based upon the industrial measurement priorities stemming from the LTCC Workshop mentioned above, as well as a number of company visits, we have expanded activities related to low temperature co-fired ceramics, including both process model development and sintering experiments.

Division personnel continue to be very involved in leadership roles in standards activities through VAMAS, ISO, and ASTM, as well as in the development of SRMs. Of particular note with respect to the latter is the agreement signed with the Bundesanstalt fur Materialforschung und –prufung (BAM) to mutually develop SRMs, the first of which on porosity measurement, will be completed next year.

A number of our Division staff have been honored this year. Said Jahanmir was presented the Mayo D. Hersey Award by ASME for his contributions in the field of tribology. Said was also elected a vice-president of ASME. Winnie Wong-Ng and George Quinn were made Fellows of the American Ceramic Society.

Stephen W. Freiman

Chief, Ceramics Division

Technical Highlights

The following Technical Highlights section includes expanded descriptions of research projects that have broad applicability and impact. These projects generally continue for several years. The results are the product of the efforts of several individuals. The Technical Highlights include:

- Advanced Small-Angle Scattering Methods Link Microstructure to Processing and Performance for Thermal Barrier coatings *in situ* on the Substrate

- Crystal Structure of Novel LTCC Microwave Ceramics

- MatML: XML for Materials Property Data

- Monolayer Film Design

- Texture Measurement and Analysis

Advanced Small-Angle Scattering Methods Link Microstructure to Processing and Performance for Thermal Barrier Coatings *in situ* on the Substrate

Coatings are used in the electric utility and aircraft industries to protect advanced gas turbines from increasingly high operating temperatures, but no single industrial technique that can quantify the component void microstructures that control thermal barrier coating performance and reliability. NIST researchers have developed advanced small-angle scattering methods which, with appropriate models, provide a microstructure characterization for thick, freestanding material, and have explored generic links between microstructure, processing and service life. Two innovations now extend these studies to coatings in situ on the substrate, and suggest that such characterization provides calibration and validation of the partial information available from other methods.

Many of the technologically important properties of thermal barrier coatings (TBCs) are governed by their strongly anisotropic void microstructures, which are in turn determined by the feedstock and spray conditions. The importance of understanding the spray-process – microstructure – property connections cannot be underestimated if performance is to be improved. A series of advances in small-angle scattering studies at NIST have enabled the porosities, sizes and surface area distributions of the intra-splat cracks, inter-lamellar pores and globular pores, together with their approximate orientation distributions, to be resolved and quantified for plasma-sprayed ceramic TBC deposits for the first time. Correlations have been revealed between feedstock morphology and TBC microstructure, as have the effects of varying the spray parameters.

Whereas most of these results apply to thick freestanding deposits, further recent innovations in the small-angle scattering technique have enabled some microstructure information to be obtained for sub-millimeter-thick deposits *in situ* on the substrate. In near-surface small-angle neutron scattering (NS-SANS) a reflection geometry is used to determine, to a typical 100 μm mean depth, the apparent void surface area, as projected along its surface-normal, *versus* the angle the surface-normal makes with the spray direction (usually an axis of symmetry). Figure 1 shows the apparent surface area distributions for an yttria-stabilized zirconia (YSZ) TBC deposited on a nickel superalloy substrate, both as-sprayed and annealed for 1 h at 1100 °C. The surface area projected along the spray direction is reduced on annealing due to the partial sintering of inter-lamellar pores that are mainly parallel with the substrate. The surface area projected along directions parallel with the substrate is significantly increased by thermal-mismatch intra-splat cracking mainly perpendicular to the substrate. This microstructure change contrasts with a preferential sintering of intra-splat cracks for freestanding deposits, and significantly modifies the properties and performance of TBCs subjected to elevated service temperatures.

For a (300 to 400) μm thick TBC on a substrate, where TBC and substrate can be sectioned perpendicular to the substrate plane to less than 300 mm in thickness, the TBC microstructure can be determined using a modified form of ultra-small-angle x-ray scattering (USAXS). Two "side-bounce" crystal reflections are added to the normal configuration. These remove the intrinsic slit smearing of standard USAXS and create the technique, SBUSAXS, suitable for the study of anisotropic materials. SBUSAXS has been applied to TBCs fabricated both by plasma

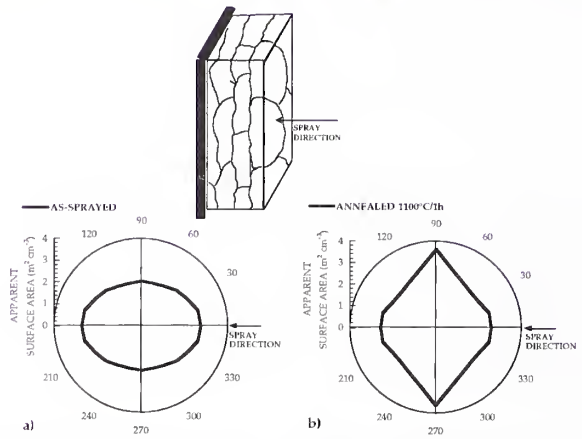

Figure 1: Apparent surface area distributions from NS-SANS studies of a YSZ deposit: a) as sprayed; b) annealed.

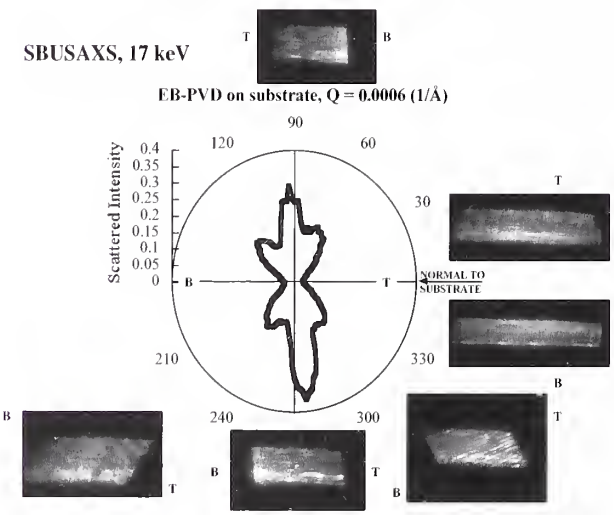

Figure 2: SBUSAXS data at Q = 0.0006 Å^{-1} *versus* angle to the substrate-normal for an EB-PVD TBC. SBUSAXS images taken at various sample orientations are also shown where T and B denote the top and bottom of the TBC, respectively.

spray and by electron-beam plasma-vapor deposition (EB-PVD). For YSZ the x-ray energy is set to 17 keV, just below the Y absorption edge, in order to minimize attenuation of the beam. Figure 2 shows the scattered intensity at a fixed Q ($Q = (4\pi/\lambda)$ in θ where θ is one half the scattering angle)) as a function of

sample orientation for a YSZ EB-PVD TBC. The two large lobes in the scattering, nearly parallel with the substrate plane, are associated with inter-columnar porosity within the EB-PVD microstructure, while the butterfly pattern is associated with nanoscale V-shaped intra-columnar voids. USAXS images of the sample, imaged using the scattered x-rays themselves, reveal different parts of the microstructure for different sample orientations. The images also show that the inter-columnar structure is most evident near the bottom of the coating while the intra-columnar voids are more evident near the top of the coating. Since the x-ray beam size can be as small as 100 µm x 100 µm, SBUSAXS can be used to determine the size, porosity, surface area and orientational distributions of the void components as a function both of the fabrication and service-life conditions, and of the depth within the coating attached to the substrate.

Returning to free standing deposits, studies of plasma sprayed YSZ TBCs have focussed on quantifying the microstructural links between the processing / feedstock conditions and the properties / performance of the TBC material, itself. For example, the effect of feedstock particle size on the deposit microstructure has been studied, together with the consequent influence on thermal conductivity. Figure 3 shows the effects of different feedstock particle size on the component microstructures of the deposits as measured by multiple-SANS (MSANS). (Standard deviations in total porosity are ± 0.1 %, those in component porosities, ± 0.5 %.) The increase in porosity, particularly for the inter-lamellar pores, with increasing feedstock particle size is responsible for the decrease in thermal conductivity shown in Figure 4. (Estimated standard deviation ± 0.03 W m^{-1} K^{-1}.)

Such data feed into models both for the spray-process and for the predicted thermo-mechanical properties. While increased inter-lamellar porosity decreases thermal conductivity, it also increases coating loss due to spalling. This has led to current industrial interest in reducing inter-lamellar porosity despite the penalty of increased thermal conductivity.

These studies are providing data needed for building reliable quantitative models to optimize feedstock and spray-process conditions for tailored TBC design. By combinations of SANS / MSANS studies of the generic TBC microstructure variations *versus* the feedstock, spray conditions and service life, with NS-SANS and SBUSAXS studies of the modifications introduced when the TBC remains *in situ* on the substrate, a valuable validation tool is becoming available to support industrial TBC design.

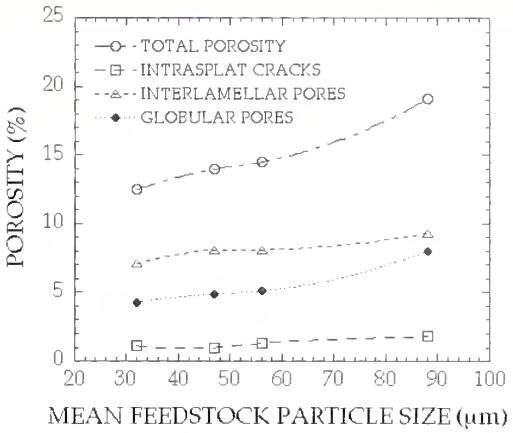

Figure 3: Total and component porosities *versus* mean feedstock particle size. (Total porosity from precision density measurements.)

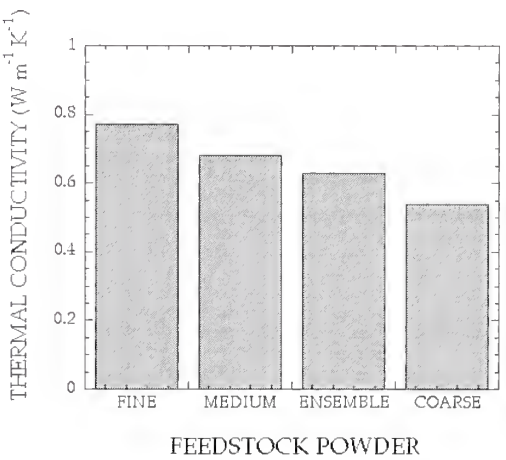

Figure 4: TBC thermal conductivity *versus* feedstock particle morphology.

For More Information On This Topic:

A. J. Allen, J. Ilavsky, G. G. Long, J. S. Wallace, C. C. Berndt and H. Herman, "Microstructural Characterization of Yttria-Stabilized Zirconia Plasma-Sprayed Deposits Using Multiple Small-Angle Neutron Scattering," Acta Materialia, **49**, 1661 - 1675 (2001).

Contact: Andrew Allen, Jan Ilavsky and Gabrielle Long

Crystal Structure of Novel LTCC Microwave Ceramics

The progress of wireless communication devices largely depends on the development of microwave resonator ceramics with improved dielectric properties and reduced cost. Microwave ceramics with low sintering temperatures become of increasing importance as they (i) can be processed at significantly reduced cost for bulk applications and (ii) can be integrated in multilayer structures co-fired with metal electrodes. Detailed knowledge of phase equilibria and crystal-chemistry in such systems is imperative for the rational optimization of both processing parameters and dielectric properties. The present work demonstrates application of high-resolution transmission electron microscopy and X-ray diffraction to the analysis of crystal structures and phase equilibria of a novel low-sintering-temperature microwave ceramic in the Li-Ti-Nb-O system.

The solid solution $Li_{1+x-y}Nb_{1-x-3y}Ti_{x+4y}O_3$, also referred to as the "M-phase", occurs over an extended phase field in the Li_2O-TiO_2-Nb_2O_5 system. Recent work at the University of Pennsylvania has demonstrated that these solid solutions exhibit a combination of low sintering temperatures (1100 °C) and chemically tunable dielectric properties of interest for use in wireless communication systems (ε=55-78, t_f tunable to zero, Qf up to 9000 GHz). Moreover, the sintering temperature of these ceramics can be reduced to 950 °C by small additions of V_2O_5, which permits co-firing with silver electrodes, thus rendering the ceramic an attractive candidate for LTCC technology.

Despite the technological potential of the $Li_{1+x-y}Nb_{1-x-3y}Ti_{x+4y}O_3$ solid solutions, their crystal-chemistry and exact chemical compositions have remained uncertain, rendering it difficult to understand and control dielectric properties. Two different models have been proposed to describe the crystal structure of the M-phase. According to one model, the structure is incommensurate and consists of intergrowths of $LiNbO_3$-type and Li_2TiO_3-type (rock-salt) blocks; the model implies stacking faults in the oxygen subcell. Another model suggested that the structure is an intergrowth of $LiNbO_3$ and $Li_4Ti_5O_{12}$ (spinel) blocks. However, no clear evidence was established to support either of these models.

In the present work, we applied electron diffraction and structural imaging in a high-resolution transmission electron microscope to clarify the crystal structure of the $Li_{1+x-y}Nb_{1-x-3y}Ti_{x+4y}O_3$ phase. Systematic studies confirmed that what actually forms is not a solid solution, but rather a homologous series of distinct compounds (Fig. 1) with structures built from $LiNbO_3$-like blocks. Successive compounds differ in the thickness of the $LiNbO_3$ blocks, expressed as the number of cation (or anion) layers, n, which increases with decreasing Ti/(Li+Nb) ratio. The total number of layers in the repeat unit is $L=n+1$. The structure of $LiNbO_3$ features a hexagonal close-packed oxygen subcell with the interstices filled by Li and Nb cations; the cation layers in turn form a cubic close-packed stacking sequence. Computer simulations of the phase contrast for $LiNbO_3$ indicated that the stacking sequences of the anion- and cation-layers can be revealed using the [210] and [110] structural projections, respectively (Fig. 2). Application of this imaging code to the interpretation of the structural images of $Li_{1+x-y}Nb_{1-x-3y}Ti_{x+4y}O_3$ specimens demonstrated that both previous models were incorrect: The "M-phase" compounds feature intergrowths of $LiNbO_3$-type blocks and corundum-like layers (Fig. 3), similar to the recently reported Nb_2O_5-stabilized $Li_{14}Ti_{19}O_{45}$ phase. The stacking sequence of the oxygen ions remains hexagonal close-packed for all homologs.

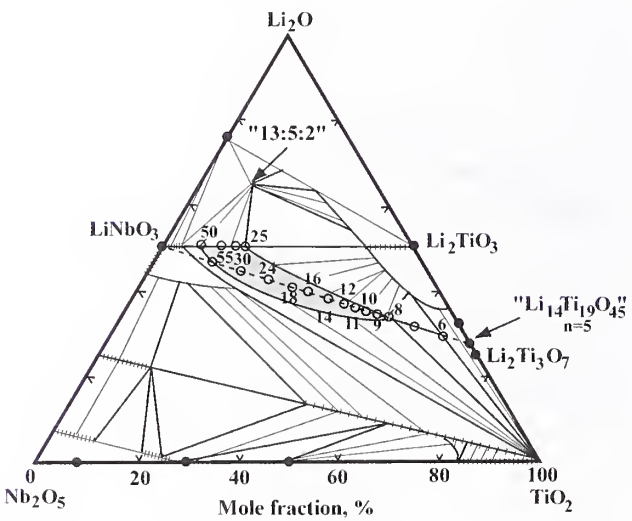

Figure 1: System Li_2O-Nb_2O_5-TiO_2 at 1100 °C (Phase Equilibria Diagrams,Vol. XI, Fig. 9451). The "single-phase" field containing $Li_{1+x-y}Nb_{1-x-3y}Ti_{x+4y}O_3$ (M-phase) is indicated by gray shading. In the present study, rather than a continuous solid solution, a homologous series of distinct compounds (indicated by empty circles) were found to occur in this phase field. The numbers correspond to the number of cation layers, L, in the repeat unit.

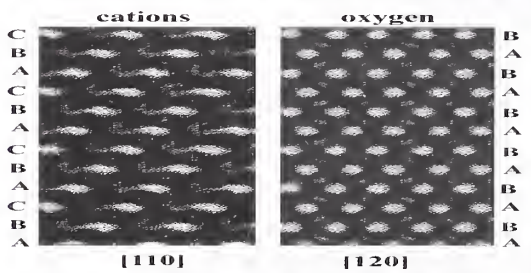

Figure 2: Computer simulated phase contrast images of $LiNbO_3$ in both the [110] and [120] orientations. These two projections reveal the stacking sequences of the cation and oxygen layers, respectively, and for the $Li_{1+x-y}Nb_{1-x-3y}Ti_{x+4y}O_3$ specimens, revealed that it is not a continuous solid solution, but rather a homologous series of distinct phases.

(Fig. 4). The M-phase field was confirmed to encompass a series of such ordered commensurate intergrowths with n ranging from 5 to 54. Specimens with compositions corresponding to fractional n-values typically contained a mixture of two compounds having the nearest integer n-values. Similarly, specimens with nominal compositions corresponding to large values of n contained a mixture of structures with a range of n-values close to the nominal value. For example, a specimen with a nominal composition corresponding to n=27 contained a mixture of structures with n=24, 25, 26, 27, 28.

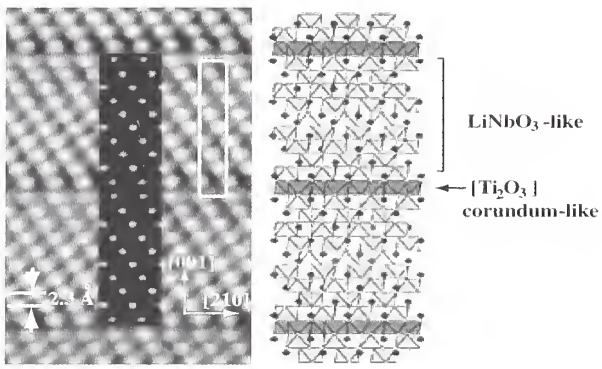

10L Structure

Figure 3: Structural image of the compound $Li_{9.5}Nb_{4.4}Ti_{7.1}O_{30}$ in the [110] orientation recorded near Scherzer defocus. The composition corresponds to a structure with n=9 (10 layers in the repeat unit). The insert shows the phase contrast calculated using the structural model shown, which features intergrowth of $LiNbO_3$- and corundum-like layers. The model was derived by structural refinements using single-crystal X-ray diffraction data.

For a few compositions corresponding to small n-values, single crystals could be grown using a flux method and the structures of these crystals were solved using X-ray diffraction, in collaboration with Dr. I.E. Grey (CSIRO Minerals, Australia). The resulting structural models were in agreement with those proposed from electron microscopy data (Fig. 3).

X-ray structural refinements provided information about the distribution of Ti and Nb in the structure which could not be obtained using electron microscopy data. In particular, the refinements indicated that Ti preferentially segregates into the corundum layers, which, thus, have a composition of $[Ti_2O_3]^{2+}$.

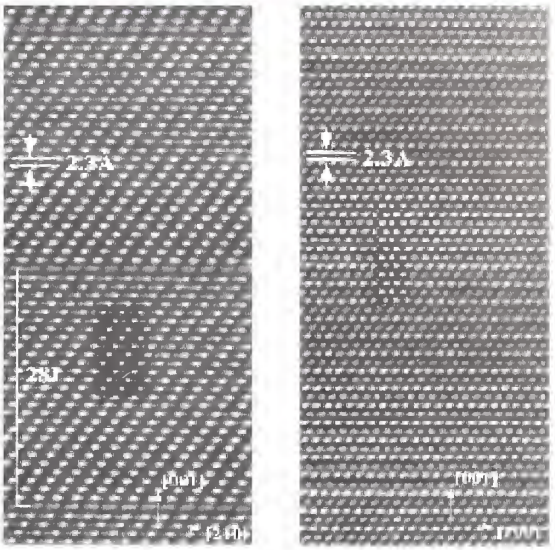

Figure 4: Structural images of the $Li_{1+x-y}Nb_{1-x-3y}Ti_{x+4y}O_3$ 28L-structure (n=27) in both [110] (left) and [120] (right) orientations. This compound is located on the $LiNbO_3$-Li_2TiO_3 join. The [110] projection reveals cubic closed packed stacking of the cation layers in the $LiNbO_3$-like blocks; the intergrowth of these blocks with the corundum-like layers is observed. The [210] projection demonstrates that the oxygen layers form a hexagonal close-packed stacking sequence which is continuous across the intergrowths. The contrast calculated for the $LiNbO_3$ structure is superimposed.

The symmetries of the $Li_{1+x-y}Nb_{1-x-3y}Ti_{x+4y}O_3$ compounds were derived theoretically for different n-values. The analysis demonstrated that all possible structures are represented by four distinct trigonal space groups; both the space group and the lattice parameter along the stacking direction are determined by the n-value. All four deduced space groups contain an inversion center (introduced by stacking of the $LiNbO_3$-like layers), so that all $Li_{1+x-y}Nb_{1-x-3y}Ti_{x+4y}O_3$ compounds are predicted to exhibit paraelectricity, in contrast to $LiNbO_3$. The predictions were in excellent agreement with experimental data.

The structural nature of the M-phase ceramics as complex mixtures of distinct compounds rather than a continuous solid solution bears important implications for their processing and properties as LTCC ceramics. The structural complexity and large number of possible phases considerably extends the "tunability" of properties in the $Li_{1+x-y}Nb_{1-x-3y}Ti_{x+4y}O_3$ system. However, processing temperatures and times will need to be carefully controlled in order to yield consistent phase assemblages and dielectric properties.

For More Information On This Topic: I. Levin, R.S. Roth, T.A. Vanderah

MatML: XML for Materials Property Data

MatML is an application of XML for exchanging materials property data distributed via the World Wide Web.

During the 24-25 May 1999, ASTM-NIST Workshop on Materials Data in the Internet Era, the materials community expressed the need for an extensible markup language (XML) for exchanging documents containing materials property data on the World Wide Web. NIST is responding to that need by leading the technical effort of an international working group to develop MatML, a markup language for materials property data. The MatML Working Group is a cross-section of the materials community composed of participants from private industry, government laboratories, universities, standards organizations, and professional societies.

To understand the significance of establishing a Web-based exchange format for materials data, consider how most of these data are encoded in Web documents today. The current *lingua franca* of the Web is hypertext markup language (HTML). Figure 1 contains a very small HTML code fragment for part of a table from a document in the NIST Ceramics WebBook (see: www.ceramics.nist.gov/webbook/webbook.htm) while Figure 2 illustrates how the code would be displayed in a browser.

In HTML, <table> and </table> are the tags used to start and end a table, respectively. Similarly, <tr> and </tr> begin and end a row within the table. Finally, <td> and </td> begin and end a cell within a row. So, the table in Figure 1 is composed of 2 rows, each containing 3 cells. The content inside each cell is centered and the entries in the first row of cells are displayed in bold font (turns bold on and turns bold off). Also, ^{and} turn superscripting on and off. Notice that the tags such as <table>, <tr>, and <td> do not describe the content, i.e., Critical Current Density is not identified as a property and Magnetic Field and Temperature are not identified as measurement parameters. The tags merely tell the browser how to display the content, as seen in Figure. 2. That the tags do not help identify the content, in this case, materials property data, is a serious drawback for those wishing to use the data in computer applications such as simulation and CAE software. One would need detailed knowledge about the data as well as the containing document's structure in order to write a computer application that could extract the data for subsequent processing. Worse yet, even if data interpretation as described were not an issue for one source, it is very likely

```
<table>
  <tr>
    <td align="center"><b>Magnetic Field (T)</b></td>
    <td align="center"><b>Temperature (K)</b></td>
    <td align="center"><b>Critical Current Density (kA/cm<sup>2</sup>)</b></td>
  </tr>
  <tr>
    <td align="center">0</td>
    <td align="center">3</td>
    <td align="center">3040</td>
  </tr>
</table>
```

Figure 1: Code fragment from the NIST Ceramics WebBook

Magnetic Field (T)	Temperature (K)	Critical Current Density (kA/cm²)
0	3	3040

Figure 2: How code fragment in Fig. 1, would appear in a web browser.

that interoperability issues would arise if one were to apply the same interpretation rules to a different source of materials property data. The MatML effort is addressing these problems of interpretation and interoperability through the development of an extensible markup language (XML) for materials property data that will allow a person or a computer application to interpret and use the data regardless of the source.

Figure 3 represents the markup for the data in Figure 2 if one were to use the current working draft of MatML. Unlike the code fragment in Figure 1, in Figure 3 it is clearly easier to understand what each datum is and one can almost see how each datum is related to others without any other assistance. Part of the power of XML is that it permits the definition of domain-specific tags that allow the data content to become self-describing. As a consequence, interpretation of the data is streamlined and amenable to automation.

For an extensive introduction to XML, see "XML, Element Types, DTD's, and All That" on the MatML web site.

Progress to date regarding the development of MatML has been a result of the assembly of the MatML Working Group, the creation of the MatML Discussion Forum, the design, development, and implementation of the MatML web site, and the development of the Annotated MatML Document Type Definition (DTD). Future progress will be driven by the action items identified by attendees of the International Workshop on the Technical and Strategic Future of MatML (NIST, 26-27 June 2001) during which the MatML effort was strongly endorsed by the materials community.

NIST Collaborators

Ceramics, Polymers, Metallurgy, Center for Theoretical and Computational Materials Science (CTCMS), Standard Reference Data, Semiconductor Electronics, Building Materials, Materials Reliability

External Collaborators

ABB ALSTOM Power (UK), Aluminum Association, ASM International, Atomic Weapons Establishment (UK), The Boeing Company, CenTOR Software, Colorado School of Mines, ESM Software, Ford Motor Company, Information Analysis Center, Instron Corp., Iowa State University, Lawrence Berkeley National Laboratory, Massachusetts Institute of Technology, MSC.Software, NIMS (Japan), University of Delaware, Nottingham University, Virtual School of Molecular Sciences (UK), William Andrew Publishing.

```
<Properties>
  <PropertyDetails>
    <Name>Critical Current Density</Name>
    <Units>kA/cm<sup>2</sup></Units>
    <DataSource>Journal</DataSource>
    <DataType>Evaluated</DataType>
  </PropertyDetails>
  <Value>3040</Value>
  <Parameters>
    <Name>Magnetic Field</Name>
    <Value type="integer">0</Value>
    <Units>T</Units>
    <Name>Temperature</Name>
    <Value type="integer">3</Value>
    <Units>K</Units>
  </Parameters>
</Properties>
```

Figure 3: Markup of Fig 1 data using MatML Working Draft Version 2.0

For More Information On This Topic:

http://www.ceramics.nist.gov/matml/matml.htm

Contact: Edwin F. Begley

Monolayer Film Design

As magnetic data storage technology moves forward with lower flight heights and thinner carbon overcoats, the monolayer of organic molecules on the surface becomes more important in achieving higher shear resistance and longer durability. A novel concept of multi-component molecular assembly is being proposed. The idea is to assemble different molecules of various function groups and molecular weights at a nanometer level and measure the films' properties. Initial results suggest that such a concept is feasible and different molecules can indeed be assembled together to impart different properties at this scale.

As devices shrink in size and many applications require control of surface properties such as adhesion, friction, and stiction, the need to develop thin films for this purpose increases. Magnetic hard disks, MEMs, actuators, and other microsystems need such control via surface thin films. Current technology utilizes fluorocarbons extensively, due to their stability and low vapor pressure. But as contact conditions become more severe, better thin films are needed. Since space is limited in many of these applications, only one or two nanometer thick films are allowed. Because of limited solubility for other molecules, molecular assembly using fluorocarbons is not easily carried out.

If a mixed molecular assembly could be constructed, the potential for effective lubrication, barrier films, and hydrophobic surface control could be significantly advanced. Before such attempts can be made, a conceptual framework is needed. We have studied the mechanisms of protection of perfluoropolyether films on magnetic disks and from the results, developed the concept of monolayer film design.

Effective films should have strong adhesive strength and cohesive strength to resist shear stresses. Organization of such films, whether single molecular or mixed species, has a profound influence on film performance. The most important property of the film is its bonding characteristics with the surface (adhesive strength of the film). The ability to resist shear is fundamental to effective lubrication.

Molecules attach themselves to a surface via either physical or chemical adsorption. The bonding force depends on the nature of the bonds, number of bonds per molecule (in high molecular weight molecules), and the molecular orientation and packing density per unit area. On engineering surfaces (atomically rough surfaces with non-uniform surface energy), molecules tend to preferentially bond to the surface defect sites and high energy sites (steps, twins, dislocations, lattice defects, etc.). In such a case, measurement of the precise adhesive strength of the monolayer will be difficult. Thus, the nature of the surface and its surface energy are important considerations in adhesion and bonding of molecules on a surface. To test such ideas, a test capable of measuring adhesion of a monolayer on engineering surfaces needs to be developed.

We have developed a ball-on-inclined plane test apparatus to measure the shear rupture strength of monolayer films on relatively rough surfaces. Figure 1 shows the schematic set up of the technique. A ball of various diameters (3 mm to 15 mm) slides on a magnetic hard disk. The load is controlled by the geometric interference of the two surfaces and the forces in the x, y, z directions are continuously recorded by a force transducer mounted on top of the ball. The angle of incline of the flat plane controls the initial loading and the rate of load increase. The large area of contact between the ball and the flat captures a large number of molecules and upon deformation of the surfaces as the load increases, the contact area increases. At a load where the monolayer cannot sustain the shear stresses, the film ruptures.

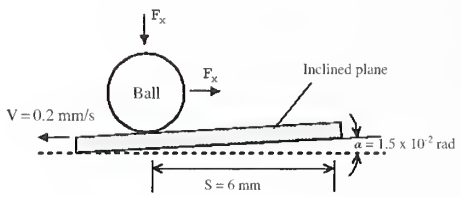

Figure 1: Ball-on-Inclined-Plane Apparatus

Figure 2 shows typical data on model compounds deposited on a single silicon surface at one nanometer film thickness. The data suggest that the adhesive strength follows somewhat the polarity of the functional groups and the packing density.

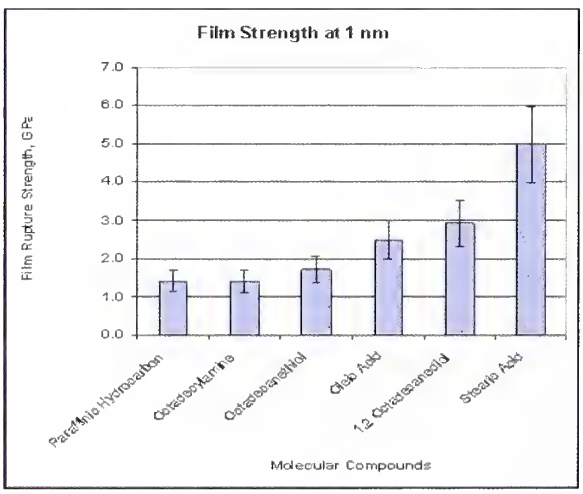

Figure 2: Film Strength Data on Different Chemical Films

The lubricating property or wear resistance of a monomolecular film can be related directly to the bonding strength and the cohesive strength of the monolayer. The classical Langmuir-Blogett films (fatty acids, alkyl thiols, siloxanes) typically behave like a solid. Solid films will deform under contact stresses, produce defects (Gauche defects), and eventually fracture, leading to film failure. The durability of such solid-behavior films under repeated contacts is typically short.

If the spacing between molecules is larger than individual molecular size or volume, then the film behaves like a liquid or a solid-liquid mixture. The durability of the film will increase due to the ease of mobility of the molecules to accommodate stresses but the magnitude of shear stress it can withstand will decrease. Molecule size (molecular weight) also influences the shear strength of the film when the size of the molecule is larger than the asperity contact radius. If the molecular size is sufficiently large and several asperities are in contact with the same molecule, shear resistance will increase due to the large energy necessary to rupture the molecule under shear.

Self-repair can be defined as the ability of the molecules to reorganize themselves into the original state after being mechanically disrupted by contacts. In order to have a self-repairing property, the ability of the molecules to self-assemble will be essential, but the requirement for self-assembly would almost dictate that molecules are free to move about on the surface. This mobility implies that the molecules cannot be chemically bonded to the surface, hence low bonding strength. This diametrically opposite requirement of strong adhesive strength and self-repairability poses an interesting challenge. To meet this dual requirement, one approach is a mixed molecular system where one species will bond to the surface and another species will be allowed to move freely on the surface.

Figure 3 provides some illustrations of the conceptual designs possible to control friction more effectively using a monolayer. Figure 3a shows the schematic representation of molecular arrangement of polar molecules distributed uniformly on the surface. In reality, surface reconstruction often occurs and some molecules will aggregate into different crystalline structures. Figure 3b shows two rows of molecules with one row of molecules chemically bonded to the surface and one row of molecules physisorbed on the surface. This way the film can have both mobility and adhesive strength. Fig. 3c shows a molecular film consisting of molecules with the same functional group but with different chain lengths. Since the adsorption is governed by the functional groups, the lower half of the film will be closely packed, behaving like a solid. The molecules with longer chain length will have part of the molecules sticking above the solid layer. Since they have much larger molecular volume to move about, they will behave like a liquid. Thus, a film with both liquid and solid properties can be constructed. The liquid layer provides damping and low friction and the solid layer provides load supporting strength. Fig. 3d is a variation of the same concept. In this case, a molecular species is first adsorbed on the surface below the monolayer coverage. They are made to bond chemically with the surface either by heat or by UV irradiation. The surface is rinsed with solvent to remove the unreacted species and deposited again with a long chain polymeric molecule similar in structure to the bonded ones with or without the same functional groups. This kind of molecular organization therefore provides a way to achieve high adhesive strength without sacrificing self-repairability.

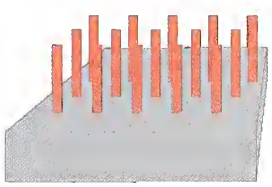

Figure 3a

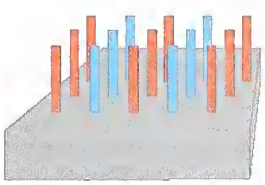

Figure 3b

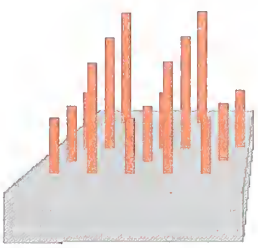

Figure 3c

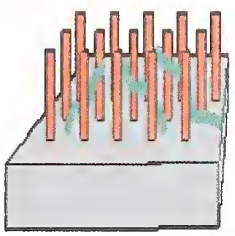

Figure 3d

For More Information On This Topic:

"Scaling Issues in the Measurement of Monolayer Films," Hsu, S.M., McGuiggan, P.M., Zhang, J., Wang, Y., Yin, F., Yeh, Y.P., and Gates, R.S., NATO/ASI Proceedings on the Fundamentals of Tribology and Bridging the Gap between Macro- and Micro/Nanoscales, Nato Science Series: II. Mathemetics, Physics and Chemistry – Vol 10, Kluwer, Amsterdam, 2001

Contact: Dr. Stephen M. Hsu

Texture Measurement and Analysis

Many components and devices in electronic systems are fabricated from materials that have a preferred crystallographic orientation or texture. The applications in which the texture of the material plays a key role in determining properties and performance are broad: complex oxides in random access memory devices, ZnO thin film resonators for cell phone applications, metallic alloys in magnetic recording media, and Al and Cu interconnects in integrated circuits are but a few examples.Texture is established during the synthesis or post-synthesis heat treatment of a material and thus has a strong dependence upon processing history. Accurate measurement of texture is not simple and a variety of tools and approaches are being actively employed in texture studies. X-ray, neutron and electron diffraction based techniques are practiced around the world at varying levels of complexity with regard to equipment and analysis methods. Despite the well-documented existence of these varied approaches, many reported texture measurements on electronic materials are based solely on the relative intensities of conventional θ-2θ x-ray diffraction peaks, which typically yield inaccurate results. NIST has developed quantitative texture measurement techniques that employ equipment commonly available in most industrial and academic settings.

Many thin film and bulk materials used in electronic applications have a preferred crystallographic orientation or texture. Properties of materials can be strongly affected by texture and it is desirable to quantify the effects of texture on properties in order to optimize the development and application of textured materials. This requires accurate characterization tools.

The impetus to develop texture measurement tools in the Ceramics Division came from American Superconductor Corporation, Westborough, MA, (ASC) in 1994. During product development, ASC needed to do rapid, accurate crystallographic texture measurements on wires (or tapes) composed of the high temperature superconductor $Bi_2Sr_2Ca_2Cu_3O_{10}$ swaged in silver. Their goal was to correlate the observed texture with measured electrical and mechanical properties, which are known to be strongly influenced by texture. A major requirement was that the texture measurement technique could be performed using the conventional x-ray powder diffractometer available at ASC. A technique was developed at NIST for quantitative measurement of texture using scans performed on a conventional 2 circle diffractometer; the scans can be obtained in about one hour. The data analysis method employs the technique of calculating the hkl ω scan from an untextured sample of the material being tested using a θ-2θ scan of the sample over the hkl peak. The experimental ω scan from the textured sample is divided by the calculated ω scan to give the texture profile of the sample. The technique is best suited to the analysis of fiber texture. The software to perform the calculations of the analysis, TexturePlus, was developed at NIST. The technology was validated at NIST using SRM676 (untextured alumina) and successfully transferred to ASC in 1995. The software package TexturePlus is available on the World Wide Web: www.ceramics.nist.gov/webbook/TexturePlus/texture.htm.

It became clear that there were many potential users of this method in industry, particularly small businesses, and academia. Since most advanced electronic materials are used in thin film form, the technique was extended to analysis of diffraction data from thin films, where the thickness and linear x-ray absorption coefficient of the film were necessary input data. Validation of the thin film correction was achieved in 1998 with data obtained from electrodeposited films of copper, which are being introduced into chip interconnection technology as a replacement for aluminum. In this study, the (111) texture of 1.6 μm thick electrodeposited Cu films was investigated with two omega scans, using 111 and 222 Bragg peaks. Figure 1 shows that the agreement between the 111 and 222 texture profiles is excellent and that when the correction algorithms in TexturePlus are applied using the correct film thickness the agreement between the 111 and 222 curves is very good. Also noted is a large randomly oriented fraction.

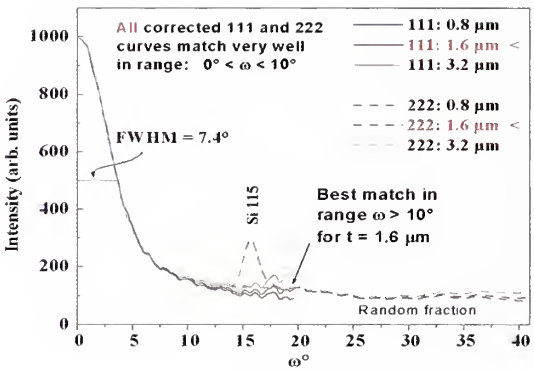

Figure 1: (111) texture measurements from 1.6 μm thick electrodeposited copper films, measured with 111 and 222 peaks and corrected for thicknesses of 0.8 μm, 1.6 μm and 3.2 μm. Specimens provided courtesy of Semitool Corporation.

In collaboration with industrial and university partners, the NIST technique has been used to successfully quantify texture in a broad range of technological materials, both thin film and bulk.

- $Ba_{1-x}Sr_xTiO_3$ for dynamic random access memory (IBM)
- $PbZr_{1-x}Ti_xO_3$ for non-volatile random access memory (Ramtron International Corporation)
- $Na_{0.5}Bi_{0.5}TiO_3$ for transducers, actuators, multilayer capacitors

In the first two cases, one of the main issues was the volume fraction of differently textured material in the films.

A particularly difficult application arose in the case of zinc oxide thin films used for high frequency acoustic resonators in cellular phones under investigation by Agere Systems. The property of importance is the electromechanical coupling coefficient of the films, which is a function of the processing temperature. The films are 750 nm of ZnO on Pt/Si substrates. Processing temperatures have a strong effect on the degree of basal plane texture (ZnO has a hexagonal crystal structure), so accurate

monitoring of this texture would constitute a valuable diagnostic for film quality assessment. Various tools have been used for this measurement – 2 and 4 circle XRD diffractometers and an area detector diffractometer. The full width at half maximum intensity (FWHM) values of the texture profile, determined by the 2 circle technique using TexturePlus, are plotted in Fig. 2 for various incident slit sizes as a function of receiving slit size, also shown are the 4 circle and area detector results. The results are not consistent, and indicate that not only do different techniques give significantly different results (1.2° difference between 4-circle and area detector) but also that the results from a single method depend on the optics of the x-ray equipment (variation of 0.58° for the 2 circle method). Such discrepancies must be understood and resolved before developing standardized texture measurement methods.

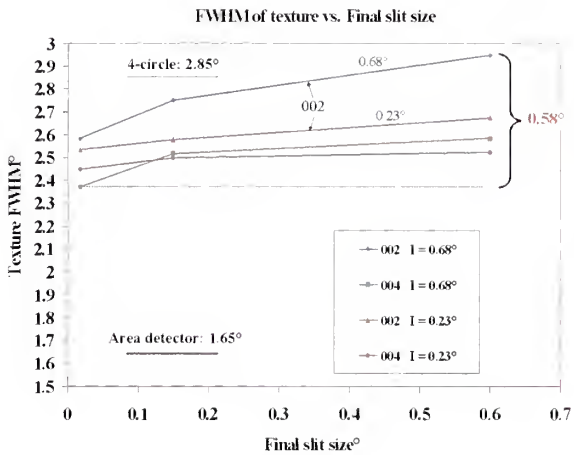

Figure 2: Texture results from ZnO film processed at 650 °C. Powder diffractometer results are plotted as function of final slit size for various incident slit sizes (I). The 4-circle and area detector results are shown as horizontal lines.

A workshop on Texture in Electronic Applications was held at NIST Gaithersburg October 10-11, 2000, and was attended by about 40 researchers evenly divided among industry, academia and national laboratories. The primary goal of the workshop was to provide a forum for the discussion of critical issues relevant to texture and texture measurement. At this meeting, the need for a texture standard was voiced by several participants; it was determined that a round robin of measurements on identical specimens using various techniques was the first step in developing a standard. The following institutions have agreed to participate: Oak Ridge National Labs, IBM, HKL Technologies and McGill University; others will be solicited. NIST will coordinate this interlaboratory activity using Pt thin films with axisymmetric preferred crystallographic texture on Si substrates (courtesy of Ramtron Corporation International) as the candidate texture standard.

For More Information On This Topic: http://www.ceramics.nist.gov/programs/thinfilms/texture.html

Mark D. Vaudin

Advanced Engine Materials

Ceramics and ceramic coatings play an enabling role as industry strives to meet demands requiring higher energy efficiencies, decreased emissions, extended engine life, and reduced warranty costs associated with diesel and turbine engines. Structural ceramics are already used in automotive and diesel engines as fuel pump and injector components, cam roller followers, water pump seals, and turbocharger rotors. These components provide increased wear and corrosion resistance and allow higher operating temperatures and thus improved engine performance. The use of ceramic coatings is increasing in both aircraft and land-based gas turbines, and in diesel engines. Most of the current use of ceramic coatings is associated with thermal barrier coatings – a thin ceramic layer deposited on metallic components to impart thermal resistance as well as resistance to environmental corrosion. The present historical trend of substantial increases in the introduction of ceramics and ceramic coatings in engines is expected to continue. However, the primary barriers to the widespread use of these materials are the cost and uncertainty associated with in-service mechanical reliability.

The primary objective of the Advanced Engine Materials Program is to provide measurement techniques, standards, basic data, and predictive models needed to develop and implement reliable and cost-effective materials for internal combustion and gas turbine engines. Research focuses on the development of test methods for the assessment of contact damage and wear, identification of machining-induced damage and its influence on mechanical properties, development of test methods and predictive models for evaluation of mechanical properties at elevated temperatures, development of techniques and reference materials for thermal conductivity measurements, and development of models for prediction of coating properties and performance. Reliability and precision of various measurement techniques and their suitability for standardization are assessed jointly with industrial partners, international measurement laboratories, and national and international standards organizations. The close working relationship developed between these organizations and NIST not only ensures the relevance of the research projects but also promotes an efficient and timely transfer of research information to industry for implementation.

Contact Information: **Said Jahanmir**

Design Guidelines for Coatings

Edwin Fuller, Mark Locatelli, Andrew Allen, Jan Ilavsky, and Stanley Dapkunas

Ceramic coatings impart thermal and wear protection to many types of heat engines and other mechanical devices. The objectives of this project are: (1) develop techniques for analysis of fine microstructural details; (2) develop models which predict physical and thermal properties based on microstructural features, and, (3) develop models which predict lifetime based on fracture mechanics analysis. Thermal barrier coatings are emphasized.

Ceramic coatings provide wear and thermal protection to metallic components in many applications. Thermal barrier coatings (TBC's) as applied to gas turbines and diesel engines used in aircraft and stationary power generation are the material systems that are the focus of our research. TBC's are typically comprised of plasma sprayed (PS) or physical vapor deposited (PVD) yttria-stabilized zirconia (YSZ) several hundred micrometers thick deposited atop metallic bondcoats on nickel base superalloys.

Two key issues face the TBC community: prediction of physical properties, such as thermal conductivity and elastic modulus; and, prediction of lifetime, as manifested by adherence of the YSZ to the bondcoat.

Microstructural features of the YSZ, the bondcoat and any thermally grown oxides largely determine properties and lifetime. Hence, the research addresses means of characterizing microstructures and predicting physical properties and lifetime based on microstructure.

The microstructural characterization aspects of the research have emphasized the use of small angle neutron scattering (SANS) and small angle x-ray scattering (SAXS) to quantatively measure fine pores and cracks. These pores and cracks are a consequence of the methods of processing and determine the thermal and mechanical properties of the zirconia overcoat. This year, techniques developed for thick PS deposits have been extended to much thinner layers typical of commercially available products and to YSZ deposited by PVD. A more detailed description of this research is provided in the Technical Highlights section of this report.

Coating microstructure can be controlled during processing. Microstructural analysis, typically via optical microscopy, is a primary method of inspection during manufacturing. Accordingly, we are engaged in the development of image-based finite-element analysis tools (the NIST OOF software) for simulating and predicting physical properties of TBC's from microstructure. Research to develop and validate such tools for thermal conductivity measurements is conducted in collaboration with the General Electric Corporate R&D Laboratory. They provide microstructural data (micrographs) and thermal conductivity data for air plasma sprayed TBC samples with a wide range of thermal conductivities (varying by approximately a factor of 3). A thermal version of OOF was developed and used to calculate thermal conductivity from optical microstructural images of these samples. A key aspect of the analysis is ascertaining the level of microstructural detail required in the input images to the simulations. To date we have established that the simulation approach correctly predicts the relative order ranking of thermal conductivity. However, the absolute value was significantly different depending upon the thermal conductivity value assigned to the gas phase in the pores. We are exploring an alternate stratagem for varying the gas-phase conductivity as a function of the microcrack opening dimension.

The ability to predict coating adherence as a function of temperature, cycling conditions, applied stress, bondcoat oxide growth and material properties, such as, coefficient of thermal expansion and elastic modulus, is key to more effective use of TBC's. We have formulated a fracture-mechanics-based description of the growth of cracks near the YSZ-bondcoat interface. The growth of this crack is a critical step in the formation of an unsupported YSZ section that can buckle and spall during cooling from elevated temperature. The model depends on interfacial roughness and the growth of a thermally grown oxide (TGO) of alumina at the YSZ-bondcoat interface. The uniqueness of this solution is the ability to properly account for the closure stresses that develop over the central portion of the crack after the TGO thickness exceeds a critical value. In contrast to initial intuition, these closure stresses actually enhance rather than retard crack growth.

In order to better address the needs of the coating community, a series of visits to engine companies was made by NIST researchers. As a result of these discussions, we are more closely linking our research to industrial interests. This linkage will include the use of data and materials supplied by industry to determine the extent of applicability of our microstructural characterization and modeling and lifetime prediction research.

Contributors and Collaborators: Stephen Langer, Information Technology Laboratory.
James Ruud, General Electric Company
NIST Center for Theoretical and Computational Materials Science

Intermediate Temperature Crack Growth in Ceramics

Sheldon M. Wiederhorn and
Ralph Krause, Jr.

Because of their excellent resistance to deformation, ceramic materials are often used at high temperatures, where they can easily resist temperatures greater than 1000 °C. The main threat to ceramics at these temperatures is subcritical crack growth due to thermal or mechanical shock. In this project, basic crack growth data needed for lifetime prediction at high temperatures are being obtained by both strength methods and by the direct measurement of crack growth rates. The goal of the work is to develop a test methodology for the safe design of structural ceramics at elevated temperatures.

In ceramics, fracture is usually preceded by crack growth from flaws or cracks present in the material. The theory of fracture mechanics provides a logical framework for understanding subcritical crack growth and for relating subcritical crack growth rates to lifetime. A substantial body of experimental data at room temperature supports the theory and its predictions. However, at high temperatures, data supporting the crack growth model of failure are much sparser than at room temperature, and the crack growth model is not as soundly based as at room temperature. In this project crack growth and strength data collected at elevated temperature are being compared to explore the applicability of crack growth theory to component lifetime at elevated temperatures.

Work over the past year concentrated on sapphire, both as a model material and as a material used as IR domes in defense applications, where high temperature fracture due to air heating can be a problem. The crack velocity, v, can usually be expressed as a power function of the applied stress-intensity factor, K_I, $v = AK_I^n$. The exponent n is an important determinant of crack growth sensitivity, $n<10$, indicating a high sensitivity.

Strength tests were carried out in dry nitrogen at room temperature and at 800 °C, on specimens aligned for fracture on the m-plane, $[10\bar{1}0]$, and the r-plane, $[\bar{1}012]$. For m-plane oriented specimens, fracture occurred on the m-plane at room temperature; n was evaluated from fracture mechanics theory as n=52. At 800 °C, fracture did not occur on the m-plane, but on the r-plane, so that each specimen broke on a crystallographic plane at an angle of approximately 32° to the principal tensile stress. At room temperature and at 800 °C, r-plane specimens did not fracture on the r-plane, but on a plane oriented 7° to 9° to the r-plane. The fracture plane was not smooth and was, therefore, not crystallographic. Crack growth measurements were also made at room temperature on both the r-plane and the m-plane using the double torsion technique, from which n=57.4±8.5 was obtained for the m-plane.

The erratic fracture behavior of the flexure specimens also occurs in crack growth studies on the r-plane. Cracks did not propagate on the r-plane. Instead they propagated on a rough surface that lay at an angle of 5° to 10° from the r-plane. Even when crack relaxation could be used to measure crack velocities, crack growth was very erratic. Cracks would propagate for a while at a small angle to the r-plane and then very suddenly jump onto the r-plane, rapidly covering a distance of from 3 mm to 5 mm, Figure 1. Just as quickly, the crack would turn from the r-plane and again propagate on a surface that lay 5° to 10° from the r-plane. A large drop in applied stress intensity factor accompanied the jump in crack position. Why the crack switches planes and why it does not normally propagate on the r-plane is not understood at this time.

The sudden jump of a moving crack onto the r-plane suggests that the transition event for propagation between the two planes may now be the critical event that controls lifetime. Under such a scenario, the transition event would have to be characterized in order to characterize the lifetime. These studies will be extended to silicon nitride materials used in diesel engines for purposes of lifetime prediction.

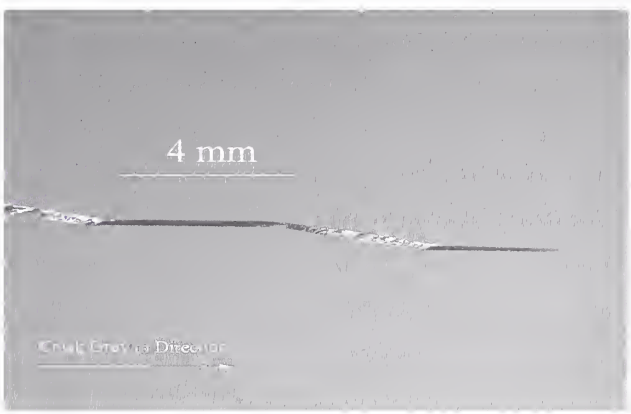

Figure 1: Erratic nature of crack growth in r-plane specimens. The dark portions of the crack represent r-plane fracture.

Machining Damage

Lewis Ives, George Quinn,
and Said Jahanmir

Manufacturers of ceramic components for advanced engine applications require cost effective grinding processes with known or minimal potential for introduction of performance limiting damage. This project determines the relationship between machining conditions and performance related requirements such as strength, surface finish, wear resistance, and fatigue life; and provides data and measurement methods to assess the effects of damage, and establishes standard test methods.

Grinding with diamond abrasive tools is the predominant machining method for shaping and finishing ceramic components Because of their brittle nature, ceramics are highly susceptible to the introduction of damage, in particular, microcracks, generated during the abrasive/material interaction This damage can have a critical influence on the capability of finished components to meet performance requirements such as those associated with strength, wear resistance, and fatigue life. In support of manufacturers' needs for improved grinding processes, this project has focussed primarily on two areas: 1) determination of the influence of grinding conditions on performance related properties of ceramic materials and 2) development of test methods and standards related to the measurement of grinding damage.

Current work has concentrated on evaluating the effect on grinding damage of different diamond-grit coatings and different bond types used in formulating grinding wheels Application has been to both silicon nitride and silicon carbide ceramics. Observed differences appear to be related to the effectiveness of grit retention and the propensity of grit to wear. The data will assist manufactures in optimizing their grinding processes.

A recent outcome of this project has been the development under ASTM Committee C28 of a standard test method for the measurement of the effect of grinding conditions on the flexure strength of advanced ceramics. The standard designated C1495 was accepted and will be issued this year

In recently completed work, a comprehensive fractographic evaluation of machining damage was conducted on a commercial, sintered reaction bonded silicon nitride. The rod and bar specimens were ground under carefully specified conditions employing diamond grinding wheels of different grit sizes. The fractographic analysis involved detailed examination of the fracture origins in all of the nearly 200 specimens subsequent to flexure strength testing. The bars and rods had appreciably different Weibull strength distribution curves in accord with the grinding conditions applied. Fractographic analysis indicated that the differences were directly attributable to the size and presence of machining induced cracks. A crucial finding was that 320 grit longitudinal ground rods experienced no strength degradation due to machining, since nearly every specimen fractured from the material's inherent flaws. Almost the same outcome was observed for 600 grit transversely-ground rods, wherein small or negligible degradations were noted and the machining cracks were very shallow (< 15 mm). This is a significant finding since transverse grinding with 600 grit wheels is much more practical than longitudinal grinding for cylindrical parts. This knowledge should translate into cost savings and greater confidence in preparing parts for the particular, commercial silicon nitride.

An equally important finding is that machining cracks often leave telltale markings on fracture surfaces. Machining damage had heretofore been notoriously difficult to discern by anyone other than an expert in fractography. To aid materials scientists and engineers in the detection of these telltale signs, a new series of schematic illustrations has been created These will be incorporated in several ASTM or ISO standards. The figure below is one such example.

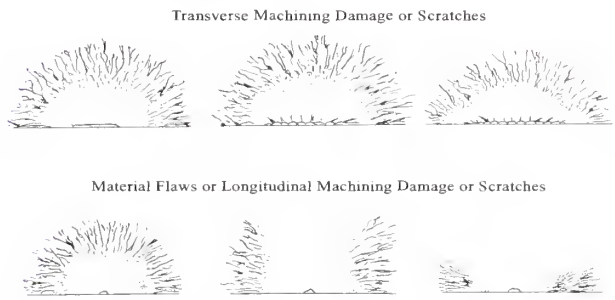

Schematic illustrating telltale features in fracture origins which can be used to identify their origin, e.g. machining damage, surface scratch, or material flaw.

Much of work for this project is carried out jointly with members of the NIST Ceramic Machining Consortium. Members are mainly from industry but several universities are also included. The results generated by the projects have helped industrial members optimize their grinding methods and thereby produce more cost effective and reliable products In one case, the results were cited as having made a significant contribution to the successful development and production of a new ceramic cam roller follower adopted for use in diesel engines by a major manufacturer.

Contributors and Collaborators:

Members of the NIST Ceramic Machining Consortium: Cabot Corp.; Ceradyne Inc.; Ferro-Ceramic Grinding Inc; Ford; Fraunhoffer USA; GE Superabrasives; Landis Gardner; Saint Gobain Norton; Michigan Tech. U.; N. C. State U.; Scientific Manufacturing Technologies, Inc.; Stevens Inst. of Tech.; U. Alaska Fairbanks; U. of Arkansas; U. of Delaware; U. of Toledo; West Manufacturing Tech., Inc.

Test Methods for Mechanical Reliability

William Luecke, Ralph Krause, Jr. George Quinn, and Said Jahanmir

Structural ceramics such as silicon nitride offer a unique combination of properties. Their light weight, high-temperature strength, and resistance to wear and corrosion make them particularly attractive replacements for metals in diesel engines. Their use as certain key engine components will allow higher operating temperatures, which will lead to higher thermal efficiencies and environmentally cleaner propulsion systems. The objective of this project is to develop standard test methods for assessing the fracture toughness, contact damage and wear resistance of ceramics for diesel engines and other heavy vehicle propulsion systems.

Reliability and cost-effectiveness are critical issues for implementing ceramics in diesel engines. Ceramic components in engines serve under demanding conditions, characterized by high contact loads, elevated temperatures, and corrosive environments. To ensure a reliable service life, standard test methods are needed to evaluate the performance of candidate ceramics. In collaboration with diesel engine companies in the U.S. as well as participants from Germany and Japan under the auspices of the International Energy Agency (IEA), we are evaluating test methods for characterizing the contact fatigue behavior of ceramics under rolling and sliding conditions that simulate the cam roller followers, valves and valve seats. An integral part of this project is evaluating the effect of machining damage on contact reliability as well as possible interactions between machining damage and contact damage that may lead to premature failure. In addition to test methods, we are studying the relation between ceramic microstructure and performance reliability. We also have on-going projects for developing and refining test methods for evaluating ceramic strength and fracture toughness.

We have initiated research in standards and standard test methods for evaluating rolling contact fatigue (RCF) and contact damage in engine ceramics with a workshop at NIST during May 2001. National Laboratory, industrial, academic, and NIST participants formed a Contact Damage Working Group to study unresolved issues in reliability of engine ceramics. Industry representatives from Caterpillar, Cummins, and Ceradyne presented their views on potential research directions that would address barriers to their adopting ceramic components. The group, which will meet biannually, adopted a three-part research plan. Firstly, it will develop a guide to practice for evaluating contact damage in ceramics. In parallel, it will study an existing test (ball-on-rod) for evaluating RCF damage to establish its suitability for standardization, including possible interlaboratory testing. Three members possess this test capability, as do a number of other potential working group members. Thirdly, the group will probe the relationship between microstructure of candidate ceramics and their RCF behavior and resistance to contact damage.
We made progress on several standards, including a new ASTM flexural strength of cylindrical rod test method, a new ISO fracture toughness test method, and revisions to the master ASTM C 1161 flexure strength standard for rectangular bars and the fracture toughness ASTM standard C 1421. This work has been closely coordinated with activities in the Machining Damage project.

We refined the surface crack in flexure (SCF) fracture toughness test method. The SCF method uses a common Knoop hardness indentation to create a classic median-controlled flaw in a bend bar as illustrated in Fig. 1. The bar is fractured after removal of the indentation and its damage zone. Fracture toughness is computed from the size of the median crack and the stress at fracture. Some discrepancies in results (5 % to 10 %) for particularly brittle materials were traced to interferences from vestigial lateral cracks in the vicinity of the indentation. A simple remedy is to observe the ground surface during the customary step of removing the indentation and its damage zone. Material should be removed until all traces of the remnant lateral cracks are eliminated. This refinement will be incorporated into a revision of the ASTM standard C 1421 and will be included in the latest ISO draft standard.

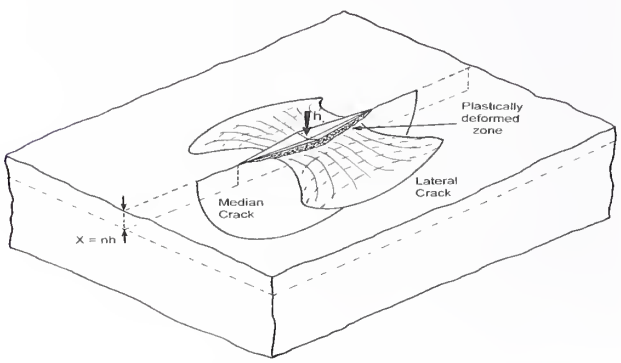

Figure 1: Lateral crack formation under the Knoop indent

Contributors and Collaborators: Biljana Mikijelj, (Ceradyne), Paul Wilbur (Colorado State U), Jonathan Salem (NASA Glenn), Kouichi Yasuda (Tokyo Institute of Technology), Seong-Jai Cho (Korean Research Institute of Standards and Science), Joseph Annese (Bomas Machine Specialties) Ronald Chand (Chand Associates), Lou Balmer-Miller (Caterpillar), Thomas Yonushonis (Cummins)

COMBINATORIAL METHODS

The Combinatorial Methods Program develops new measurement techniques and experimental strategies needed for rapid acquisition and analysis of physical and chemical data of materials by industrial and research communities. A multi-disciplinary team from the NIST Laboratories participates to address key mission driven objectives in this new field, including needed measurement infrastructure, expanded capability, standards and evaluated data.

Measurement tools and techniques are developed to prepare and characterize materials over a controlled range of physical and chemical properties on a miniaturized scale with high degree of automation and parallelization. Combinatorial approaches are used to validate measurement methods and predictive models when applied to small sample sizes. All aspects of the combinatorial process from sample "library" design and library preparation to high-throughput assay and analysis are integrated through the combinatorial informatics cycle for iterative refinement of measurements. The applicability of combinatorial methods to new materials and research problems is demonstrated to provide scientific credibility for this new R&D paradigm. One anticipated measure of the success of the program would be more efficient output of traditional NIST products of standard reference materials and evaluated data.

Through a set of cross-NIST collaborations in current research areas, we are working to establish the infrastructure that will serve as a basis for a broader effort in combinatorial research. A Combinatorial Methods Working Group (CMWG) actively discusses technical progress within NIST on combinatorial methods through regular meetings. The technical areas and activities of the CMWG are available in a brochure "Combinatorial Methods at NIST" (NISTIR 6730). Within MSEL, novel methods for combinatorial library preparation of polymer coatings have been designed to encompass variations of diverse physical and chemical properties, such as composition, coating thickness, processing temperature, surface texture and patterning. Vast amounts of data are generated in a few hours that promote our understanding of how these variables affect material properties, such as coatings wettability or phase miscibility. Additional focus areas for both organic and inorganic materials include multiphase materials, electronic materials, magnetic materials, biomaterials assay, and materials structure and properties characterization. State of the art on-line data analysis tools, process control methodology, and data archival methods are being developed as part of the program.

In order to promote communication and technology transfer with a wide range of industrial partners, an industry-national laboratories-university combinatorial consortium, the NIST Combinatorial Methods Center (NCMC) is being organized by MSEL. The NCMC will facilitate direct interactions on combinatorial measurement problems of broad industrial interest and efficient transfer of the methods developed to U.S. industry.

Contact Information: **Alamgir Karim**

Combinatorial Tools for Oxide Thin Films

Peter K. Schenck and Debra L. Kaiser

Combinatorial methods are increasing being used by industry for the discovery and optimization of inorganic thin film materials for electronic, optical and magnetic applications. We have developed novel approaches for thin film library fabrication and high throughput thickness and optical property measurement that are broadly applicable to a wide variety of ceramic, metal, and ceramic/metal composite systems. These techniques are demonstrated for model $BaTiO_3$-$SrTiO_3$ film libraries of interest for next generation wireless, memory and logic devices.

Our work has focused on the development of two combinatorial tools that can be applied to a broad range of inorganic materials: a pulsed laser deposition (PLD) system for thin film library fabrication and a rapid throughput, spatially-resolved spectroscopic reflectometry technique for mapping film thickness and refractive index. To date, $BaTiO_3$-$SrTiO_3$ film libraries have been deposited and characterized using these tools.

PLD is a versatile rapid prototyping tool for thin films that has the following advantages: complex target compositions are possible; congruent vaporization leads to stoichiometric material transfer; high energy process; low substrate temperatures; and high deposition rates. A conventional single-target PLD system was retrofitted to a novel dual-beam, dual-target configuration designed for the fabrication of graded composition films. A positionable horizontal mask is installed to allow variation of an additional process parameter such as temperature or gas pressure during deposition. Substrate temperatures up to 800 °C can be achieved. The system is outfitted with a high-speed intensified charge-coupled device camera for *in situ* imaging of the laser-generated plumes at 5 ns resolution; this diagnostic capability has been used to fine-tune the process in real time. A 500 nm thick film library spanning the entire composition range between the two target compositions is deposited in less than 1 h.

Thickness and optical property assays are performed on the film libraries using a semi-automated spectroscopic reflectometry apparatus designed and fabricated in our laboratory. This instrument is equipped with a bifurcated fiber optic probe to both illuminate the sample and obtain the reflected light, and a miniature fiber optic coupled spectrometer to collect the entire spectrum simultaneously at each measurement position. The reflectivity of the film-substrate system relative to the bare substrate is calculated and fit to a model from which thickness, refractive index and absorption coefficient can be derived. The data collection and analysis takes ≈ 5 s per point, so a 1 mm x 1 mm grid on a 2 cm square film can be mapped in about ½ h. Spatial resolution is 0.5 mm and the spectral range is 385 nm to 885 nm; films with thicknesses ranging from 20 nm to ≈ 3 μm can be measured.

Composition assays are performed by electron microprobe analysis in the NIST Chemical Sciences and Technology Laboratory. Also under development in this laboratory is a scanning evanescent microwave microscope for mapping dielectric properties at frequencies up to 20 GHz.

To demonstrate the applicability of these tools, library films were prepared using $BaTiO_3$ and $SrTiO_3$ ceramic targets. The Ba/Sr ratio varied from 6.5 to 0.5 across a 2 cm segment of a film, verifying that the dual target PLD approach yields the desired composition spread library. Using the *in situ* diagnostic capabilities, the plumes were fine-tuned to yield a film with a uniform thickness within ± 3 % over a 1 cm x 1 cm area.

A procedure was developed to predict the composition map in a film using the measured thickness map or deposition pattern from films deposited from the individual targets. Correlation of the pattern obtained by summation of the two individual target patterns with the pattern from a film deposited using both targets under otherwise identical conditions was excellent. Assuming negligible diffusion of the deposited species, it was then possible to predict the composition map from the individual target deposition patterns. Using this approach and the in situ diagnostic instruments, the process was fine tuned to yield a film having regions of fairly uniform thickness with large composition gradients; for example, the line y = 10 mm and x = 19 mm to 30 mm in Figure 1.

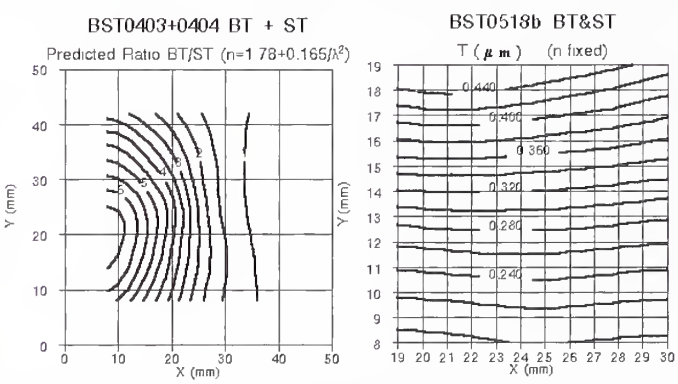

Figure 1: Predicted Ba/Sr ratio (left) and measured thickness map (right) for a $BaTiO_3$-$SrTiO_3$ film library

Contributors and Collaborators: John T. Armstrong, Ryna B. Marinenko, Steven W. Robey, Stephan J. Stranick, Chemical Science and Technology Laboratory, NIST

DATA EVALUATION AND DELIVERY

Materials data are critical to the rapid and decentralized design and manufacture of communication, transportation and other devices, which characterize 21st century life. The goal of the Data Evaluation and Delivery Program is to provide the producers and users of materials with the means of fulfilling their data requirements in the most efficient ways. This goal is accomplished by providing improved access to materials data, development of methods for transferring materials data across the World Wide Web, providing protocols for data evaluation, and enhancing the functionality of existing collections of evaluated data. Much of this research is based on information technology and includes: the development of a materials mark-up language (MatML), the linkage of digitized crystallographic information with full structure analysis in cooperation with the International Center for Diffraction Data and Fachinformationszentrum (FIZ) Germany, and the production of phase diagrams through the NIST/American Ceramic Society Phase Equilibria Program. Other informatics available to the community are contained in the Ceramic WebBook at the Ceramics Division Website. The Ceramics WebBook provides links to other sources of ceramic data and manufacturer's information, selected evaluated data sets, structural ceramics and high temperature superconductor databases, glossaries, and tools for analysis of ceramic materials.

Databases for metals will be developed on web pages in the form of phase diagrams, deformation mechanism maps, and simple - but useful - interactive calculations of thermodynamic and mechanical properties. Annotation and interpretation will be conducted by the Metallurgy Division.

Contact Information: **Stanley J. Dapkunas**

Automotive Headlights for Forensic Utility

This activity is a is a collaborative effort with the automotive industry to develop and establish a database on the identification details of front lighting systems of motor vehicles sold in the United States. The database is intended to serve law-enforcement and the forensic community in investigations in which fragments of automotive headlights exhibited as evidence can be linked to a specific vehicle involved in a crime.

Mario J. Cellarosi

Activities in this effort are to replace the NBS Special Publication 480-17, 1978 (SP 480), on Glass Auto Headlights for Forensic Utility. SP 480 has served the forensic community and law enforcement as an effective tool in investigations aimed at determining a specific vehicle identification from fragments of headlights left at the scene of hit-and-run crimes. However, this publication is at present of very limited use because it covers only headlights of the sealed-beam type, which were installed in passenger-type vehicles made between the years 1962 and 1974. Therefore, a replacement for this forensic publication with a computerized database that reflects the present state of auto headlights is warranted.

There are significant differences now from 1978, when the SP 480 was issued. Today, there are many more front lighting designs to go along with the great increase in vehicle models. Prior to 1978, headlights were made from borosilicate glass produced principally by three companies. Several lamp makers then assembled lens and reflectors glass components as single unit sealed-beam headlights. Nearly all of these production facilities were located in the United States. Sealed-beam headlamps were then installed in passenger vehicles in both right and left front locations.

Today, glass, plastics, and glass-plastic hybrids, are used for headlight systems. These systems are installed in variety of vehicles, passenger cars, sport utility vehicles (SUVs), light trucks, and minivans. For the North American market, headlights are made and assembled by a large number of companies, many of which are located overseas. In this development, the identification details and the purchasing and referencing system for headlights is exceedingly intricate.

There are other major differences between SP 480 and the current situation. 1) SP 480 covered only passenger cars, principally U.S. built. Today, vehicle sales in the United States are about sixteen million units per year. Approximately fifty percent of these sales are light trucks, SUVs, vans, and hybrids of these models. Furthermore, the present U.S. market comprises vehicles that are about 30 % imports. 2) SP 480 covered 22 types of sealed-beam headlights, which were installed in both left and right positions, in all passenger cars, models 1962 to 1974. In the present scenario, one major company alone, in the last ten years, has installed 1,200 different types of headlights in their vehicles. 3) In 1974, the "Big Three" (GM, Ford, Chrysler) together produced 67 different models. Today, each one of the major carmakers has a similar number of vehicles. 4) The present worldwide market for automotive components is very competitive. Carmakers and suppliers consider their parts source information and other pertinent data company proprietary. For these reasons, a databank for headlights installed in all vehicle makes and models manufactured since 1978, is a massive, complex, and expensive task.

NIST/industry collaborations have been established with the purpose to create a new database on headlights. These collaborations now include the major automakers, parts suppliers, and the SAE International Committee on Headlights. This partnership is designed to generate and establish a running system for data collection on automotive front lighting, from present to future production and application. The new database encompasses the identification details, visual characteristics, and information of single headlights and front lighting assemblies, for both the right and left positions. Covered data comprises the headlamp, materials, inner and outer lens, park and turn signals, side marker, side reflex, and daylight running lights (DRL).

Because each headlight design is specific for a particular year, type and model of a vehicle, the output of this project provides a significantly improved diagnostic tool as compared to the use of the previous SP 480, in forensic investigations in which fragments of automotive headlights exhibited as evidence can conclusively be linked to a vehicle involved in a crime.

A formal presentation on this project was given to the Academy of Forensic Sciences, Annual Meeting, Seattle, WA (February 2001). Similar presentations were given to the Society of Automotive Engineers and in other organized meetings with representatives of the Automotive Industry. All recognized the value of the NIST project, which addresses important needs in law enforcement and the forensic community in investigations involving auto headlights.

Contributors and Collaborators: DaimlerChrysler Corp., Ford Motor Co., General Motors Corp., Honda Co., Nissan Co., Toyota Co., Corning Inc., Guide Corp., Visteon Corp., Society of Automotive Engineers, S. Dapkunas (852), S. Ballou and K. Higgins (NIST Office of Law Enforcement Standards).

Full Structural Crystallographic Data for Non-Organic Materials

Vicky Lynn Karen and Alec Belsky

The materials community in both science and industry use crystallographic data models on a daily basis to visualize, explain, and predict the behavior of chemicals and materials. Access to reliable information on the structure of crystalline materials helps researchers concentrate experimental work in directions that optimize the discovery process. This project develops, maintains, and disseminates evaluated full structural crystallographic data in modern computerized formats, along with scientific software tools to exploit the content of these databases.

To meet the needs of the industrial, scientific and technical communities, the scope of this project covers three areas: a) building and maintaining state-of-the-art databases containing the structures of non-organic substances, including ceramic, metals and inorganic materials; b) developing software tools for the calculation and standardization of derived data items as well as modules for the intelligent access of these data, and c) providing access to these databases through modern user interfaces and networking capabilities. Access to crystal structure data can be a key step in solving research and applications problems involving materials, as in the chemical (catalytic materials), petroleum (zeolites), and the electronics (epitaxial growth and thin films) industries. These data are of interest to analysts in areas such as materials design, properties prediction, and compound identification. Better quality data and modern products facilitate increased understanding of materials properties, and help companies reduce costs and increase research efficiency.

The Inorganic Crystal Structure Database (ICSD) is produced cooperatively by the Fachinformationszentrum Karlsruhe and NIST. The ICSD is a comprehensive collection of crystal structure data of inorganic compounds containing more than 57,000 entries and covering the literature from 1915 to the present. The initial focus of this project has been on modernizing and evaluating the ICSD. This has included a complete re-design of the ICSD database structure, conversion and loading of the data into a relational database management system, designing graphical user interfaces to access the data, and creating scientific application modules to analyze the results of a database search.

A Windows-based graphical user interface and underlying search algorithms have been designed and implemented for the ICSD. The user interface is tabular in design, allows for searching in five general categories of Chemistry, Crystal Data, Reduced Cell, Symmetry, and Reference Data, and includes enhanced features for the characterization of materials based on lattice and chemistry search modules, and 3-dimensional visualization and powder pattern simulation of inorganic structures. An iterative process of review, test and revision of this database and software is being conducted

As entries are added to the ICSD, the data are evaluated by experts in specific disciplines and by specialized computer programs. Several types of evaluation are performed, including examination of an individual data item and looking for consistency within a complete entry. During this year, NIST has continued its crystallographic evaluation of the ICSD to determine the relationship of an individual entry to the entire database; scientific strategies and code are used to identify which entries may represent related and duplicate crystal structure determinations. Database searches have been carried out to locate entries which are identical with respect to reduced cell parameters, space groups, Wyckoff positions, sum formula, among other criteria. Various subsets of the data were prepared and more than 1,500 entries were examined in detail by an expert in crystallography. This expert evaluation is an ongoing activity at NIST.

In a parallel effort, the NIST Structural Database (NSD) contains crystallographic and atomic positional information for metallic crystalline substances, including alloys, intermetallics and minerals. About half of the entries represent experimentally refined structures; in the remaining half, the structure type has been published by the authors or editorially assigned. This year, an Agreement has been signed with HKL Technology, Inc. to incorporate the NSD into an electron diffraction instrument package. The planned electron diffraction software will search the NSD by elemental composition, retrieve the full structural crystallographic information, and use this to generate a calculated or simulated electron diffraction pattern. Unknown phases can then be identified automatically by matching the calculated and observed patterns.

Contributors and Collaborators: Fachinformationszentrum Karlsruhe, Germany D. Watson (Cambridge Crystallographic Data Centre, UK) S. Young (NIST Standard Reference Data Program)

Materials Property Data and Data Delivery

Ronald G. Munro and Edwin F. Begley

Advances in materials science and engineering, from the production of new material phases (such as superconducting MgB_2) and the refinement of measurement capabilities (such as SRM 2100 for fracture toughness of ceramics) to the modeling of material behavior (such as via OOF), create greater demands for data that are evaluated and readily available in a directly functional format. Projects focused on the development of evaluation methodology, comprehensive databases, and the advanced materials markup language (MatML) are responding to those needs.

The technologies of manufacturing and materials modeling advance at rates that are limited, in general, by information. These applied technologies advance rapidly only when pertinent and reliable data are readily accessible. New materials, for example, are widely integrated with product development only when designers have sufficient data on which their designs can be based or supported. Increasingly, simulation models of potential products are being developed using finite element techniques prior to any investment in prototype construction. There are two important aspects in this trend that depend significantly on information technology. First, the range of physical, mechanical, and thermal property data must be sufficient to accommodate a variety of potential operating conditions. Second, the data need to be accessible in a manner that allows the information to be acquired without a substantial expenditure of time or other resources. Work in the Ceramics Division addresses both of these issues, not only to promote current applications, but also to anticipate the evolution of technological demands.

Central to the Division's strategic plan for property data and information technology is the NIST Ceramics WebBook, one of the principal components of the Divisions's web site (http://www.ceramics.nist.gov). Currently, the Ceramics WebBook is composed of three parts: evaluated data, a guide to data centers and sources, and links to other resources useful to materials research. The component devoted to evaluated data is divided further into three sections addressing structural ceramics, high temperature superconductors, and a collection of more focused topical data sets known as the NIST Property Data Summaries. In the present reporting period, a major update has been completed for the Structural Ceramics Database (SCD).

The first version of the SCD was completed in October 1990 and released through the NIST Standard Reference Data Program as NIST Standard Reference Database Number 30. That first version of the SCD was developed in support of research on advanced ceramic heat exchangers and contained only 127 data sets for selected varieties of silicon carbide and silicon nitride. In 1993, the first upgrade of the data set increased the number of citations to approximately 225. The second upgrade did not occur until 1998 at which time the number of citations rose to approximately 400. In the three years that have lapsed since then, the data set has been expanded significantly to encompass a broader range of materials including borides (TaB_2, TiB_2, ZrB_2, ...), carbides (B_4C, SiC, TiC, C(diamond),...), nitrides (AlN, BN, Si_3N_4,...), oxides (Al_2O_3, BeO, MgO, SiO_2, TiO_2, ZrO_2,...), and oxynitrides ($[Al_2O_3]_{1-x}[AlN]_x$, $Si_{6-x}Al_xO_xN_{28-x}$, Si_2N_2O,...). Concurrently, the number of citations has been increased to approximately 700, while the total number of property values has increased approximately from 15000 to 31000.

Access to the SCD data is provided by means of the Ceramics WebBook. Currently, the WebBook displays the database using the hypertext markup language (HTML). While HTML is adequate for displaying data to be read on a display screen, it has serious deficiencies with respect to the growing need for automated data retrieval. The internet has created a realistic opportunity for worldwide distributed computing in which, for example, one computer may execute a computational program (such as OOF) while accessing databases (such as the SCD) on other computers. To achieve this interaction, however, the database must be encoded with considerably more information than is provided in HTML. This situation arises because HTML, in essence, treats all information as merely a collection of symbols that are to be placed somewhere on the display screen. The HTML code specifies where and how to display each symbol. Consequently, a computer reading an HTML file would encounter a stream of symbols and display codes and would be very hard pressed to determine whether a symbol was part of a material name, a property name, a value, a unit, or any other parameter or qualifier that might be recorded in the file. To resolve this dilemma, the NIST Ceramics Division has taken the lead in developing a new materials markup language called MatML. MatML retains the display capability of HTML while simultaneously enabling meaningful automated data retrieval for distributed computing. For a more comprehensive discussion of this development, see MatML by E. F. Begley in the Technical Highlights section of this report.

Contributors and Collaborators: Stephen Freiman, Stanley Dapkunas, Mario Cellarosi, and Joyce Harris, Ceramics Division (852), MSEL
The members of the MatML Working Group

Phase Equilibria Diagrams

Mary A. Harne, Peter K. Schenck, and
Terrell A. Vanderah

The Phase Equilibria Diagram program is a long-standing cooperative effort with the American Ceramic Society to maintain and develop a state-of-the-art database of critically evaluated ceramic phase equilibria data for industrial and academic customers

Phase diagrams are used throughout the ceramics industry to understand and control the complex phenomena which increasingly underlie advanced industrial production and materials performance. To service the need for reliable phase diagram data, the Phase Equilibria Data Center along with the American Ceramic Society jointly publish a series of critically evaluated collections of phase diagrams. The series originally was published under the title "Phase Diagrams for Ceramists" (1964-1992). It is now published under the more general title "Phase Equilibria Diagrams" to emphasize that the data are useful to a broader materials community than just ceramists.

The series "Phase Equilibria Diagrams" provides current, evaluated data on the phase equilibria of ceramics and related materials and also provides bibliographic, graphical and analytical services, so that researchers have access to reliable up-to-date data for designing, using, applying, analyzing, and selecting those materials.

The database is currently being modernized from the 1980's IIP-based system to a PC-based system. The new system will be capable of electronic publishing in a variety of formats, including a Web-based version, which must incorporate all of the scientific data relationships embodied in the original database. In addition, NIST-ACerS data center personnel have substantially completed required modernization tasks including upgrading of the digitization software originally written by NIST staff, and input of 2,000 commentaries and 6,955 diagrams from older volumes of the series that did not exist as electronic files.

Accomplishments this year include the publication of Volume XIII - Oxides. This volume, edited by Robert S. Roth, contains 892 diagrams and 595 commentaries. Collection and preparation of technical data for a second monograph entitled "Electronic Ceramics I: Oxides of Ti, Nb, and Ta", is now in progress, and will be edited by R.S. Roth and T.A. Vanderah. Most of the systems to be included in this monograph will be of major interest to the fields of dielectric, ferroelectric, and piezoelectric ceramics. Also in preparation is Volume XIV - Oxides which will contain a wide variety of metal, non-metal, and semi-metal oxide systems.

Contributors and Collaborators: The American Ceramic Society; R.S.Roth, C. Cedeno, H. Ondik, H.F. McMurdie, N. Swanson, E. Farabaugh

Materials for Magnetic Data Storage

For the magnetic data storage industry, the market potential is vast and growing, but global competition is intense, and the technical challenges extreme. Leading commercial magnetic disk drives today store about 25 gigabits of data per square inch. The National Storage Industry Consortium (NSIC) plans to demonstrate a recording density of 1 terabit per square inch—40 times today's level—by 2006.

To reach these goals, new materials are needed that have smaller grain structures, can be produced as thin films, and can be deposited uniformly and economically. Recording heads must be designed to produce higher output signals and lower noise. Component dimensions must be made smaller, and the measurements more precise. New lubricants are needed to prevent wear as spacing between the disk and head becomes smaller than the mean free path of air molecules. New methods are needed to standardize components and increase yields.

The National Institute of Standards and Technology is working with the magnetic recoding industry to develop measurement tools, modeling software, and standards to help achieve their goals. Staff expertise at NIST spans all fields relevant to magnetic data storage, including materials science, electrical engineering, physics, mathematics and modeling, manufacturing engineering, chemistry, metrology, and computer science, with the Materials Science and Engineering Laboratory, the Electronics and Electrical Engineering Laboratory, the Physics Laboratory, the Information Technology Laboratory, and the Manufacturing Engineering Laboratory working as partners in this effort. By addressing important measurement issues in magnetism, by the development and preparation of appropriate standards, and by bringing together the industrial and scientific communities through the organization of workshops and conferences in the area, NIST acts to accelerate the use of advanced magnetic data storage materials and technologies by the industrial sector, and to enable industry to take advantage of new discoveries and innovations. In addition, close linkage with NSIC increases the industrial relevance of our program and improves technology transfer. Additional collaborations with Xerox, General Motors, Hewlett Packard, IBM, Seagate, Motorola, and Carnegie Mellon University, for example, enable NIST to leverage its activities with the much larger, but complementary, capabilities of other organizations.

In FY2001, the Program on Materials for Magnetic Data Storage in the Materials Science and Engineering Laboratory focused on the following projects that were continued from the previous year:

- Processing of magnetic multilayers for optimal giant magnetoresistance effect (Metallurgy Division)
- Magnetic domain imaging and micromagnetic modeling of magnetic domains for understanding magnetization statics and dynamics in recording heads and magnetic media (Metallurgy Division)
- Understanding the nanotribology of magnetic hard disks through the measurement of stiction, friction, and wear at the nanometer scale (Ceramics Division)
- Measuring nanoscale magnetic interactions and structure in multilayers, nanocomposites, and low dimensional systems, needed for understanding and applying materials physics at small scales (Metallurgy Division, NIST Center for Neutron Research)
- Measuring and understanding the origin of magnetic exchange bias in conventional and advanced magnetic structures and devices (Metallurgy Division, NIST Center for Neutron Research)
- Developing a measurement system for magnetic susceptibility of small samples at high frequencies (Metallurgy Division)
- Preparing magnetic measurement standard reference materials. (Metallurgy Division)

Two new projects were initiated in FY2001:

- Processing and measuring the properties of "spintronic" systems wherein spin-dependent magnetic devices are integrated directly onto semiconductor chips (DARPA-sponsored; Metallurgy Division)
- Developing measurements of magnetic damping (NIST Nanotechnology Initiative Funding with EEEL; Metallurgy and Materials Reliability Divisions.)

Contact Information: **Robert Shull**

Nanotribology

Stephen Hsu, Richard Gates, Patrick Pei, Pu-Sen Wang, Jerry Chuang, and Daniel Fischer

The magnetic spacing on disks is becoming smaller to accommodate higher data storage density and data transfer rates. Thinner diamond-like carbon overcoats and improved lubricant monolayers are expected to provide improved protection against occasional head-disk impacts. Working with the National Storage Industry Consortium (NSIC), we address the measurement needs of the head-disk interface contacts. We also explore the fundamentals of how to achieve better protection through a novel multi-component molecular assembly for the disks in conjunction with our CRADA partner Pennzoil-Quaker State Company.

Current magnetic hard disks are protected by a one nanometer thick perfluoroalkylpolyether (PFPE) film and 7.5 nm thick carbon overcoat. In order to increase the storage density, the fly height and carbon overcoat need to be reduced to 5 nm and 3 nm respectively. At these conditions, durability of the disk is reduced by occasional collisions and impacts. Additionally, the data transfer rate needs to be increased to take advantage of the higher density. Higher data transfer rate means the linear velocity of the head flying over the disk will be increased from the current 10 m/s towards 40 m/s. This results in a higher impact force. Such impact force is very difficult to measure, therefore its consequences are difficult to ascertain. Because of these difficulties, the disk drive design is changed from the current start-stop sequence to ramp load and unload (the head is always flying over the disk and parks on a ramp outside the disk).

We have initiated a project to develop a one-pass high-speed impact test using a ruby ball colliding against an artificially created deformation ridge on a disk. A microscratch test was used to create such a ridge which should be high enough (50 nm to 100 nm) and the slope shallow enough (0.5°-2°) to control the shear stresses imposed by such a collision. Acoustic signals are monitored to quantify the impact forces and damage. Since the disk consists of many nanometer-thick layers, the strain distribution as a function of such imposed stresses is of great interest. A simple, approximate closed form formula was developed for the prediction of the critical stress as a function of the ratios of layer thicknesses, elastic properties of layers as well as the impact load. As the hard disk consists of multi-layer thin films coated on an elastic substrate, the derivation follows the bending theory of a circular plate resting on an elastic foundation. Results indicate that the critical stress is always located at the bottom of the magnetic media layer underneath the impact site, and is linearly dependent on the impact load so long as the disk remains elastic.

The current disk lubricant (a PFPE with terminal alcohol functional groups) works by diffusing into the contact area after the head passes over, thus creating a "self-repairing" property. The ability to move about also dictates that the molecules cannot be bonded chemically to the disk. Hence the resistance to shear impacts is low. To balance the shear resistance and surface mobility, the concept of multi-component monolayer organization has been explored. Using a hydrocarbon system, a solution of different molecular species was prepared and a one nanometer thick film was deposited onto the disk surface using dip coating and vapor phase deposition. Initial test results suggested that films can be organized to achieve shear resistance, wear protection, and durability. But each performance characteristic such as shear resistance demands a different molecular structure than the other characteristics. Also, if the film thickness is too large relative to the disk roughness at the atomic scale, stiction and friction are higher. This is attributable to high surface tension and meniscus force. Preferential adsorption of the polar species has been identified as an important contributor to film behavior. Ultra-soft X-ray near edge fine structure spectroscopy at the Brookhaven Synchrotron Radiation Facility has been used and has been successful in determining the relative concentration of each species and the nature of interactions between the monolayers with a disk surface. Collaboration with Wayne State University on high resolution modulated AFM provides additional insight of where the molecules are on a typical surface.

We have initiated an effort to study the chemical nature of the diamond-like carbon overcoats using nuclear magnetic resonance (NMR) and electron spin resonance (ESR). Special disk overcoats with different chemistries (CH_x, CN_x, and CH_xN_y) on glass substrates were received from our industrial partner, MMC (MaxMedia Corp.). Initial experiments suggested that sufficient NMR and ESR signals on dangling bonds in the carbon overcoats could be obtained. We will attempt to develop these techniques to obtain quantitative measure of these dangling bonds and relate them to surface reactivity between carbon coating and lubricants.

Contributors and Collaborators: Sujeet Sinha (NIST), Takuya Ohzono (NIST), Mingwu Bai (NIST), Singh Batia (IBM), Jun Zhang (DSI), G. Y. Liu (Wayne State), Frank Talke (UCSD), Selda Gunsel (Pennzoil), Jing Gui (Seagate), P. Mazumdar (NIST/ATP), Ken Johnson (MMC)

Materials for Microelectronics

Today's U.S. microelectronics and supporting infrastructure industries are in fierce international competition to design and produce new smaller, lighter, faster, more functional, and more reliable electronics products more quickly and economically than ever before.

Recognizing this trend, in 1994 the NIST Materials Science and Engineering Laboratory (MSEL) began working very closely with the U.S. semiconductor, component and packaging, and assembly industries. These early efforts led to the development of an interdivisional MSEL program committed to addressing industry's most pressing materials measurement and standards issues central to the development and utilization of advanced materials and material processes within new product technologies, as outlined within leading industry roadmaps. The vision that accompanies this program – to be the key resource within the Federal Government for materials metrology development for commercial microelectronics manufacturing – may be realized through the following objectives:

- Develop and deliver standard measurements and data;
- Develop and apply *in situ* measurements on materials and material assemblies having micrometer- and submicrometer-scale dimensions;
- Quantify and document the divergence of material properties from their bulk values as dimensions are reduced and interfaces contribute strongly to properties;
- Develop models of small, complex structures to substitute for or provide guidance for experimental measurement techniques; and
- Develop fundamental understanding of materials needed in future microelectronics.

With these objectives in mind, the program presently consists of twenty separate projects that examine and inform industry on key materials-related issues, such as: electrical, thermal, microstructural, and mechanical characteristics of polymer, ceramic, and metal thin films; solders, solderability and solder joint design; photoresists, interfaces, adhesion and structural behavior; electrodeposition, electromigration and stress voiding; and the characterization of next generation interlevel and gate dielectrics. These projects are conducted in concert with partners from industrial consortia, individual companies, academia, and other government agencies. The program is strongly coupled with other microelectronics programs within government and industry, including the National Semiconductor Metrology Program (NSMP) at NIST.

FY2001 Projects (and division leading project)
Lithography/Front End Processing
Characterization of Ultrathin Dielectric Films (Ceramics)
Lithographic Polymers (Polymers)

On-chip Interconnects
Interconnect Materials and Reliability Metrology (Materials Reliability)
Measurements and Modeling of Electrodeposited Interconnects (Metallurgy)
Thin Film Metrology for Low K Dielectrics (Polymers)

Packaging and Assembly
Packaging Reliability (Materials Reliability)
Solder Interconnect Design (Metallurgy)
Solders and Solderability Measurements for Microelectronics (Metallurgy)
Tin Whisker Mechanisms (Metallurgy)
Wafer Level Underfill Experiment and Modeling (Metallurgy)
Wire Bonding to Cu/Low-k Semiconductor Devices (Metallurgy)
X-ray Studies of Electronic Materials (Materials Reliability)

Crosscutting Measurements
Dielectric Constant and Loss in Thin Films and Composites (Polymers)
Electron Beam Moiré (Materials Reliability)
Ferroelectric Domain Stability Measurements (Ceramics)
Measurement of In-Plane CTE and Modulus of Polymer Thin Films (Polymers)
Mechanical Properties of Thin Films (Ceramics)
Permittivity of Polymer Films in the Microwave Range (Polymers)
Polymer Thin Films and Interfaces (Polymers)
Texture Measurements in Thin Film Electronic Materials (Ceramics)
Thermal Conductivity of Microelectronic Structures (Materials Reliability)

Contact Information: **Frank Gayle**

Characterization of Ultra-thin Dielectric Oxide Films

Debra L. Kaiser, Charles E. Bouldin,
Igor Levin, and Mark D. Vaudin

The International Technology Roadmap for Semiconductors projects that traditional silicon dioxide gate stacks will need to be replaced by higher dielectric constant materials by the year 2005 to meet the industry's device scaling goals. As a result there has been intensive research on alternative gate dielectric materials. We have studied crystallization and homogeneity in ultra-thin films of two potential materials, zirconium oxide and zirconium silicate, both deposited by spin coating.

Two of the key materials issues in the development of alternate gate dielectric layers with comparable electrical performance to silicon dioxide are crystallinity and homogeneity. In this work, we have used extended x-ray absorption fine structure (EXAFS), high resolution transmission electron microscopy (HRTEM), energy dispersive x-ray spectrometry (EDS) and glancing angle x-ray diffraction (XRD) to study crystallization behavior and homogeneity in ultra-thin (<5 nm) zirconia (ZrO_2) and zirconium silicate films.

ZrO_2 films were deposited by spin-coating solutions containing zirconium acetate, propylene glycol, isopropanol and glacial acetic acid onto (100) Si wafers. The films were dried at 200 °C; and annealed in air for 30 min at 400 °C to 800 °C. Solution compositions and spin conditions were selected to give films with a thickness of about 5 nm as determined by HRTEM. Glancing angle XRD measurements revealed the presence of cubic ZrO_2 in films heated above 500 °C; below 400 °C the films were amorphous. These results were confirmed by HRTEM examination of films annealed at 400 °C (amorphous) and 500 °C (<111> oriented ZrO_2).

EXAFS measurements were performed on the series of films to probe the local structural evolution as a function of annealing temperature (Fig. 1). The first shell Zr-O peak remains relatively unchanged in the series, indicating that the Zr atoms have the full 8 nearest neighbor oxygen coordination in all of the films. The evolution of the second shell Zr-Zr peak with increasing temperature shows a sharpening of the Zr-O-Zr bridging bond angle indicated in the inset. This bond angle has a disorder of 3° to 5° in the 200 °C film, and decreases with increasing temperature, approaching the thermal disorder of the crystal in the 800 °C film. Both the first and the second shell peaks appear to be doublets, suggesting the formation of two Zr-O phases with similar structures but different lattice parameters.

Zirconium silicate films were fabricated by spin coating solutions of tetraethoxysilicon, zirconium acetate or nitrate, propylene glycol and isopropanol onto (100) Si wafers. Heat treatment to 1000 °C resulted in the crystallization of ZrO_2, but not zircon ($ZrSiO_4$) as determined by XRD. HRTEM studies on a film heated to 700 °C for 1 h in air showed an amorphous structure with non-uniform contrast that can be attributed to a compositional heterogeneity (Fig. 2).

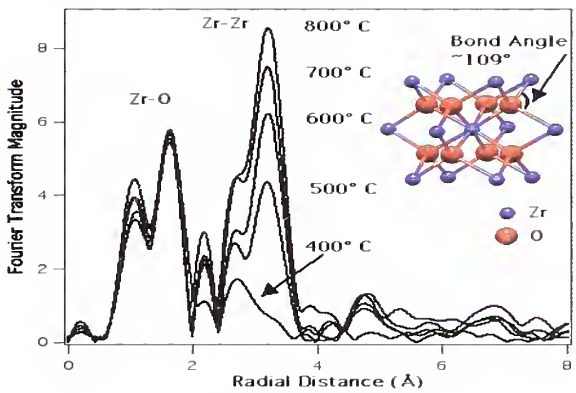

Figure 1: Radial distribution function of 5 nm ZrO_2 films annealed at temperatures indicated

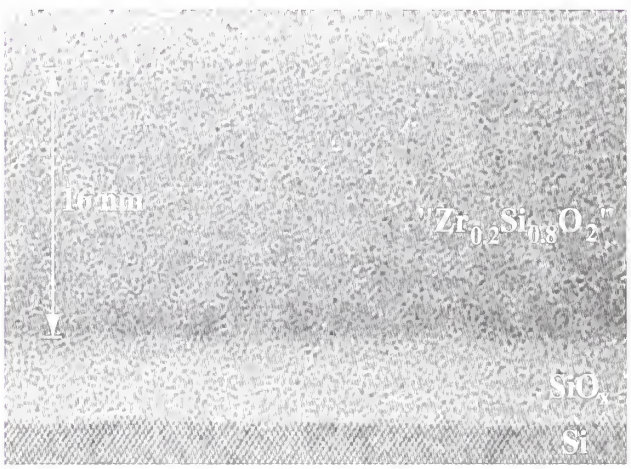

Figure 2: HRTEM image of amorphous zirconium silicate with nominal composition $Zr_{0.2}Si_{0.8}O_2$; the actual composition measured by EDS is close to $Zr_{0.5}Si_{0.5}O_2$.

Contributors and Collaborators: Joseph Ritter and Joseph Woicik, Ceramics Division, MSEL; Eric Vogel, Electronics and Electrical Engineering Laboratory, NIST

Domain Stability in Ferroelectric Thin Films

Grady S. White and John E. Blendell

Ferroelectric thin films have the potential for making major impacts in applications as diverse as non-volatile RAM, uncooled detectors, and MEMs. The material properties required for these applications, switchable electric dipoles, large pyroelectric coefficients, and piezoelectric response, are all controlled by the domain stability in the films. The relationship between microstructure and the physics of domain stability is being modeled and is being compared to real time nanometer scale measurements of the domain behavior.

We are measuring domain stability in $Pb(Zr,Ti)O_3$ (PZT) thin films as a function of film microstructure and electric history. Although domain stability issues, i.e. pinning, aging, fatigue and retention, limit the use of ferroelectric films in nonvolatile memory and micro-actuator applications, the physics and materials science that affect them are not understood. We have demonstrated that domain pinning in a PZT film appears to be associated with specific grain boundary sites. These sites can occur at different locations along the grain boundary. We are examining these sites to ascertain what features of the grain boundary control pinning. Modeling of the stresses which may effect pinning are being carried out using an object oriented finite element technique (OOF) developed at NIST.

In the measurements, an applied AC electric field (»1 MV/m) changes the shape of the grains in the ferroelectric film due to piezoelectric response. Both normal and lateral changes are observed by atomic force microscopy, Figure 1, allowing a more complete determination of the orientation of the polarization of individual grains. The spatial resolution is limited to »20 nm due to the contact area of the tip and spreading of the electric field.

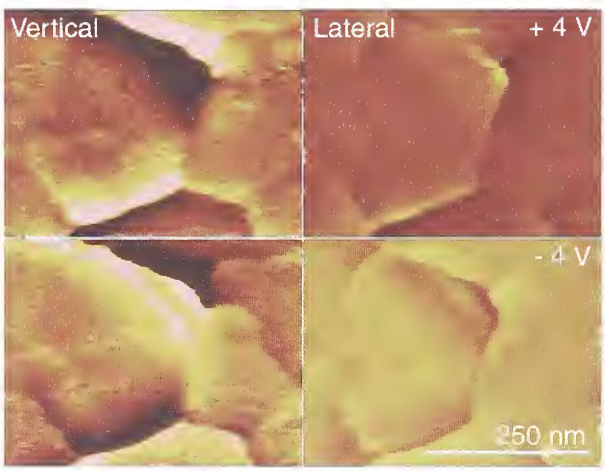

Figure 1 Piezoresponse microscopy shows contrast reversal with changes in the DC bias field applied. The contrast reversal in both the lateral and normal response demonstrates that 180° switching of domains has occurred rather than 90° switching.

A two-dimensional finite element code was used to model the stresses associated with grain misorientations in plane strain mode, Figure 2. Only stresses resulting from mechanical constraints were considered; electric field effects were not included in these calculations. All the grains were assumed to be aligned with <111> normal to the film surface and with different orientations of <001>. Stresses were generated by converting the grains from cubic to tetragonal symmetry; the c/a ratio in the tetragonal grains was set at 1.02, similar to a bulk hard PZT.

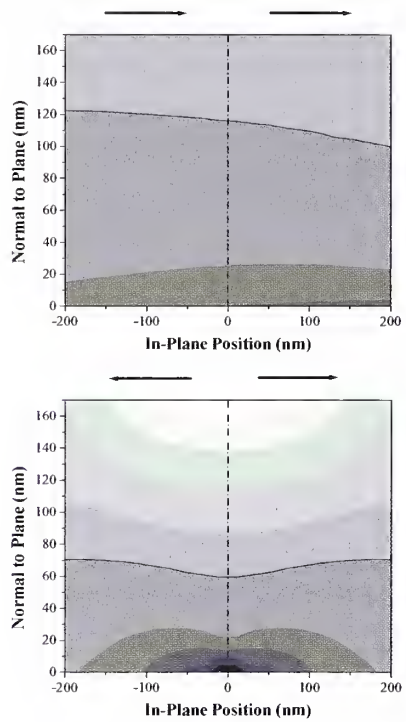

Figure 2 Stress maps of the calculated normal stress for different grain boundary misorientations. The arrows show the projection of the polarization vector on the top surface of the film. When the polarization vectors are aligned, the stresses through the film are minimal and for a 180 °C; misalignment, high stress (0.5 GPa) are found at the grain boundary.

Contributors and Collaborators:

Edwin R. Fuller, Jr., Ceramics Division, MSEL

Evan Pickett, (Penn State University)

Yong-Eui Lee (Seoul National University)

Mechanical Properties of Thin Films

Douglas T. Smith

The use of thin films in a wide range of applications has grown dramatically in recent years. In applications such as wear or scratch resistant films for cutting tool or optical systems, it is clear that a knowledge of film mechanical properties is essential for design. In other applications, materials may be chosen primarily for their electronic or optical properties, but some knowledge of their mechanical properties is often needed. We work on the development and standardization of test methods to obtain elastic, plastic and adhesion properties for thin films.

Thin films, and multilayer thin film structures, are a critical part of many electronic and optoelectronic devices. They also are often used, in thicknesses anywhere from a few nanometers to micrometers, to provide wear resistance for surfaces as diverse as magnetic storage media and cutting tools. In some of these applications, knowledge of the mechanical properties of the film is essential to the design. However, even in applications where thin film materials are chosen on the basis of other properties, such as electronic, magnetic or optical performance, knowledge of the mechanical properties of each film or layer can be very important. One example of such a situation would be the need to know the elastic properties of each layer in a multilayer electronic component in order to analyze the stresses that would develop in the system in thermal cycling. Because the structure of a thin film is often significantly different from a bulk specimen of the same material, in general it is not safe to assign bulk values to a film. In some cases, a particular material can be created only in thin-film form; no bulk specimens of that material exist for testing. In response to these needs, a number of techniques have been developed to measure mechanical properties of very small volumes of material, or of a thin film. For measuring both elastic and plastic deformation properties, the most commonly used method is Instrumented Indentation Testing (IIT), also referred to as Nanoindentation when used at low forces. In addition, Surface Acoustic Wave (SAW) techniques are being pushed to higher frequencies (> 100 MHz), allowing elastic properties to be determined for thinner films (< 1 μm). Finally, a wide range of adhesion tests have been developed to measure the strength of the film/substrate interface. Commercial machines are available to perform each of these test methods. The problem with many of these tests, however, is that because they are relatively new, often no standard test methods exist for their use. This situation is particularly acute for IIT, where there are more than 1000 commercial test machines in daily use around the world characterizing materials, but there is no U.S. or international standard test method available. As a result, properties obtained from instrumented indentation testing cannot be used in product specifications, and a reliable determination of the accuracy of a test result typically is not made. In this Project, we are actively involved in national and international efforts to develop standard test methods for IIT, and to compare the results of IIT tests to those obtained by other methods (such as SAW measurements made at NIST Boulder and BAM). A major effort in this area is underway within the Versailles Project on Advanced Materials and Standards (VAMAS) Technical Working Area 22 (TWA 22). A large international round robin IIT test of thin film specimens was organized and carried out with substantial NIST involvement to compare the results from different machines and different analysis methods. A report on the project is nearly complete. A second project is underway in TWA 22 to compare the results of several adhesion tests (scratch, bend and indentation) on several thin film systems, and a third is proposed in the area of stress measurements for thin films. In addition, NIST and BAM in Germany have a joint program in progress to develop standard or certified reference film systems for mechanical test methods. We are also active in efforts to develop an American Society for Testing and Materials (ASTM) standard for IIT, in Task Group E28.06.11. This effort began three years ago, and a draft of an ASTM document "Standard Practice for Instrumented Indentation Testing" has been prepared for sub-committee ballot

Contributors and Collaborators:

Stuart Saunders and Nigel Jennett, National Physical Laboratory (NPL), U.K.; Uwe Beck, Bundesanstalt für Materialforschung und –prüfung (BAM), Germany; Toyonobu Yoshida, University of Tokyo, Japan; Takahito Ohmura, National Institute for Materials Science (NIMS), Japan; Donna Hurley, Materials Reliability Division, MSEL, NIST; ASTM Task Group E28.06.11 for instrumented indentation

Materials for Wireless Communication

Today, wireless technologies constitute one of the most important growth areas in the global electronics industry. The current revolution in wireless communications would not have been possible without the discovery and development of oxide ceramics exhibiting the coincidence of high, temperature-independent resonant frequency with low dielectric loss. Technically important ceramic materials fall into two major dielectric categories: bulk ceramics for base station resonators/filter and those needed for low-power, miniaturized hand-held devices. Paramount in achieving smaller and lower cost devices are guidelines that facilitate the rational design of advanced materials to provide temperature stability, frequency, and size-reduction requirements for the next generation of devices for cellular, PCS, and many other niches of the wireless communications industry.

A collaboration between the Ceramics Division and the Electrical and Electronics Engineering Laboratory at NIST on ceramic materials for base station applications includes experimental determination of selected complex-oxide phase diagrams integrated with in-depth structural (x-rays, electrons, neutrons), crystal-chemical, spectroscopic, and dielectric property characterization. The objective of this multidisciplinary project is to determine the fundamental relationships between phase chemistry, crystal structure, and dielectric performance at wireless frequencies.

Another project in the Ceramics Division uses first-principles calculations to elucidate the roles of cation order-disorder and ferroelastic phenomena in determining the phase relations and physical properties of complex ceramic oxide systems. These calculations are used to predict cation ordering phenomena, physical properties, and how they vary with chemical composition. Critical experiments are performed to test the predictions.

Microstructural modeling and experimental studies are also underway to determine the dimensional changes in low-temperature-cofired ceramics used for portable communication devices. Processing models were identified by a large segment of industrial producers as being crucial to reducing the time currently needed to design and produce components. Wireless devices, often hand-held, are especially susceptible to mechanical damage; assuring the reliability of electronic products is especially critical for such devices. Work in the Materials Reliability Division includes development of noncontact acoustic metrology to characterize wireless materials in both thin-film and bulk form. Also, the mechanical properties of thin films are investigated using laser-ultrasonic methods to generate and detect surface acoustic waves. The elastic property information obtained will result in improved predictive modeling of film performance. In addition, resonant-ultrasonic techniques are applied to new piezoelectric materials for SAW devices, used extensively as oscillators in hand-held devices.

Researchers in the Polymers Division developed a new test method that permits dielectric measurements of film substrates at frequencies of 1 GHz to10 GHz. The project is exploring the relationships between dielectric properties and structure in a variety of polymer resins, blends and composites, e.g., hybrid materials based on polymer resins and ferroelectric ceramics. Microstructural modeling and experimental studies are being undertaken to determine the effect of polarizability of the polymer matrix on the apparent dielectric permittivity of the composite. A need for models and measurement techniques has been identified by a large segment of industrial producers as being crucial in new designs and reducing the development time of new products. A consortium involving the National Center for Manufacturing Science and industry has been organized to help address these issues.

Contact Information: **Terrell Vanderah**

First-Principles Studies of Electronic Oxides

Benjamin P. Burton and Eric Cockayne

Ceramic compounds with exploitable ferroelectric, dielectric, or magnetic properties are widely used in technical applications such as actuators, transducers, and dielectric resonators. We are using first-principles (FP) calculations to elucidate the roles of cation order-disorder and ferroelastic phenomena in dictating the phase relations and physical properties of these technologically important materials.

Ferroelectric, dielectric, magnetic, and transport properties of ceramics are typically sensitive functions of the state of cation order. Therefore, First-Principles Phase Diagram (FPPD) calculations are used to predict cation ordering phenomena and physical properties, and how they vary with chemical composition. Critical experiments are performed to test the predictions. An additional technical objective is to benchmark various FP techniques that are used for calculating physical properties (e.g. dielectric constant), and the formation energies on which FPPD calculations are based.

The intended outcome is to predict ordering behavior in complex technologically important oxide systems, with the objectives of (1) minimizing the experimental work necessary to elucidate phase relations; (2) optimizing theoretical techniques; (3) optimizing processing strategies; (4) predicting the existence of new, technologically relevant ordered phases; (5) predicting how physical properties vary as functions of composition, temperature, and heat treatment.

The inclusion of degrees of freedom, derived from ionic motion, in the first-principles models will facilitate simulation and physical understanding of important properties. For example, the ferroelastic transitions in PZT, experimentally associated with large piezoelectricity, can be simulated as a function of temperature, composition and stress. Molecular dynamics methods, with time-varying external fields, can be used to model the dielectric properties as a function of frequency in systems of interest for microwave applications, such as $CaTiO_3$-$CaAl_{1/2}Nb_{1/2}O_3$. We have addressed several issues important to the processing and applications of electronic ceramics and accomplished several advances in the modeling of these materials.

A first-principles-based model of cation ordering in $[Na_{1/2}Bi_{1/2}]TiO_3$ has been formulated, and the ground-state ordered structure predicted. As observed experimentally, the predicted pseudocubic structure has a primitive cell with doubled cell constants in all three (x, y and z) Cartesian directions, but it has a different cation ordering configuration than the expected NaCl-related type. This is a particularly interesting result because much of the literature on $[Na_{1/2}Bi_{1/2}]TiO_3$ reports (erroneously) that NaCl-type ordering was observed. Our first-principles calculations, however, indicate that many other cation ordering configurations have lower energy than the NaCl-type.

We developed an effective Hamiltonian for the relaxor ferroelectric $PbSc_{1/2}Nb_{1/2}O_3$ (PSN), based on first-principles calculations. The model allows one to simulate the structure and dielectric properties of of PSN as a function of cation ordering, temperature, applied fields, etc. We compared the temperature dependent properties of PSN in an ordered NaCl-type Sc/Nb cation configuration with those of PSN in a random configuration, and found a significantly (35 %) lower ferroelectric transition temperature in the random state.

A working group has been formed to develop a Unified Effective Hamiltonian theory for modeling systems that exhibit both cation order-disorder and ferroelastic transitions. The first workshop was held June 2000 at NIST. The second, co-organized by B.P. Burton, will be combined with an alloy theory workshop on "Thermodynamic and Structural Properties Of Materials," and will be held in Avignon, France September 9-14, 2001. This important workshop will bring together scientists working on first-principles calculations for alloys with those carrying out analogous research on ferroelectrics and minerals.

Contributors and Collaborators: I. Levin and T.A. Vanderah (Ceramics Division), G. Ceder and A. Van der Ven (MIT), A. Van de Walle (Northwestern U.), L. Bellaiche (U. Arkansas), V. Zelezny and J. Petzelt (Czech Academy of Sciences), U. Waghmare (JNCASR, Bangalore, India)

Phase Equilibria and Structure-Property Relationships

TerrellA. Vanderah and Igor Levin

Every modern commercial wireless communication system incorporates dielectric oxide ceramics with unique electrical properties as critical elements. The commercial competitiveness of next-generation devices depends on new ceramics with improved properties and/or reduced processing costs. Experimental phase equilibria determination integrated with systematic chemistry-structure-property studies contribute to the fundamental understanding of these ceramics. In addition, the existence of potentially useful phases and phase assemblages in selected oxide systems is revealed.

Dielectric oxide ceramics with unique electrical properties are used to fabricate a variety of components in cellular communications circuits that store, filter, and/or transfer electromagnetic energy with minimal loss (e.g., resonators, bandpass filters, circulators). The required properties for these ceramics include high dielectric constant (E_r), minimal dielectric loss (or high Q, quality factor), and essentially zero temperature dependence of resonant frequency (t_f). Knowledge of the materials science underpinning the appearance of these useful properties does not exist, hence all ceramic systems currently in use were empirically "discovered" and developed. Fundamental understanding of the chemical and structural basis of dielectric performance at wireless frequencies is needed to reduce the processing costs of existing ceramics, and to improve the design and discovery of next-generation materials needed for higher-frequency and higher-power applications.

This research activity includes experimental studies of phase equilibria and chemistry-structure-property relations of complex oxide systems containing one or more components or compounds that exhibit potentially useful dielectric properties. Systems are selected for study on the basis of empirical knowledge, results from integrated computational-experimental studies, and information from industry regarding next-generation needs. In addition to revealing the existence of new, possibly useful materials, knowledge of phase equilibria relations is important because all commercial ceramic components are processed as controlled mixtures to tune dielectric constants and to achieve temperature compensation; i.e., near-zero t_f values. The technical work is multi-disciplinary and includes synthesis and crystal growth; experimental determination of phase relations; structural analysis by X-ray, electron, and neutron diffraction; characterization (via collaborative efforts) of dielectric properties at wireless frequencies; and measurement of vibrational spectra.

Recent studies include analysis of phase transitions and microwave dielectric properties in the perovskite-related $(1\text{-}x)CaAl_{0.5}Nb_{0.5}O_3$–$xCaTiO_3$ system using X-ray and neutron powder diffraction, transmission electronmicroscopy, Raman spectroscopy, and dielectric measurements at microwave frequencies (2 GHz to 8 GHz).

This system is of practical interest since it contains a temperature-stable ($t_f = 0$) compound at $x \sim 0.5$ with a permittivity of 50 and good dielectric loss. Furthermore, it serves as an important model for the study of structure-property relations since the end-members display very different dielectric properties ($CaAl_{0.5}Nb_{0.5}O_3$: E_r=27, t_f= -88 x 10^{-6} /°C; $CaTiO_3$: E_r=170, t_f= +800 x 10^{-6} /°C), despite having nearly identical crystal structures. Rietveld structural refinements confirmed that both end-compounds exhibit similar octahedral tilted frameworks. In $CaAl_{0.5}Nb_{0.5}O_3$, the tilting is superimposed onto NaCl-type ordering of Al and Nb on the B-sites. The $(1\text{-}x)Ca(Al_{0.5}Nb_{0.5})O_3$–$xCaTiO_3$ system therefore features both cation ordering and octahedral tilting phase transitions, both of which are known to affect dielectric behavior. The temperature of the order/disorder transition decreased rapidly with increasing Ti-content, which correlated with a progressive increase of cation disorder in the specimens; a disordered structure is attained at the $x = 0.5$ temperature-stable composition. For the "solid solutions", the non-linear dependence of both E_r and t_f on Ti-content corresponded to a linear dependence of the macroscopic polarizability on composition; that is, the oxide additivity rule was closely obeyed. Therefore, this rule can be used to predict E_r and t_f for any intermediate composition from the permittivities and temperature coefficients of the end compounds.

Contributors and Collaborators: R.S. Roth, E. Cockayne, B.P. Burton, W. Wong-Ng, L. Bendersky, D. Minor, MSEL; J.E. Maslar, CSTL; R.G. Geyer, EEEL; V. Miller, Rider University; T. Lindsey, Appalachian State University; R. Coutts, Univ. Maryland; T. Negas and S.Bell, TRAK Ceramics, Inc.

Sintering Behavior of Low Temperature Co-fired Ceramics

John E. Blendell, Jay S. Wallace,
Mark R. Locatelli and Bernard J. Hockey

Low temperature co-fired ceramics (LTCC) are rapidly becoming the technology of choice for RF components and modules for portable wireless applications. LTCC has demonstrated that it can enable the high density integrated packages meeting the requirements for portable wireless. Commercialization of these ceramics requires the accurate prediction of dimensional changes during sintering in order to design passive integrated components (resistors, capacitors and inductors) in the LTCC module.

Low temperature co-fired ceramics (LTCC) are finding increasing use in portable wireless applications due to their high dielectric constant, low loss and high Q. These features allow a reduction in the size of modules used in high frequency applications. In addition, LTCC can have integrated passive components, are environmentally robust and can be rapidly produced. This leads to a significant cost advantage for LTCC modules. Because dimensional tolerances are critical, accurate predictive models of dimensional changes during sintering are necessary for the commercialization of LTCC modules.

We have constructed a hot-stage optical microscope for direct examination of the surface of the LTCC tapes during sintering. By measuring both the overall shrinkage and the local variations in sintering near vias and interconnects the effect of inhomogeneities in the system can be determined. The system will be able to locate markers placed on the surface and follow the trajectory of these markers during the sintering process as shown in Figure 1. The effects of different processing parameters such as lamination pressure, texture, heating rate and peak sintering temperature can be measured. In addition, by measuring local shrinkage the effect of interactions of the inks used to form interconnects and integrated passive components can also be determined.

Modeling of evolution of the microstructure and dimensional changes during sintering will be carried out using a combination of phase field methods with object-oriented finite element analysis. This should allow for more accurate modeling of sintering processes with arbitrary boundary conditions. The finite element models will be used to solve for the stress state of the powder compact and these stress profiles will be used in the phase field model to more accurately predict mass flow and microstructural evolution during firing.

TEM investigations of sintered tapes have been used to investigate the reactions of the glass and the Al_2O_3 grains in the LTCC. At the low temperatures used in these systems there is minimal reaction as shown in Figure 2. However, the reactions between the integrated passive components and the glass are expected to be significant.

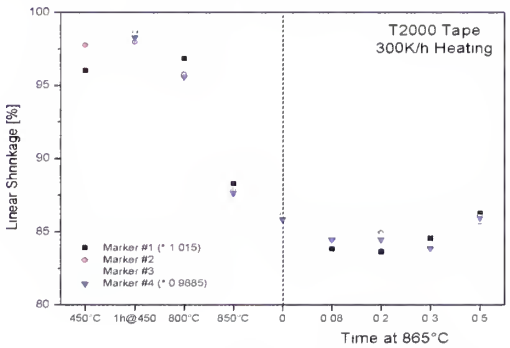

Figure 1: Shrinkage of individual markers on the surface of LTCC tape during heating and isothermal hold at 865 °C. The majority of the shrinkage occurs during heating.

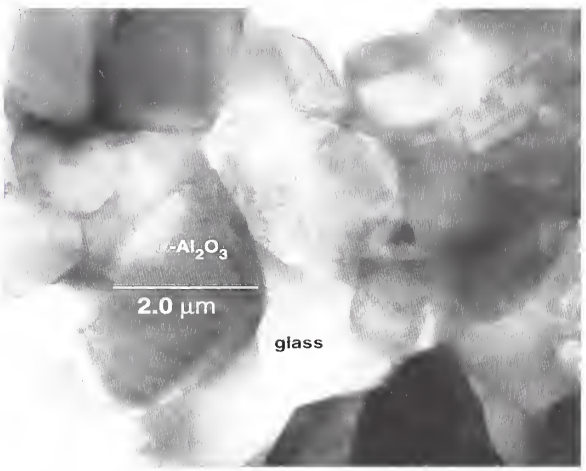

Figure 2: TEM micrograph of LTCC production device consisting of alpha-Al_2O_3 particles with sizes ranging up to » 5 µm contained within a continuous glass phase. For this particular device, the glass phase was found to be a calcium-aluminum-silicate, containing various concentrations of Pb, Ti, Na and K.

Contributors and Collaborators: Brent Smith, Hereaus Inc.; David Wilcox, Motorola Corp.; Daniel Amey, Dupont Co.; Michael Ehlert, National Semiconductor Corp.; Don Brown, IWPC

Powder Measurements

Powders are the precursors for well over 80 % ceramic manufacturing processes. Accurate and reliable measurements of the physical and chemical properties of ceramic powders are critical to ensuring processes and products of high quality, minimal defects, and consequent economic benefits. The primary objective of this program is to provide measurement techniques, standards, fundamental science, and predictive models needed for economical and globally competitive manufacturing of ceramic products. Fundamental understanding, test methods, data, and other results generated from this program are also of value to industries such as powder metallurgy, pharmaceutical, food processing, construction, and cosmetics.

Accurate particle size and size distribution determination of ceramic powders is an area of particular interest in this program. In view of the increasing consumption and projected use of sub-micrometer and nano-sized powders a new task focused on this particle size range was initiated this year. Conventional methods of sample preparation and size measurement often cannot be used for accurate analysis in this size range due to physical limitations of commonly used instruments or the basis of the measurement technique. The need for new methods of sample handling, preparation, and protocols for measurement is addressed.

In ceramic manufacturing, powder is frequently dispersed into a fluid vehicle for shape forming and other unit operations that require deagglomeration of the constituent particulate matter. Large interfacial areas that exert a dominant influence on the dispersion properties characterize sub-micrometer powders. These highly loaded suspensions require strict control of interfacial properties in order to obtain homogeneous and well-dispersed systems. The chemical and physical characteristics of powders dispersed in liquids are evaluated to understand the influence of surface charge, dissolution, precipitation, adsorption, and other physicochemical processes on the dispersion behavior. Significant challenges lie in measuring the properties of suspensions at the high solids concentrations typically used in industrial applications. Tools are being developed to measure and model the interaction and flow of complex multicomponent fluids at high concentrations.

A major area of emphasis in this program is the development of standard reference materials for use as primary calibration standards and national/international standards for particle size and size distribution, pore volume, and particle dispersion measurements. These projects involve extensive collaborations with industrial partners, measurement laboratories, and academic institutions in the U.S., Europe, and Asia.

Contact Information: **Said Jahanmir**

Particle Dispersion Measurements

Vincent A. Hackley and Lin-Sien Lum

The manufacture of ceramics with ultrafine microstructures and enhanced performance requires starting materials that are extremely small in scale. To handle such fine particulates, complex mixtures (dispersions) are formed that include ceramic particles, chemical additives and electrolytes in a liquid medium. We provide methods, standards and data relating to dispersion measurements. Our mission is to enable industry to develop reliable, robust dispersion-based manufacturing processes for advanced materials. Our focus is on colloidal and nanosize materials for the electronics industry.

The objective of this project is to develop the necessary knowledge and measurement tools to enable manufacturers and users of ceramic suspension technology to control their processes in a reliable and cost-effective manner. Our work focuses on non-dilute colloidal and nanoparticulate systems, where interfacial forces play a dominant role in dispersion properties. We measure particle size distribution, electrokinetics, surface charge, viscosity, yield stress, adsorption of additives, and suspension structure.

A cooperative research effort between NIST and standards development laboratories in Germany and Japan continues to provide improvements in methodology for dispersion measurements in concentrated ceramic suspensions. The objective of these joint studies is to establish international standards for dispersion measurements in cooperation with the Versailles Advanced Materials Project (VAMAS) Technical Working Area 27. To date, we have developed and successfully implemented a draft method for the determination of the isoelectric point (IEP) in moderately concentrated ceramic dispersions using colloid vibration current (CVI), electrokinetic sonic amplitude (ESA) and particle charge detection (PCD) techniques. The IEP is a key powder parameter describing the acid-base properties of the material.

In addition to methods development, we have examined the overall precision and reproducibility of IEP measurements (see Figure 1) and have developed a large database that includes the results of a systematic investigation of the underlying factors influencing the electroacoustic measurement of IEP. For instance, it was determined that sample mixing and pH measurement are critical sources of error for IEP determination in non-dilute systems. In particular, poor mixing can result in accretion of material on the sensor surface, which in turn produces large hysteresis effects and artificial IEP values. Lesser effects were noted for factors relating to sample preparation and solids concentration. We are currently compiling guidelines for the implementation of CVI, ESA and PCD techniques.

We are developing new methodologies to extract relevant acoustic and electroacoustic signatures from complex concentrated dispersions. We have successfully used these

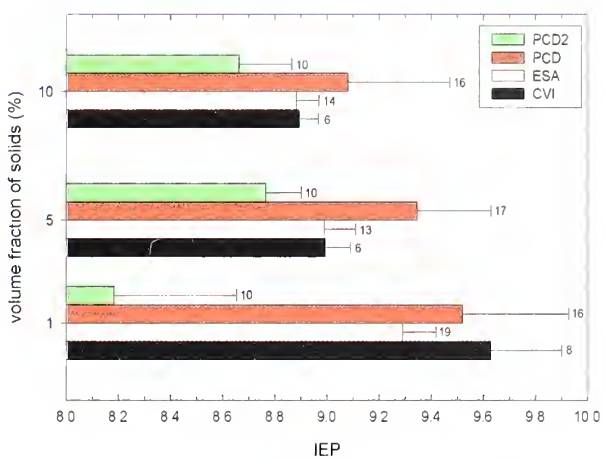

Figure 1: Variation of IEP as a function of solids loading and technique. Data was derived from one hundred and forty five titrations performed in Germany, Japan, and at NIST.

methods to monitor the physical and chemical changes occurring during hydration of tricalcium silicate at up to 30 % solids. We are currently applying these methods to the characterization of chemical-mechanical polishing slurries.

We are developing a series of special publications on the use of technical nomenclature and data relating to dispersed systems. The second of these guides, NIST Special Publication 946, focusing on rheological measurements, was published in January and distributed to over fifty industrial and academic organizations. SP945 and SP946 were selected to form the basis for a new *NIST Recommended Practice Guide*.

A NIST/industry consortium was initiated this year as a cooperative effort between BFRL, ITL, MSEL and six industry partners to develop a Virtual Cement and Concrete Testing Laboratory (VCCTL). The Dispersion Measurements project is developing particle characterization methods and providing data for the cooperative effort to further the state-of-the-art in computational materials science of cement-based materials.

Contributors and Collaborators: Chiara Ferraris (Building Materials Division), Ming Tung (Polymers Division), Makio Naito & Hiroya Abe (Japan Fine Ceramics Center), Rolf Wäsche (Federal Institute for Materials Research and Testing, Germany), Hemant Pendse (University of Maine), Ungyu Paik (Hanyang University, S. Korea)

Powder Characterization

James Kelly, Dennis Minor and
Ajit Jillavenkatesa

Standard reference materials (SRMs) and standardized techniques for measurement of particle size, size distribution and porosity are critical to the ceramics community for reliable, cost-effective manufacturing. This program has led to the development of such materials and systems and is establishing the groundwork for new efforts in the emerging area of submicrometer and nanosized powders.

This project focuses on issues associated with reliable measurements of physical properties of ceramic powders. The properties of interest include, but are not limited to, particle size and size distribution, specific surface area and porosity. Inadequate characterization and control of these characteristics during manufacturing can lead to undesirable properties, high rejection rates and consequent economic losses.

A cooperative program for joint certification of a primary reference material was initiated with the Federal Institute for Materials Research and Testing (BAM), in Germany. This program will result in a jointly certified SRM/CRM for pore size distribution by Hg intrusion porosimetry to be issued by both NIST and the BAM. Participating laboratories both in the United States and Europe have completed the analysis of a test material using mercury porosimetry and submitted their results for analysis to NIST and BAM. Work conducted during this year has progressed to the completion of the pre-qualification testing program. Completion of the certification testing phase of this project is expected in late October 2001 and final certification by June 2002.

A new project was initiated to develop suitable techniques for reliable and reproducible dispersion and size analysis of submicrometer and nanosized ceramic powders. The emphasis for this new area of investigation arises due to the significant interest and increasing applications of ceramic powders in this size range. Initial work included identification of a suitable powder system satisfying size distribution and shape requirements. It was determined that very few ceramic powders with uniform shapes and narrow size distribution are available in the 200 nm to 500 nm size range. Attempting to reduce larger particles to this size range leads to significant broadening of the size distribution, while attempting to nucleate and grow particles is extremely time consuming, expensive and typically results in very small yields. Some candidate materials have been identified and are currently being examined for ease of dispersion and stability in that state. Dispersion stability is being achieved both by addition of dispersion agents and pH control. Investigations have focussed on the types of dispersing agent used, the concentration, and the efficacy of pH control to maintain long-term stability.

Size and size distribution measurements are being conducted by x-ray centrifugal sedimentation techniques and by laser light scattering techniques. The influence of instrumental parameters in x-ray centrifugal sedimentation, such as sample volume and disc speed, have been studied and optimal values for different powder systems have been identified. Sample preparation methodologies have been developed and are being tested. Size and size distribution results obtained by these techniques will be complemented and verified using scanning electron and field-emission microscopy. The ground work for a NIST-sponsored workshop on issues pertaining to standards and characterization of submicrometer and nanosized powders has been laid. This workshop will be held in October 2001, and will focus on assessing the existing state of technology for physical property measurement of submicrometer and nanosized powders. The strengths and limitations of this technology will be evaluated. Recommendations for new measurement standards, reference materials and techniques for property characterization will be made.

During the past year, developmental work on various SRMs was completed. SRM 1897 is a new material for the calibration of nitrogen BET Specific Surface Area (SSA) instruments using the volumetric method. This effort includes work done at NIST and a round robin testing program that included eight industrial, academic and commercial laboratories within the United States. This SRM will replace the former RM 8572. SRM 1918 is a new reference material being developed for the calibration of instruments used for mercury porosimetry, operating at pressures up to 412 MPa. This SRM will be certified initially for pore volume and mean pore diameter. The development of SRM 1003c comprised of glass beads was completed and awaits certification. This material will be certified for particle size and size distribution over a size range of 20 μm to 50 μm. Size and size distribution was measured using laser light scattering and an instrument based on the electro-zone sensing principle, and scanning electron microscopy. Development of a complimentary SRM comprised of glass beads to be certified over the 1 μm to 20 μm range is currently underway.

Contributors and Collaborators: P. Klobes, Federal Institute for Materials Research and Testing (BAM), Berlin. C. Kreller, U. of Maryland-Baltimore County. Collaborations with 40 material characterization laboratories in industry, government and academia through participation in round-robin testing for powder property characterization.

X-Ray Characterization

The X-ray Characterization Program at NIST/MSEL is based on the development and application of advanced microstructural characterization tools and techniques. This includes the development and operation of experimental stations at the National Synchrotron Light Source (NSLS) at Brookhaven National Laboratory, and at the Advanced Photon Source (APS) at Argonne National Laboratory. It also includes the development and operation of unique laboratory x-ray facilities.

Synchrotron radiation sources provide intense beams of x-rays enabling leading-edge research in a broad range of scientific disciplines. At the NSLS, NIST operates one experimental station independently, and two others in partnership with Dow, Brookhaven National Laboratory, and with the NIST/Chemical Science and Technology Laboratory. At the APS, NIST is a partner with the University of Illinois at Urbana/Champaign, Oak Ridge National Laboratory, and UOP, in a collaboration called UNICAT (University Collaborative Access Team). At the NSLS and the APS, NIST scientists, and researchers from industry, universities, and other government laboratories, perform a variety of state-of-the-art measurements on a wide range of advanced materials. Studies currently underway include: the microstructure of ceramic coatings; the evolution of defect structures during the deformation of metals, ceramics, and polymers; the evaluation of crystalline perfection in single-crystal proteins, semiconductors, and ceramics; and the atomic-scale and the molecular-scale structures at surfaces and interfaces in polymeric, catalytic, and metal/semiconductor systems.

The experimental stations at the NSLS offer both hard and soft x-ray absorption spectroscopy as well as standing wave and diffraction anomalous fine structure (DAFS) capabilities. The first UNICAT beam line became operational November 1, 2000; a second beam line is currently being commissioned; and a third is under construction. These facilities incorporate the newest technology, enabling NIST scientists to improve significantly our capabilities in ultra-small-angle x-ray scattering, x-ray topography and x-ray absorption fine structure. They also offer opportunities for cutting-edge experiments in structural crystallography, time-resolved structural scattering, surface / interface scattering, diffuse scattering, and magnetic scattering. NIST scientists anticipate extending our present portfolio of characterization capabilities to include an even wider range of materials and measurements of importance to materials scientists and to U.S. industry.

Complementary to the synchrotron radiation techniques, a new laboratory x-ray diffractometer is nearing completion. It features three optical configurations: (1) high resolution parallel beam for the analysis of thin films, (2) "low" resolution parallel beam for the analysis of powders, and (3) a divergent beam optic also for the analysis of powders. Integral to its design is an ability to perform first principles lattice spacing measurements on powders and thin films that are traceable to the SI. The new machine will be used for certification of the next generation of NIST Standard Reference Materials, which serve both the powder diffraction and high-resolution diffraction communities.

Contact Information: Gabrielle Long

Non-Dipole Effects in Photoelectron Emission Measured Using an X-ray Interference Field

Erik J. Nelson and Joseph C. Woicik

Angle-resolved photoelectron-yield standing waves (XSW) is a new experimental method to test the atomic theory of non-dipole effects in photoelectron emission. It relies on the interference of the incident and reflected x-ray-beam matrix elements that occurs near a crystal x-ray Bragg reflection. Consequently, unlike conventional angle-resolved measurements, both the amplitude and phase of the quadrapole (non-dipole) contributions to the photoelectron process may be measured. By monitoring the photoelectron yield as a function of photon energy near the (11-1) Bragg back-reflection condition of crystalline Ge, sizable contributions of non-dipole effects to Ge 3d photoelectron emission are observed.

We have calculated the photoelectron emission matrix element under excitation by an x-ray standing-wave (XSW) interference field by considering the sum of the individual matrix elements from the incident and reflected fields:

$$M_{if} = E_o e^{ik_o r_{core}} \langle f | e^{ik_o r_e} (\mathbf{e}_o \mathbf{p}) | i \rangle$$

$$+ E_h e^{ik_h r_{core}} \langle f | e^{ik_h r_e} (\mathbf{e}_h \mathbf{p}) | i \rangle .$$

In the dipole approximation, $e^{ik_o r_{core}} \approx 1$, the cross section (amplitude squared of the matrix element) is proportional to the electric field intensity at the position of the core.

Higher-order quadrupole effects in the photoemission process are included by considering the next order Taylor-series term of the electric field about the position of the atomic core, i.e., $e^{ik_o r_e} \approx 1 + i\mathbf{k}_o \mathbf{r}_e$. Unlike the dipole terms, quadrupole terms probe the spatial extent of the initial electron wave function $| i \rangle$. The photoelectron cross-section in the XSW field including quadrupole effects is $ds/d\Omega \propto 1 + [(1 + Q) / (1 - Q)] R + 2 F_c \sqrt{R} [1 - Q]^{-1} \cos(2p D_c + n - y)$, where the parameters $D_c = \mathbf{h} \mathbf{r}_{core}$ and F_c are the phase and amplitude of the charge-density Fourier coefficient for the $\mathbf{h}$ reflection. The quantity n is the phase of the complex-field amplitude ratio $E_h/E_o = \sqrt{R} e^{in}$, and R is the reflectivity function $R = | E_h/E_o |^2$. Both R and n are functions of photon energy.

This expression differs from the usual dipole-only XSW expression by the introduction of both the quadrupole strength parameter Q and the quadrupole phase shift y, which are related to the amplitude and phase of the complex dipole-quadrupole matrix element product. Q and y depend on $\mathbf{k}_o \mathbf{r}_e$ and are maximized by detecting electrons in a small azimuthal window about the "backwards" direction relative to the incident wavevector $\mathbf{k}_o$. Experimentally, we achieved this by constructing a 15° azimuthal shutter in front of the cylindrical mirror electron analyzer (CMA). In contrast, with no shutter, electrons are detected in the full 2p azimuthal range of the CMA cone, and the $\mathbf{k}_o \mathbf{r}_e$ dependence averages to zero, so Q = y = 0.

The Ge 3*d* photoelectron XSW yield (Figure 1(a)) exhibits a change in XSW amplitude for the Ge (11-1) back-reflection with and without the 15° azimuthal shutter. The fit to the Ge 3*d* photoelectron XSW yield renders a quadrupole strength parameter $Q_{3d} = 0.24 \pm 0.03$, which is in excellent agreement with the theoretical result of $Q_{3d} = 0.23$ derived from calculated atomic angular distribution parameters. In addition, the fit renders a nonzero phase shift $y = +0.027 \pm 0.006$. This is the first experiment to directly measure a phase shift due to quadrupole effects on photoelectron emission from a solid in an XSW field.

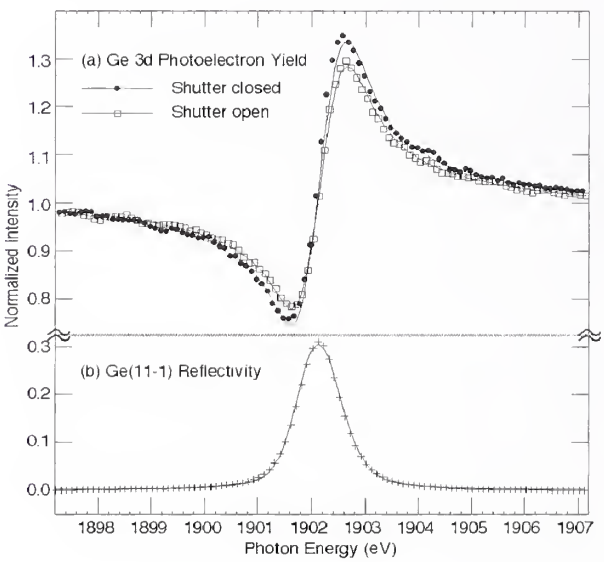

Figure 1: (a) The Ge 3*d* photoelectron yield as a function of photon energy around the Ge(11-1) Bragg back-reflection condition. Both the quadrupole-sensitive data, taken with the analyzer shutter closed (filled circles), and the angle-averaged data, taken with the analyzer shutter open (open squares), are compared. The solid lines are the best fits to the data using the dipole-only XSW yield equation. (b) Reflectivity data and best fit.

Contributors and Collaborators:

John W. Cooper (Institute for Physical Science and Technology, University of Maryland), Ivan A. Vartanyants (University of Illinois), Piero Pianetta (Stanford Synchrotron Radiation Laboratory)

Powder Diffraction Standards

James P. Cline

The realization that structural imperfections in material specimens caused line broadening in an X-ray diffraction experiment led to the investigations of said broadening dating to the1930s and 1940s. Moreover, by relating the specimen broadening to physical properties of the material specimen, it was proposed that a microscopic "picture" encompassing size distribution and shape of crystallites, as well as distortions of the crystallite lattice, could be developed. The implications of developing such an understanding at a microscopic level are immense for both scientific and commercial reasons

The broadening of X-ray powder diffraction line profiles due to particle size and micro-strain effects is a well known phenomenon. Several methods have been developed which purport to yield credible data on the particle size and the level of microstrain from analyses of profile shape. Unfortunately, for the most part, they are either applicable only to specific types of instrument configurations and/or specimens, or they make *a priori* assumptions about the data which impart limitations or biases to the results. The development of a NIST Standard Reference Material (SRM) for microstructure analysis would require that a method be developed which would not impart any bias on the result. Furthermore, to be useful to the community, the method should be applicable to a range of instrument configurations. While the analysis of profile broadening provides data on both the crystallite size and lattice strain, it was decided to concentrate initially on an SRM exhibiting broadening due to size effects only, i.e., a strain free powder. The development of such an SRM is of particular importance, especially with present developments in nanotechnology and the use of nano-powders in industry.

The first step in developing an SRM involved a series of x-ray diffraction experiments performed in conjunction with numerical simulations to develop an understanding of the principal factors affecting the recorded size-broadened line-profile. These included: the instrument profile function, counting statistics, background level, and lastly, the "common-volume function" of the crystallites and their size-distribution. The common-volume function simply defines the shape and dimensions of a single crystallite. It is convoluted with the size distribution of the crystallites to describe the intensity distribution of the entire specimen. Thus, the crystallite-size distribution can be linked to the observed specimen profile.

The problem of developing a "picture" of structural imperfections is made more difficult by the manner in which intensity distributions are recorded. That is, for a conventional diffractometer the intensity distribution in a three dimensional reciprocal space is mapped into a one-dimensional space. In order to develop a picture of the microscopic properties of the material, we must work backwards from the one-dimensional space into a three-dimensional space. The problem is further compounded by the fact that the diffractometer introduces an intrinsic broadening and statistical errors into the recorded line-profile. The underlying problem we face is determining the most plausible or probable of many possible solutions with respect to both the removal of the instrumental broadening and determining the shape of the crystallites and their size distribution.

The method developed for extracting size data from observed profiles must yield results which meet two basic properties concerning line-profiles and size-distributions: the first property is that these distributions are positive definite. That is, the recorded profile and specimen profile represent intensities which have a positive value, while the size distribution represents a probability of a crystallite having a particular dimension. The second property is that these distributions are additive. That is, the sum of the intensities over a region represents a physically meaningful quantity, while the sum of the size-distribution must be unity over its entire range.

The maximum entropy principle is employed to determine the most probable solution , while preserving the positivity and additivity of these distributions. The size-distribution (or specimen line-profile) which has a maximum entropy with respect to the recorded line-profile is the most probable or plausible solution. The maximum entropy principle can be placed on a firm statistical basis by introducing Bayesian statistics and formulating a Bayesian/maximum entropy method for determining the crystallite-size distribution. This approach allows each of the principal terms that define a recorded line-profile to be defined and the corresponding, most probable, size-distribution to be determined. The Bayesian/maximum entropy method also allows any available *a priori* information concerning the shape and type of size distribution to be included in the analysis.

The final stage in the development of a size broadened SRM has been the preparation of the feedstock. The SRM itself is likely to consist of two materials: cerium-oxide and zinc-oxide. Cerium oxide forms crystallites that are spherical in shape and thus require the simplest shape model. On the other hand, zinc oxide exhibits a columnar crystal habit which requires a more complex shape model. Completion is estimated to be in 2002.

Contributors and Collaborators: Armstrong, N.A., Kaleeff W. (University of Technology, Sydney, Australia)

Soft X-ray Characterization of Surfaces and Bulk

We utilize polarized soft x-rays to probe the structure and molecular orientation of nanometer thick layers on a variety of surfaces in partnership with industries and academic institutions. Practical industrial problems are currently being investigated, such as model catalyst systems, polymer surfaces and their interfaces, magnetic hard disk surface chemistry, bio-materials and high temperature superconductors.

Daniel A. Fischer

The discovery of superconductivity at 39 K in the MgB_2 may open a door to a deeper understanding of superconductivity at higher temperatures. This material differs greatly from the high temperature superconducting oxides by its simple structure, but it is similar in that (1) it is a layered material and (2) Hall voltage measurements as well as electronic structure calculations suggest that electron holes are the charge carriers.

We use near edge x-ray absorption spectroscopy (NEXAFS) and electron energy loss spectroscopy (EELS) to study the near edge fine structure at the K-edge of boron in the superconductor MgB_2. These techniques are based on the same fundamental physical process. The incident x-rays in NEXAFS, or the incident fast electrons in EELS, excite core electrons to hole states above the Fermi level. These two techniques also have several complementary features: for example, NEXAFS has a better energy resolution, and EELS a much better spatial resolution.

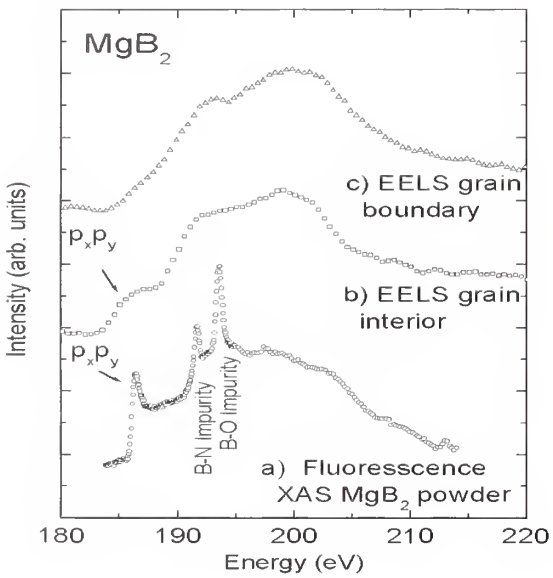

We observe in the NEXAFS a peak of width 0.6 eV at the threshold of this K-edge, signaling a narrow energy region with empty boron p-states near the Fermi level. Our observations are consistent with several electronic structure calculations reporting a narrow energy window of empty p_xp_y states that has fallen to zero at 0.8 eV above the Fermi level. The disappearance of the p_xp_y feature in EELS spectra from grain boundaries suggests that this signature may become powerful in probing the superconducting properties at the nanoscale.

Next generation lithographic materials and processes that are able to fabricate features less than 100 nm in size are critical for the continued improvements in device performance of integrated circuit devices. This tolerance imposes very demanding challenges on both lithographic materials and processing methods. In particular, it is important to be able to control the distribution of the resist components in order to obtain high quality line profiles. Advanced photoresist formulations make use of photosensitive molecules, photoacid generators (PAGs), which decompose to form acids after illumination with radiation. Surface and bulk sensitive NEXAFS measurements were performed on thin films of poly(hydroxystyrene) loaded with a mass fraction of 20 % of the bis(p-tert-butylphenyl) iodonium perfluorooctanesulfonate (PFOS) photoacid generator (PAG) to determine the surface behavior of the PAG in the resist matrix. We find that for 20 % PFOS in PHS, the fluorinated component is observed at the film surface for the as prepared film and for thermal bakes at 130 °C for up to 14 h. However, after a UV dose of $\approx$ 75 mJ/cm^2, and a 5 min post-exposure bake at 130 °C, the fluorinated component is apparently *absent* from the film surface. However, the overall mass fraction of fluorine through the entire film remains essentially unchanged. These results demonstrate the surface sensitivity of NEXAFS to distinguish the surface behavior of important resist components.

Contributors and Collaborators: Y. Zhu and A. R. Moodenbaugh (Brookhaven National Laboratory), E. K. Lin and W. L. Wu (Polymers Divison)

Synchrotron Beam Line Operation and Development

Gabrielle Long

The Synchrotron Radiation Program at NIST/MSEL includes the development and operation of beam stations at the National Synchrotron Light Source (NSLS) at Brookhaven National Laboratory, and at the Advanced Photon Source (APS) at Argonne National Laboratory. The emphasis is on microstructure characterization, where NIST scientists, and researchers from industry, universities and government laboratories perform state-of-the-art measurements on advanced materials.

The UNICAT collaboration at the Advanced Photon Source, which includes NIST, the University of Illinois, Oak Ridge National Laboratory, and UOP Research Center, supports a range of research techniques that require widely varying characteristics of the incident X-ray beam. To meet the technical demands of our diverse experimental portfolio, the UNICAT beam lines on Sector 33 exploit the brilliance of the APS source to deliver X-rays with high flux and with energy resolution better than or equal to the lifetime-broadened core-hole widths for all accessible K and L shells. The insertion device beam line, 33-ID, became operational November 1, 1999, and as of November 1, 2000, has entertained independent investigators as well as collaborative access team members. The bending magnet beam line, 33-BM, began commissioning in March 2001 and is expected to become fully operational by the end of 2001.

Ultra-small-angle X-ray scattering (USAXS), which was the first of the NIST-responsible experiments to come on line, provides data in the usually inaccessible Q range (where $Q = (4\pi/\lambda) \sin\theta$, λ is the x-ray wavelength and θ is one-half the angle of scatter) down to 1.5×10^{-4} Å^{-1}. The UNICAT instrument, which has had nearly two years of full operation, includes several capabilities that make it among the best in the world. It covers an unprecedented Q range out to 1 Å^{-1}; it can operate in this range as an "effective pinhole" instrument, where the scattering data are not line-smeared, anomalous-USAXS can be used to uncover and quantify previously inseparable microstructures; and it supports the remarkable new technique of USAXS-imaging. In the past year, the USAXS instrument continued to receive the highest demand of any instrument on UNICAT.

This year, we are commissioning two new NIST-responsible experiments: X-ray topography and X-ray absorption fine structure. A third, microtomography, is still under development.

At the NSLS, we operate beam line X23A2 and we are partners in the operation of U7A and X24A. Numerous improvements have been made to the ultra-soft X-ray (U7A) Materials Science End Station over the past year. A rapidly interchangeable sample pod was designed, delivered and tested. A low-light TV camera and mirror system was developed for aligning samples in the soft X-ray beam spot. The product of a Phase I SBIR, an ultra-high efficiency Si(Li) energy dispersive detector, was developed, delivered and tested. This successful development provides a significant advance in the quantitative analysis of light elements. Finally, a newly reconfigured materials characterization end station and a six-axis sample manipulator and load lock were designed and are currently being added to the station. The reconfigured facility accommodates all of our detector capabilities, including a planned XPS electron analyzer.

The X23A2 beam line provides a stable, scanning, highly monochromatic X-ray beam in the energy range from 4.9 keV to over 30 keV. The X-ray absorption fine structure (XAFS) spectroscopy done on this line is capable of probing: the short range order in crystals, one element at a time, and it provides information on the number, distance and chemical identity of the neighbors of the absorbing atom.

Future opportunities for development include the possibility of becoming a part of UNICAT-II: a synchrotron X-ray micro-beam capability for probing materials at the sub-micrometer level. High-throughput parallel detection X-ray diffraction and X-ray fluorescence on this instrument offer a unique capability for combinatorial materials science. Additional advantages include characterizing sub-micrometer strain and stress and selected interface structures. Commissioning exercises are currently underway, and the new instruments are expected to be fully operational by the end of the year.

Contributors and Collaborators:

A.J. Allen, D.R. Black, H.E. Burdette, D.A. Fischer, R.D. Spal and J.C. Woicik (Ceramics Division); P.R. Jemian, H. Chen, H. Hong and P. Zschack (University of Illinois); J. Ilavsky (University of Maryland); G.E. Ice, J.Z. Tischler and B.C. Larson (Oak Ridge National Laboratory); and R. W. Broach (UOP Research).

Ultra-Small Angle X-ray Scattering

Andrew Allen and Gabrielle Long

Ultra-small x-ray scattering (USAXS) studies using the NIST USAXS instrument now routinely supply data in the unprecedented Q range (where $Q = (4\pi / \lambda)\sin\theta$, λ is the x-ray wavelength and θ is one-half the angle of scatter): 0.00015 $Å^{-1}$ to 1.0 $Å^{-1}$ at x-ray energies from below 7 keV to above 17 keV. A special configuration for the study of anisotropic materials reduces the maximum Q to 0.05 $Å^{-1}$, but retains the impressive performance in other respects. This versatility, coupled with a rare primary calibration capability, makes practical the quantitative study of a wide range of technological materials.

USAXS Study of Powder Agglomeration. The formation of agglomerates during ceramic powder processing is a pervasive problem that frequently prohibits the fabrication of fully-dense ceramics. While it is well-known that drying of liquid-borne powders creates agglomerates, it is not known exactly how or why those agglomerates evolve. Agglomeration during drying is particularly acute at the nanometer scale, where heightened powder dissolution and diminished electrostatic repulsion are likely to be strong driving forces for agglomerate formation. Ultra-small-angle x-ray scattering (USAXS) and field emission scanning electron microscopy (SEM) have been combined to examine agglomerate shape and size development during the drying of different nanocrystalline zirconia powder suspensions. USAXS data for the fresh suspensions, Figure 1, show hallmarks of various aggregation effects at different length scales. Away from the pH 8 isoelectric point, aggregation of the mutually-repulsive primary particles into agglomerates seems to be "reaction-limited" (i.e., there are many contacts before aggregation occurs), and this leads to the formation of large, dense, fractally-rough agglomerates from the entanglement of short chains of primary particles. At pH 8, where electrostatic repulsion is minimized, aggregation of the primary particles is diffusion-limited and large mass-fractal aggregates form. Differences with pH in the micrometer-scale morphology of fully-dried suspensions, seen by SEM, seem to be related to the nanometer-scale aggregation of primary particles, studied by USAXS. For example, where SEM shows large lamellae and coarse grains with lamellar sub-structure, USAXS suggests the presence of sheets of primary particles in the suspension prior to full drying.

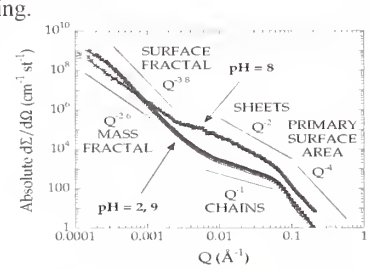

Figure 1: USAXS data for nanoparticulate zirconia suspensions

USAXS Imaging Study of Creep Cavitation. USAXS imaging is a new technique in which images are formed from angle-filtered X rays scattered by electron density variations in a sample. It greatly expands the usefulness of small-angle scattering by providing direct images of the spatial arrangement of the scattering objects. Current USAXS imaging activities include studies of ceramic coatings, metals, and polymer composites. In the example here, the sample is taken from a copper rod that was deformed in uniaxial tension at a constant strain rate, producing a volume fraction of creep cavities of $(4.5 \pm 2.3) \cdot 10^{-4}$. Such low volume fractions of cavities are rarely observed in the thin cross sections required for transmission electron microscopy, but are readily observed in USAXS images. Figure 2a shows a region of the sample containing a large circular arrangement of creep cavities, presumably surrounding a single grain. In scattering from polycrystalline Cu, some of the grains may be oriented for Bragg diffraction. A portion of this diffracted intensity can undergo a second Bragg reflection and appear as increased scattering at small angles. Such effects are also seen in USAXS images, but the double-Bragg contributions are very sensitive to rotation about the scattering vector while contributions from the scattering features are not. Figure 2b shows the same volume of the sample after rotating to a local Bragg condition; we have also used a larger scattering vector to enhance the double-diffraction contrast relative to the contrast of the cavities. A large darkened region appears within the circular area enclosed by the creep cavities, demonstrating that this area is indeed a single grain. Strain fields within the grain cause the irregular shape of the

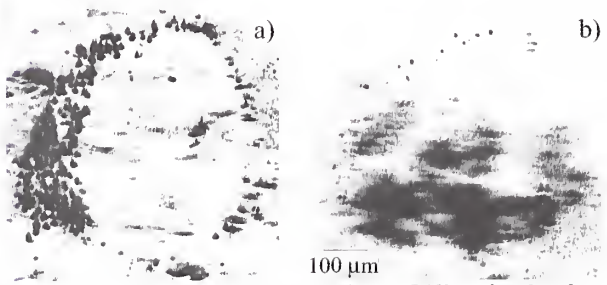

Figure 2: a) Cavities around a grain. b) Diffraction by the grain.

Contributors and Collaborators: Jan Ilavsky (University of Maryland), Pete Jemian (University of Illinois), Alejandro Vertanessian, Sujarinee Kochwattana and Merrilea Mayo (Pennsylvania State University), Lyle Levine (Metallurgy Division, MSEL)

Other

Several important projects in the Ceramics Division are unique and are not constituent parts of Programs. These projects are highly visible and have significant broad impact in several application areas but generally involve a commitment of personnel and resources less than that considered to be a program. The Ceramics Division relies on these projects for enhanced technology transfer and for more effective delivery of the results of the research programs to the technical community.

Contact Information: **Stephen Freiman and Stanley Dapkunas**

Grain Growth in Relaxor Ferroelectrics

Jay S. Wallace and John E. Blendell

Lead magnesium niobate-lead titanate, $Pb(Mg_{1/3}Nb_{2/3})O_3$ - $PbTiO_3$ (PMN-PT), is a relaxor ferroelectric that shows excellent piezoelectric response and is a good candidate for transducers. However, conventionally sintered polycrystalline PMN - PT ceramic materials exhibit inferior piezoelectric properties compared with single crystals. Understanding the grain growth mechanisms operating in this system can be used to define the microstructural evolution paths and processing parameters for increasing the size of PMN - PT single crystals, providing a low-cost alternative to growing single crystals.

The present work focuses on the determination of grain growth mechanisms of PMN-PT grains. Measurements of growth rate with varying amounts of liquid phase were used to determine the rate limiting step of growth and the effect of grain-to-grain impingement.

During grain growth, the presence of a PbO-rich liquid allows rearrangement of PMN-PT grains to occur and also acts as the transport path for solution-precipitation grain growth. The mechanisms of grain growth were determined by changing the amount of PbO-rich liquid present during sintering. At low liquid fractions insufficient liquid exists to allow significant grain movement or allow grains to attain their equilibrium shape, resulting in small, rounded grains. For higher liquid fractions, when grain-to-grain impingement no longer limits the size or shape of grains, the mechanisms controlling material transport, thus grain growth, can be studied. A change in the growth kinetics was observed at liquid fractions of approximately 0.2. For liquid fractions greater than 0.3, the grains were facetted cubes with growth rates, independent of liquid fraction, and grew at a much faster rate than for lower liquid fractions (Figure 1).

Based on the independence of the growth rate on volume fraction liquid above 0.3 and the observed faceted grain shape, growth was determined to be controlled by a surface nucleation mechanism rather than diffusion through the liquid.

Exaggerated grains, those significantly larger than the average grain size, were observed for liquid fractions greater than 0.2 (Figure 2). Orientation Imaging Microscopy determined that all of the exaggerated grains contained 60° <111> twins but none of the matrix grains was twinned. These reentrant edges from the twin planes allowed rapid nucleation of growth ledges and gave the twinned grains a growth advantage over grains with only singular, facetted surfaces. It is expected that these exaggerated grains, which contain twins and reentrant angles, can be used as seeds for further grain growth, allowing production of sintered bodies with very large grains that approach the properties of single crystals.

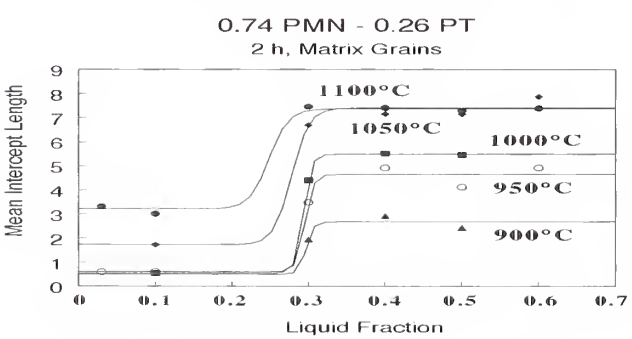

Figure 1: The size of matrix grains increases rapidly for liquid fractions about 0.2 and is independent of liquid fracture above 0.3, indicating that growth is not controlled by diffusion through the liquid phase

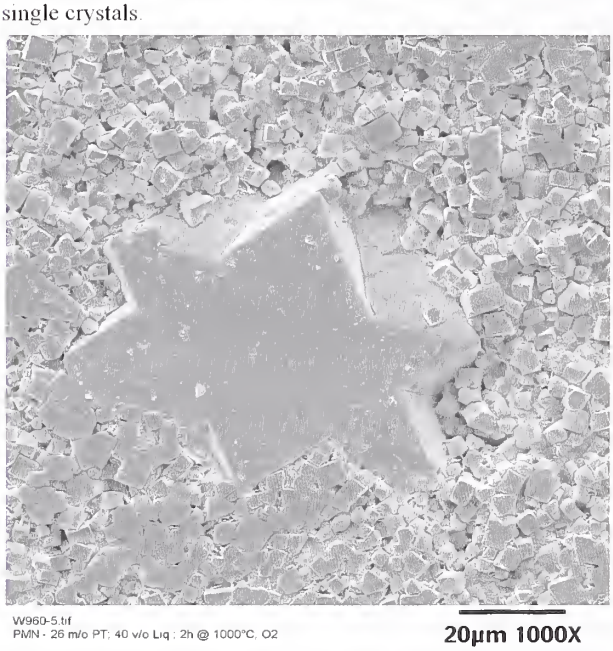

Figure 2: Scanning Electron Microscope image of an exaggerated PMN-PT grain in a polished section. Note the reentrant angles on the grain interface which give such grains a growth advantage over the surrounding cube-shaped grains.

Contributors and Collaborators: Jong-Moo Huh (KAIST, Korea) and William T. Petusky (Arizona State University, Tempe, AZ)

Optical and Structural Characterization of Optoelectronic Semiconductors

Lawrence H. Robins

Photonic device manufacturers need to better understand how inhomogeneous electronic structure in III-nitride alloys (AlGaN and InGaN) and III-nitride/metal interfaces affects the performance of optical emitters and detectors. To address these issues, we are performing measurements on GaN/InGaN and n-GaN/metal structures. The primary characterization method is high-spatial-resolution cathodoluminescence spectroscopy in a scanning electron microscope, supported by other optical and structural probes of the samples.

We are measuring critical optical and structural properties of III nitride thin films (GaN, AlN, InN and their alloys). The III nitrides are leading materials for short-wavelength solid-state optical emitters and detectors, and also show promise for high-power, high-frequency microelectronics. Our current objective is to better understand the mechanisms for inhomogeneous electronic structure in III-nitride alloys and III-nitride/metal interfaces, and the impact of non-uniform structure on device performance. InGaN and AlGaN alloy layers are critical to the fabrication of optical emitters and detectors. Spatial non-uniformity in alloy layers may arise from compositional inhomogeneity (including clustering of Al, Ga or In atoms, phase separation, and long-range ordering), inhomogeneous residual strain, and piezoelectric fields associated with the presence of strain. III-nitride/metal interfaces are critical to the fabrication of electrical contacts to all types of electronic and optoelectronic devices. Non-uniform electronic structure in the near-interfacial region may arise from band-bending effects, defects created during the metallization process, and formation of new interfacial structural phases (e.g. Ga-N-metal ternaries).

$In_xGa_{1-x}N$ films examined in this project were grown by metalorganic chemical vapor deposition on GaN/sapphire or AlGaN/sapphire substrates. The alloy compositions (x) of the films, measured by wavelength dispersive x-ray spectroscopy (WDS), are in the range 0£x£0.47 and the film thicknesses range from 0.4 mm to 1.1 mm. The structure of the films was examined by x-ray diffraction (XRD, q-2q scans of the 0006 diffraction peak) and indium K-edge extended x-ray absorption fine structure (EXAFS). Comparison of the XRD and WDS results shows that the (0001) lattice constant is a linear function of x, and the linewidth of the diffraction peak increases significantly with x. Comparison of the EXAFS and WDS results shows that the indium fraction in the indium second shell is equal to the average indium fraction (x) within the measurement uncertainty. These results indicate that the local atomic structure is closer to a random alloy (a random mixture of In and Ga atoms on the cation sublattice) than to separate In-rich and Ga-rich phases (which would show strong In-In correlation).

Optical properties of the films were characterized by the following spectroscopic methods: room-temperature optical transmittance, room-temperature spatially integrated cathodoluminescence (CL), low-temperature spatially integrated CL, and low-temperature spatially resolved CL. As reported previously, the room-temperature electronic bandgap (E_G) was determined from the absorption edge energy in optical transmittance and, independently, from the highest-energy peak in the CL spectrum. These two measures of E_G were found to be in good agreement. The composition dependence $E_G(x)$ is well-described by a quadratic function with a second-order (bowing) parameter equal to -4.57±0.75 eV, which is large compared to most semiconductor alloys.

Inhomogeneous electronic structure was investigated by low-temperature spatially resolved CL, at T~15 K and electron excitation energy of 6 keV, with an estimated electron-beam spot size of 200 nm. A striking result was obtained from these measurements. While the main exciton peak shows very little temperature shift from T=295 K to T=15 K, a new, higher-energy peak, from 0.15 eV to 0.4 eV above the main peak, is observed from selected spots on all the samples with compositions x<0.31. Further, the new high-energy peak is most intense relative to the main peak, and best defined (narrowest line-width), in the lower-indium alloys, those with x»0.06. The high-energy peak becomes less distinct with increasing indium fraction and is not observed in samples with x=0.35 and x=0.37. While we are still trying to develop a model to understand these results, a model based on formation of indium-rich clusters or "InN quantum dots," as some researchers have proposed, does not appear consistent with our data. Indium-rich clusters are expected to give rise to a CL peak on the low-energy side of the main exciton peak, and to increase in prominence with increasing indium fraction. (Formation of a distinct high-indium phase has been observed by XRD and TEM, but only in samples with x~0.4.) Spatially varying piezoelectric fields are being considered as an alternative mechanism. Measurements of III-nitride quantum well structures show that the Stark effect in a strong piezoelectric field can give rise to a red-shift of the exciton CL peak as large as several tenths of an eV.

Contributors and Collaborators:

Charles E. Bouldin, Igor Levin, Mark D. Vaudin, and Joseph C. Woicik, Ceramics Division, MSEL; Albert V. Davydov and William J. Boettinger, Metallurgy Division, MSEL; C.A. Parker, J.C. Roberts, and S.M. Bedair, Dept. of Electrical and Computer Engineering, North Carolina State University; Denis Tsvetkov, Technology and Devices International, Inc., Gaithersburg, MD

Phase Relationships in High Temperature Superconductors

Winnie Wong-Ng and Lawrence Cook

Successful processing of high T_c superconductor materials requires phase diagrams as 'road maps'. Of current interest are the $Ba_2YCu_3O_{6+x}$ (Y-213), $Ba_2NdCu_3O_{6+x}$ (Nd-213), and the $Ba_2SmCu_3O_{6+x}$ (Sm-213) superconductors. The construction of subsolidus phase diagrams of these three systems, and the role of phase equilibria and kinetics in the formation of the $Ba_2YCu_3O_{6+x}$ phase via barium fluoride amorphous precursor films, are deemed important for rapid advancement of second generation coated conductor technology.

The high T_c superconductor industry currently is pursuing two parallel technologies for the development of practical bulk conductors using cuprate high-temperature superconductors: the first generation Bi-Pb-Sr-Ca-Cu-O (BSCCO)-based wire/tape produced by the Ag-Powder-in-tube technique, and the second generation $Ba_2RCu_3O_7$-type (R-213, R=lanthanide and yttrium) coated-conductors. We have recently determined the primary phase fields for the principal superconducting phases in the BSCCO system and the effect of Ag on phase equilibria. In the past two years, we have concentrated our research efforts on supporting the rolling assisted by biaxially textured substrate/ion beam assisted deposition (RABiTS/IBAD) coated-conductor technology, in which the superconductor phase is used as a coating on a thin metallic ribbon substrate. The majority of the BaO-R_2O_3-CuO phase equilibrium studies reported to date have used $BaCO_3$-derived starting materials. Our current research is focused on the understanding of the dependence of carbonate-free BaO-R_2O_3-CuO_x subsolidus relations on both pO_2 and choice of lanthanides (R = Nd, Sm, and Y). Nd-213 and Y-213 demonstrate high T_c as well as high J_c values. The Sm-system was studied because of the potential use of the Sm-213 phase as a buffer layer for the IBAD process.

An experimental procedure for minimizing the presence of CO_2 by using BaO was established. The BaO-Y_2O_3-CuO_x phase equilibrium was investigated at pO_2 of 100 Pa and 21 kPa using carbonate-free precursors based on BaO. Different tie-line distributions among $Ba_2YCu_3O_x$, $Ba_4YCu_3O_x$, BaY_2CuO_5, and $BaCuO_{2+x}$ under carbonate-free conditions relative to those obtained using $BaCO_3$ were found to occur. Other than the different solid solution ranges of several ternary phases, the phase diagrams of the BaO-Nd_2O_3-CuO_x system under pO_2 of 100 Pa and 21 kPa were mostly similar. The Nd-213 solid solution range was found to extend from $Ba_2NdCu_3O_z$ to $Ba_{1.7}Nd_{1.3}Cu_3O_z$ under 100 Pa pO_2, and from $Ba_2NdCu_3O_z$ to $Ba_{1.05}Nd_{1.95}Cu_3O_z$ under 21 kPa pO_2. The BaO-Sm_2O_3-CuO_x phase diagram was investigated under pO_2 of 100 Pa and was found to be similar to the Nd-analog, except for different solid solution extent of phases due to the lesser substitution of Sm relative to Nd on the Ba sites, and the structure of the $BaSm_2CuO_5$ phase is different from that of Ba_2NdCuO_5.

The investigation of the phase relationships in the system BaF_2-BaO-Y_2O_3-CuO_x-H_2O is a second area of concentration. The "BaF_2 *ex situ*" process is one of the most promising methods for producing long-length high quality Y-213 superconductor. This method uses e-beam co-evaporated BaF_2-Y-Cu-precursor films on RABiTS, followed by a post-annealing in the presence of H_2O vapor. The details of phase evolution of the Y-213 phase during this process, however, are not understood. It is also important to determine whether an intermediate fluorine-containing low-temperature liquid forms, and, whether its formation plays a role governing the formation of the Y-213 phase.

The high-temperature X-ray diffractometer and the gas-flow system for studying the BaF_2 process have been set up. Using amorphous precursor films of Y-213 which contain BaF_2, Cu and Y (provided by R. Feenstra of the Oak Ridge National Laboratory), we have successfully followed the phase formation of BaF_2 and Y- 213 using high-temperature X-ray diffraction. Depending on the flow rate of water vapor, different intermediate phases were observed. Preferred orientation of Y-213 was partly governed by the thickness of the films. Also, using sol-gel methods, we have prepared fluorinated precursors of Y-213 and related compositions, and investigated the defluorination process thermogravimetrically.

Our research has been reported at three international conferences in FY2001, and was also presented in two invited lectures. Outside interest in our work has led to collaborations with the US Air Force, Oak Ridge National Laboratory, Los Alamos Laboratory, University of Houston, and Brookhaven National Laboratory. The potential for a wide variety of technological applications, including power distribution and energy storage, and advanced motors and magnets, provides the motivation for the continued rapid pace of high T_c-superconductor research activity. The Department of Energy has supported this activity through a program of intensive R&D focused on wire and cable for high-impact commercial applications, of which the NIST project is an integral part.

Contributors and Collaborators:

NIST participants: I. Levin, M. Vaudin, J.P. Cline (Ceramics); NIST MSEL collaborators: Q. Huang, B. Toby (Reactor), L. Swartzendruber (Metallurgy), A. Kearsley (Mathematical and Computational Sciences); Industrial, government and academic collaborators: T. Holesinger (LANL), R. Feenstra (ORNL), G. Riley (ASC), J. Kaduk (BP-Amoco), R. Meng (U. Houston), and M. Suenaga (BNL).

Stress Measurement in Optoelectronic Films

Grady S. White and Albert J. Paul

Optoelectronic devices, composed of multiple thin film layers, inherently contain residual stresses resulting from variations in lattice constants and coefficients of thermal expansion. These stresses affect optical, electronic, and vibrational properties in the final devices and can lead to catastrophic mechanical failure. Currently, no techniques exist to measure these stresses, which can vary substantially over micrometer distances. Consequently, we are developing measurement tools to allow stress and composition to be determined in areas of a few square millimeters, using Raman and PL spectroscopy.

We are developing techniques using Raman and photoluminescence (PL) spectroscopy to measure stresses and compositions in optoelectronic films of $Al_xGa_{(1-x)}As$. Although both Raman and PL line positions are known to be sensitive to the presence of stress and variations in [Al]/[Ga], no calibration procedures have been developed to quantify stress-induced peak shifts and no measurement techniques have been developed to deconvolute peak shifts due to stress from those due to composition variations.

The approach that is being used involves measuring the phonon deformation potential values, i.e., the constants that relate changes in Raman peak position to strain, as a function of [Al]/[Ga] using the loading rig in Figure 1. Similarly, the PL piezospectroscopic coefficients relating changes in PL peak position to stress will be determined. In addition, both PL and Raman peak position as a function of [Al]/[Ga] will be obtained in the absence of strain.

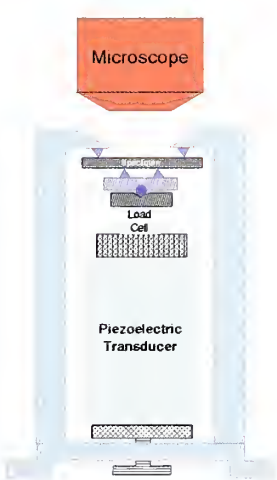

Figure 1: 4-point loading rig used for piezospectroscopic and phonon deformation potential values. Uniaxial stress is applied mechanically or through the transducer; Raman/PL measurements are made through the microscope objective.

In the case of unknown biaxial stress and unknown [Al], combining the observed shifts in the Raman and PL lines is expected to provide values for both the stress and composition. In addition to the PL and Raman measurements, x-ray experiments are planned at the Synchrotron. These measurements will provide an absolute calibration of the strain in the specimens.

Currently, measurements are being made on GaAs (i.e., [Al] = 0) as a function of incident polarization angle and applied stress. Figure 2 is a typical spectrum; the increasing background results from the excitation laser line. Substrate materials with orientations of (100), (111), and (110) are being measured. Thin film specimens with [Al] = 20%, 30%, and 90% are in preparation.

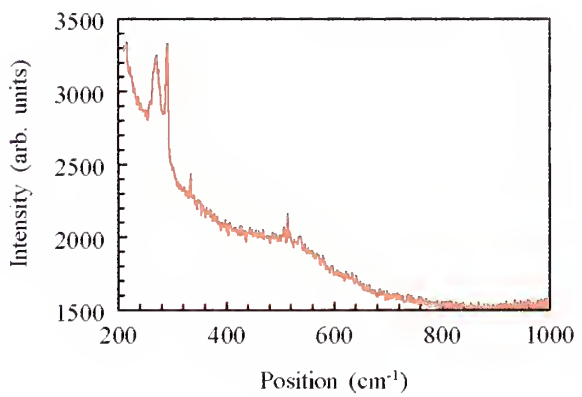

Figure 2: Spectrum of Si-doped (100) GaAs in the absence of an applied stress. The doublet consists of a sharp line near 292 cm^{-1} and a broader line near 280 cm^{-1}. The sharp line results from an LO phonon mode. The source of the broader peak is not known at this time, but may result from the Si doping. The very broad peak around 520 cm^{-1} results from a phonon-plasmon interaction. The sensitivity of the latter two peaks to stress is under investigation.

Contributors and Collaborators:

Joseph Woicik, Ceramics Division, MSEL; Alexana Roshko , Kris Burtness, Electronics and Electrical Engineering Laboratory

Publications

Allen, A.J., Long, G.G., Boukari, H., Ilavsky, J, Kulkarni, A., Sampath, S., Herman, H., and Goland, A.N., "Microstructural Characterization Studies to Relate the Properties of Thermal Spray Coatings to Feedstock and Spray Conditions," Thin Solid Films, in press (2001).

Allen, A.J., Illavsky, J., Long, G.G., Wallace, J., Berndt, C.C. and Herman, H., "Microstructural Characterization of Yttria Stabilized Zirconia Plasma Sprayed Deposits Using Multiple Small Angle Neutron Seattering," Acta Mater **49**: (9) 1661-1675 (2001).

Begley, E. F. and Sturrock, C.P., "MatML: An XML for Standardizing Web-based Materials Property Data", JOM, July 2000, p. 56.

Begley, E.F. and Sturrock, C.P. "MatML: XML for Materials," ASM International Advanced Materials & Processes, Vol. 158, No. 5, November 2000, pp. 72-74.

Bendersky, L.A., Levin, I., Roth, R.S., and Shapiro, A., "$Ca_4Nb_2O_9$-$CaTiO_3$ Phase Equilibria and Microstructures," J. Solid State Chem., in press.

Blendell, J. and Handwerker, C.A., "Grain Growth in Ceramics," Encyclopedia of Materials: Science & Technology, accepted.

Boukari H, Long G.G., Harris M.T., "Polydispersity during the formation and growth of the Stober silica particles from small-angle X-ray scattering measurements," J Colloid Interf Sci 229: (1) 129-139 September 1 2000.

Bouldin, C., Sims, J., Hung, H., Rehr, J.J., and Ankudinov, A.L., "Rapid calculation of x-ray absorption near edge structure using parallel computing," J. of X-ray Spectrometry, accepted.

Burton, B.P., Dupin, N., Fries, S.G., Grimvall, G., Fernandez Guillermet, A., Miodownik, P., Oates, W.A., and Vinograd, V., "Ab Initio Calculations in the CALPHAD Environment", Z. Metallk., in press (2001).

Burton, B.P., "Why $Pb(B,B')O_3$ Perovskites Disorder More Easily than $Ba(B,B')O_3$ Perovskites, and the Thermodynamics of 1:1-type Short Range Order in PMN," J. Phys. Chem. Solids **61**, 327 (2000).

Burton, B.P., "Long-range versus Short-range Interactions and the Configurational Energies of Ba(B, B')O3 Perovskites", Modelling and Simulation in Materials Science and Engineering, **8**, 211 (2000).

Burton, B.P., and Cockayne, E., "Prediction of the $Na_{1/2}Bi_{1/2}O_3$ Ground State," to appear in "Fundamental Physics of Ferroelectrics 2001" (AIP Conference Proceedings Series).

Chan, J.Y., Levin, I., Vanderah, T.A., Geyer, R.G., Roth, R.S., "Subsolidus Phase Relations and Dielectric Properties in the SrO-Al_2O_3-Nb_2O_5 System," Int'l. J. Inorg. Mats. **2**(1), 107-114 (2000).

Cockayne, E., "Generation of Quasicrystals via a Single Cluster," Mat. Sci. Eng. A 294, 224 (2000).

Cockayne, E. and Burton, B.P. "Phonons and Static Dielectric Constant in $CaTiO_3$ from First Principles," Phys. Rev. B **62**, 3735 (2000).

Cockayne, E., "Comparative Dielectric Response in $CaTiO_3$ and $CaAl_{1/2}Nb_{1/2}O_3$ from First Principles," J. Appl. Phys., in press (2001).

Cockayne, E., Burton, B.P., and Bellaiche, L., "Temperature-Dependent Behavior of $PbSe_{1/2}Nb_{1/2}O_3$ from First Principles," to appear in "Fundamental Physics of Ferroelectrics 2001" (AIP Conference Proceedings Series).

Cook, L.P., Wong-Ng, W., and Suh, J. "DTA/TGA study of eutectic melting in the system BaF_2-BaO-Y_2O_3-CuO_x-H_2O", MRS Proceeding, **659**, Balachandran et al eds., High-Temperature Superconductors-Crystal Chemistry, Processing and Properties, in press.

Dillingham, J., Wong-Ng, W., Levin, I., "Phase Equilibria of the SrO-Yb_2O_3-CuO_x System", Int. J. Inorg. Mater., in press.

Dong, X., Yin, L., Jahanmir, S., and Ives, L. K., "Abrasive Machining of Glass-Ceramics with a Dental Handpiece," Machining Science and Technology, 4 (2000) 209-233.

Fang, H.W., Sengers, J.V., and Hsu, S.M., "Controlled Size and Shape UHMWPE Wear Particle Generation using a Silicon Micro-Fabricated Surface Texturing Technique," Proceedings of the Society for Biomaterials 2001 Annual Meeting.

Fang, H.W., Sengers, J.V., and Hsu, S.M., "Generation of Controlled UHMWPE Wear Particles Size and Shape by Surface Texturing: Relationship between Surface Feature Dimensions to Particle Size and Shape," Proceedings of the Society for Biomaterials 2001 Annual Meeting.

Gates, R.S., and Hsu, S.M. "Oxygen-containing Compounds as Boundary Lubricants for Silicon Nitride Ceramics," U.S.Patent 6,207,627. Issued March 27, 2001.

Grey, I.E., Roth, R.S., Muimme, W.G., Planes, J., Bendersky, L., Li, C., and Chevenas, J., "Characterization of New 5M and 7M Polytypes of Niobia-Doped $Ca_2Ta_2O_7$", J. Solid State Chem., in press.

Hackley, V.A., Guide to the Nomenclature of Particle Dispersion Technology for Ceramic Systems, Special Publication 945, US DoC, Technology Administration, National Institute of Standards and Technology, Gaithersburg, MD, 2000.

Hackley, V.A. and Ferraris, C.F., Guide to Rheological Nomenclature: Measurements in Ceramic Particulate Systems, NIST Special Publication 946, US DoC, Technology Administration, National Institute of Standards and Technology, Gaithersburg, MD, 2001.

Hastie, J.W., Bonnell, D.W., and Schenck, P.K., "Application of a new thermochemical measurement method for nuclear materials at temperatures beyond 300K," J. Nuclear Materials, accepted

Haugan, T., Wong-Ng, W., Cook, L.P., Geyer, R.G., Brown, H.J., Swartzendruber, L., and Kaduk, J., "Development of Low Cost $(Sr,Ca)_3Al_2O_6$ Dielectrics for $Bi_2Sr_2CaCu_2O_{8+d}$ Applications," IEEE Transactions on Applied Superconductivity, Part III, **11** (No. 1) 3305 (2001)

Hayakawa T., Wang J., Xiang M., Li X., Ueda M., Ober C.K., Genzer J., Sivaniah E., Kramer E.J., Fischer D.A., "The Effect of Changing End Groups on Surface Properties: Synthesis and Characterization of Poly(Styrene-b-Semifluorinated Isoprene) Block Copolymers with $-CF_2H$ End Groups," Macromolecules, **33**,8012-8019, (2000)

Hockey, B.J., Kang, M.K., Wiederhorn, S.M. and Blendell, J., "Low Angle Grain Boundary Dewetting in Sapphire," Microscopy and Microanalysis Journal, accepted.

Hryniewics, P., Szeri, A.Z., and Jahanmir, S., "Application of Lubrication Theory to Fluid Flow in Grinding. Part I: Flow Between Smooth Surfaces," Journal of Tribology, 123(2001) 94-100.

Hryniewicz, P., Szeri, A.Z., and Jahanmir, S., "Application of Lubrication Theory to Fluid Flow in Grinding. Part II: Influence of Wheel and Workpiece Roughness," Journal of Tribology, 123(2001)101-107.

Hryniewicz, P., Szeri, A. Z., and Jahanmir, S., "Coolant Flow in Surface Grinding with Non-Porous Wheels," International Journal of Mechanical Sciences, 42(2000) 2347-2367.

Hsu, S.M., Ying, T.N., Gu, J.M., Wang, Y.S., and Gates, R.S., "Methods for Machining Hard Materials using Alcohols," U.S. Patent 6,206,764. Issued March 27, 2001

Hsu, S.M., McGuiggan, P.M., Zhang, J., Wang, Y., Yin, F., Yeh, Y.P., and Gates, R.S., "Scaling Issues in the Measurement of Monolayer Films," NATO/ASI Proceedings on the Fundamentals of Tribology and Bridging the Gap between Macro- and Micro/Nanoscales, NATO Science Series: II Mathemetics, Physics and Chemistry – Vol 10, Kluwer, Amsterdam, 2001.

Hsu, S.M., and Shen, M.C., "Wear Maps," Chapter 9 of the Modern Tribology Handbook, Volume I, Edited by Bharat Bhushan, CRC Press, NY, 2001.

Hsu, S.M., and Gates, R.S., "Boundary Lubrication and Boundary Lubricating Film," Chapter 11 of the Modern Tribology Handbook, Volume I, Edited by Bharat Bhushan, CRC Press, NY, 2001.

Ilavsky, J., Stalick, J. and Wallace, J., "Thermal-Spray Yttria-Stabilized Zirconia Phase Changes During Annealing," J. Thermal Spray Technology, in press.

Ilavsky, J., Stalick, J. and Wallace, J., "Thermal-Spray Yttria-Stabilized Zirconia Phase Changes During Annealing," pp 1185-1189 in "Thermal Spray Surface Engineering via Applied Research," Proceedings of the 1st Thermal Spray Conference, 8-11 May 2000, Montreal Quebec, Canada, C. C. Berndt (ed.), ASM International, Materials Park, Ohio, USA (2000).

Jeffrey, G.A., Karen, V.L., "Crystallography," in the AIP Physicists Desk Reference, 3rd ed., Eds. A. Cohen, B. Lide and C. Trigg, Chapter 9, pp. 304-306 (2001).

Jensen, R.P., Luecke, W.E., Padture, N.P., and Wiederhorn, S. M., "High-Temperature Properties of Liquid-Phase-Sintered alpha-SiC," Materials Science and Engineering A, 2000, 282, 1-2, 109-114.

Jillavenkatesa, A., Dapkunas, S. J., and Lum, L., "NIST Recommended Practice Guide: Particle Size Characterization," SP 960-1, Jan. 2001

Jin Q., Wilkinson D. S., Weatherly G. C., Luecke W. E., and Wiederhorn S. M., "Thickness Alteration of Grain-Boundary Amorphous Films during Creep of a Multiphase Silicon Nitride Ceramic," Journal of The American Ceramic Society 84. (6) 1296-1300, 2001

Kaiser, D.L. and Schneemeyer, L.S., "Single Crystal Growth," Handbook of Superconducting Materials, in press.

Kanematsu, W., Sando, M., Ives, L., Marinenko, R., and Quinn, G., "Determination of Machining Crack Geometry by Dye Penetration Technique," J. Amer. Ceram. Soc., 84 [4] (2001) 795-800.

Karen, V.L., Young, S., and Mighell, A., "CDROM Guide for NIST Crystal Data," NIST Standard Reference Database 3, NISTIR (2001).

Karen, V.L., "NIST Standard Reference Database 83," NIST Structural Database (April 2001).

Krause, R. F., Jr., Wiederhorn, S.M., and Kueber, J.J., "Misalignment-Induced Bending in Pin-Loaded Tensile-Creep Specimens," J. Am. Ceram. Soc. 84 145-52 (2001).

Krause, R.F., Jr., Wiederhorn, S.M., and Li, Chien-Wei, "Tensile Creep Behavior of a Gas-Pressure Sintered Silicon Nitride Containing Silicon Carbide," J. Am. Ceram. Soc. 84 (in press) 2001.

Langer, S.A and Fuller, E.R., "OOF: An Image-Based Finite-Element Analysis of Material Microstructures," Computing in Science and Engineering, 15-23, (2001).

Levin, I., Chan, J.Y., Maslar, J.E., and Vanderah, T.A., "Phase Transitions and Microwave Dielectric Properties in the Perovskite-Like $CaAl_{0.5}Nb_{0.5}O_3$–$CaTiO_3$ System," J. Appl. Phys., in press.

Levin, I., Bendersky, L.A., Cline, J.P., Roth, R.S., and Vanderah, T.A., "Octahedral Tilting and Cation Ordering in Perovskite-Like $Ca_4Nb_2O_9 = 3Ca(Ca_{1/3}Nb_{2/3})O_3$ Polymorphs," J. Solid State Chem. **150**, 43-61 (2000).

Levin, I., Chan, J.Y., Geyer, R.G., Maslar, J.E., and Vanderah, T.A., "Cation Ordering Types and Dielectric Properties in Complex Perovskite $Ca(Ca_{1/3}Nb_{2/3})O_3$," J. Solid State Chem., 156, 122-134 (2001).

Livingston, R.A., Neumann, D.A., Allen, A.J., FitzGerald, S., and Berliner, R.. "Application of Neutron Scattering to Portland Cement," Neutron News. **11.4**, 18 - 24 (2000).

Long G G., Levine L.E., Thomson R., "In-situ observation of small-angle X-ray scattering by dislocations," J Appl Crystallogr 33: (1) 456-460 Part 3 June 1, 2000.

Long G.G., Levine L.E., and Fields R.J., "X-ray scattering and imaging from plastically deformed metals," Mat Sci Eng A-Struct 309: 28-31 July 15, 2001.

Luecke, W., "Results of an International Round-Robin for Tensile Creep Rupture of Silicon Nitride," accepted for publication in J. Am. Ceram. Soc. July 15, 2001.

Lupascu, D., Nuffer, J., Wallace, J. and Roedel, J., "Role of Crack Formation in the Electric Fatigue Behavior of Ferroelectric Ceramics," published in Proceedings of 1999 SPIE Annual Meeting.

Marsh A.L., Burnett D.J., Fischer D.A., Rasmussen J.P., and Gland J.L., "Near Edge X-ray Absorption Fine Structure Characterization of Polymers Based on 2-Vinyl-4,5-Dicyanoimidazole," ACS preprints, Polymeric Materials: Science & Engineering 2001, **84**, 1016-1017.

Maslar, J.E., Hurst, W.S., Bowers, W.J., Hendricks, J.H., Aquino, M.I., and Levin, I., "*In-Situ* Raman Spectroscopic Investigation of Chromium Surfaces Under Hydrothermal Conditions," Appl. Surf. Science, in press.

McGuiggan P.M., Zhang J., Hsu S.M., "Comparison of friction measurements using the atomic force microscope and the surface forces apparatus: the issue of scale," Tribology Letters 10, (4), 217-223 May 2001.

McGuiggan, P.M., "The Boundary Lubrication Properties of Model Esters," Tribology Letters 11, (1), 49-53, July 2001.

Mighell, A., Karen, V.L., Munro, R., "Determination of Reduced Cells in Crystallography," published in "A Century of Excellence in Measurments, Standards, and Technology-A Chronicle of Selected NBS/NIST Publications." 1901-2000, Edited by David R. Lide, NIST Special Publication 958, pp. 188-190.

Mighell, A.D., "Lattice Metric Singularities and their Impact on the Indexing of Powder Patterns," Powder Diffraction **15**(2), 82-85.

Mighell, A.D., "Ambiguities in Powder Pattern Indexing: A Ternary Lattice Metric Singularity," Powder Diffraction **16** (in press).

Munro, R.G. ,"Effective Medium Theory of the Porosity Dependence of Bulk Moduli," J. Am. Ceram. Soc., **84** [5], 1190 (2001).

Nagarajan, V. S., Hockey, B., Jahanmir, S., and Thompson, V. P., "Contact Wear Mechanisms of a Dental Composite with a High Filler Content," J. Mat. Science, 35(2000) 487-496.

Nakao, H., Ohwada, K., Takesue, N., Fujii, Y., Isobe, M., Ueda, Y., Zimmermann, M.V., Hill, J.P., Gibbs, D., Woicik, J.C., Koyama, I., and Murakami, Y., "X-ray anomalous scattering study of a charge-ordered state in NaV_2O_5," Phys. Rev. Lett. 85, 4349 (2000).

Newell, D.B., Pratt, J.R., Kramar, J.A., Smith, D.T., Feeney, L.A., and Williams, E.," Si Traceability of Force at the Nanonewton Level," 2001 NCSL International Workshop and Symposium Proceedings, accepted.

Paik, U. and Hackley, V.A., "Influence of Solids Concentration on the Isoelectric Point of Aqueous Barium Titanate", J. Am. Ceram. Soc., **83**[10], 2381-84 (2000).

Potrepka D.M., Budnick J.I., Moodenbaugh A.R., Fischer D.A., Hines W.A., "Combined ^{63,65}Cu NQR and NMR study of $Y_{1-x}Ca_xBa_2Cu_3O_y$," Physica C, **341-348**, 611-612 (2000).

Pratt, J.R., Newell, D.B., Williams, E.R., Smith, D.T., and Krama, J.A., "Towards a Traceable Nanoscale Force Standard," Proc. of the International Conference and General Meeting of European Society for Precision Engineering and Nanotechnology, accepted.

Quinn, G. and Swab, J., "Elastic Modulus by Resonance of Rectangular Prisms: Corrections for Chamfers," J. Am. Ceram. Soc., 83 [2] 317-320 (2000). Also published as U. S. Army ARL TN 165, July 2000.

Quinn, G.D., "Indentation Hardness Testing of Ceramics," in Materials Testing and Evaluation, Vol. 8, Mechanical Testing, ASM, Materials Park, OH, 2000, pp. 244-251.

Quinn, G.D., Ives, L.K., Jahanmir, S., and Kosh, P., "Fractographic Analysis of Machining Cracks in Silicon Nitride Rods and Bars," 4th International Conference on Fractography of Glasses and Ceramics, J. Varner, G. Quinn, and V. Frechette (eds.), American Ceramic Society, July 2000.

Ravikiran, A. and Jahanmir, S., "Effect of Interfacial Layers on Wear Behavior of a Dental Ceramic," Journal of the American Ceramic Society, 83 (2000) 1831-1833.

Ravikiran, A. and Jahanmir, S., Effect of Contact Pressure and Load on Wear of Alumina," Wear, (2001) in press.

Reidy, R.F., Allen, A.J., and Krueger, S., "Small-Angle Scattering Characterization of Colloidal and Fractal Aerogels," J. Non-Cryst. Solids, **285**, 181-186 (2001).

Robins, L.H., Armstrong, J.T., Vaudin, M.D., Bouldin, C.E., Woicik, J., Paul, A.J., Thurber, W.R., Miyano, K.E., Parker, C.A., Roberts, J.C., Bedair, S.M., Piner, E.L., Reed, M.J., El-Masry, N.A., Donovan, S.M., and Peraton, S.J., "Optical and structural studies of compositional inhomogeneity in strain-relaxed indium gallium nitride films," Proc. of the 27th Int. Symp. on Compound Semiconductors, IEEE (2001).

Roth, R.S., Phase Equilibria Diagrams, Vol. XIII Oxides, Robert S. Roth, Ed., The American Ceramic Society, Westerville, Ohio, 472 pp., 2001.

Sahiner, M.A., Novak, S.W., Woicik, J.C., Liu, J., Krishnamoorty, V., "Arsenic clustering and precipitation analysis in ion-implanted Si wafers by x-ray absorption spectroscopy and SIMS," IEEE proceedings of the XIIIth International Conference on Ion Implementation Technology (IIT 2001).

Sambasivan S., Fischer D.A., Kuperman A., DeKoven B.M., "Direct Observation of Propylene Transformation Chemistry on and in the Pores of Silver Exchanged Faujasite Catalyst," Advanced Materials, **12**, 1809-1813 (2000).

Schwarz, J., Liu, R., Newell, D.B., Steiner, R., Williams, E.R., Smith, D.T., Erdemir, A., and Woodford, J., "Hysteresis and Related Error Mechanisms in the NIST Watt Balance Experiment," J. Res. Natl. Inst. Stand. Technol., accepted.

Skirl, S., Krause, R.F., Jr., Wiederhorn, S.M., and Roedel, J., "Processing and Mechanical Properties of Al2O3/Ni3Al Composites with Interpenetrating Network Microstructure," J. Am. Ceram. Soc. 84 (in press) 2001.

Sims, J.S., Hagedorn, J.G., Ketcham, P.M., Satterfield, S.G., Griffin, T., George, W.L., Fowler, H.A., am Ende, B.A., Hung, H.K., Bohn, R.B., Koontz, J.E., Martys, N.S., Bouldin, C.E., Warren, J., Feder, D.L., Clark, C.W., Filla, B.J., Devaney, J.E., "Accelerating Scientific Discovery Through Computation and Visualization," J. Res. Natl. Inst. Stand. Technol., **185**, 875 (2000).

Sitepu, H., Prask, H.J., and Vaudin, M.D., "Texture Characterization in X-ray and Neutron Powder Diffraction Data Using the Gneralized Spherical-Harmonic," Proc. of the Annual Conf. on Applications of X-ray Analysis 2001, accepted.

Spal, R.D., "Submicrometer Resolution Hard X-ray Holography with the Asymmetric Bragg Diffraction Microscope," Phys. Rev. Lett. 86, 3304 (2001).

Valincius, G., Reipa, V., Woodward, J. and Vaudin, M., "Electrochemical properties of nanocrystalline cadmium stannate films," J. Electrochem. Soc., accepted.

Vanderah, T.A., Febo, W., Chan, J.Y., Roth, R.S., Loezos, J.M., Rotter, L.D., Geyer, R.G., and Minor, D.B., "Phase Equilibria and Dielectric Behavior in the CaO-Al_2O_3-Nb_2O_5 System", J. Solid State Chem. **155**, 78-85 (2000).

Vaudin, M.D., "Accurate measurement of texture in thin films," J. Materials Processing Tech., accepted.

Vaudin, M.D., and Kaiser, D.L., "Workshop on texture in electronic applications," J. Res. Natl. Inst. Stand. Technol., **106** (2001).

Vogel, E.M., Edelstein, M.D., Richter, C.A., Nguyen, N.V., Levin, I., Kaiser, D.L., Wu, H. and Bernstein, J., "Issues in High-k Gate Dielectrics for Future MOS Devices," Microelectronics Reliability and Qualification Workshop Proc., IEEE (2001).

Vogelsan, R., Grimsdich, M. and Wallace, J., "Elastic Constants of Single Crystal Beta-Si_3N_4," Appl Phys Lett 76 (8) 982-984, Feb 21 2000.

Wallace, W.E., Fischer, D.A., Efimenko, K., Wu, W.L., and Genzer, J., "Polymer Chain Relaxation: Surface Outpaces Bulk," Macromolecules, **34(15)**, 5081-5082(2001).

Wasche, R., Naito, M., and Jahanmir, S., "Characterization Methods for Ceramic Powders and Green Bodies," VAMAS Bulletin No. 23, November 2000, 21-27.

Weber, M.D., Ankem, S., Fields, R.J., and Quinn, G.D., "Green Strength of Particle Reinforced Aluminum Composites," proceedings of the second international conference on Powder Metallurgy, Aluminum and Light Alloys for Automotive Applications, eds. W. Jandeska and R. Chernakoff, publ. by the Metals Powders Industrial Federation, Princeton, NJ, 2000.

White, G.S. and Braun, L.M., "Difficulties Making Reliability Predictions for Si, GaAs, and InP," Optical Fiber and Fiber Component Mechanical Reliability and Testing, M. John Matthewson, ed., SPIE Proceedings Series Volume 4215, 81-89 (2001).

White, G.S., Blendell, J.E., and Fuller, Jr., E.R., "Domain Stability in PZT Thin Films," ISIF 2001 Proceedings, accepted.

Widom, M., Al-Lehyani, I., Wang, Y., and Cockayne, E., "Ab Initio Energetics of Transition Metal Ordering in Decagonal Al-Co-Cu," Mat. Sci. Eng. A. 294, 295 (2000).

Woicik, J.C., Nelson, E.J., Kendelewicz, T., Pianetta, P., Jain, M., Kronik, L., and Chelikowsky, J.R., "Partial density of occupied valence states by x-ray standing waves and high resolution valence electron spectroscopy," Phys. Rev. B **63** Rapid Communications, 041403 (2001).

Woicik, J.C., Nelson, E.J., Heskett, D., Warner, J., Berman, L.E., Karlin, B.A., Vartanyants, I.A., Hasan, M.Z., Kendelewicz, T., Shen, Z.X., and Pianetta, P., "X-ray standing-wave investigations of valence-electronic structure," Phys. Rev. B. in press.

Woicik, J.C., Nelson, E.J., Kendelewicz, T., and Pianetta, P., "Partial density of occupied valence states by x-ray standing waves and high-resolution photoelectron spectroscopy," Superficies y Vacio 11, 20 (2000).

Wong-Ng, W., Kaduk, J.A. Huang, Q., Roth, R.S. "Crystal Structure of Monoclinic Perovskite $Sr_{3.94}Ca_{1.31}Bi_{2.7}O_{12}$," Powd. Diffr., **15**(4) 227 (2000).

Wong-Ng, W., Cook, L. P., Kearsley, A. and Roosen, W., "Role of melting equilibria in the Processing of high T_c Superconductors in the BSCCO System," Physica C **335** (1-4) 120-124 (2000).

Wong-Ng, W., Cline, J.P., Cook, L.P., and Greenwood, W., "X-ray characterization of Compounds in the SrO-PbO system," Adv. X-Ray Anal. **42**, 355-365 (2000).

Wong-Ng, W., Kaduk, J.A., Greenwood, W., and Dillingham, J.A., "Powder X-ray Reference Patterns of $Sr_2RGaCu_2O_7$ (R=Pr, Nd, Sm, Eu, Gd, Dy, Ho, Er, Tm, Yb and Y)," J. Res. Natl. Inst. Stand. Technol., **106** (4), in press.

Wong-Ng, W., Huang, Q., Levin, I., Kaduk, J.A., Dillingham, J., Haugan, T., Suh, J., and Cook, L.P., "Crystal Chemistry and Phase Equilibria of Selected SrO-R_2O_3-CuO_x and Related Systems, R= Lanthanides and yttrium," Int. J. Inorg. Mater., in press.

Wong-Ng, W., Kaduk, J. A., Dillingham, J. "Crystallographic studies and x-ray reference patterns of $Ba_5R_8Zn_4O_{21}$ by Rietveld Refinements," Powder Diffraction, in press.

Woo, H., Tyson, T.A., Croft, M., Cheong, S-W., Woicik, J.C., and Bandt, B.L., "Correlations between the magnetic and structural properties of Ca doped BiMnO3," Phys. Rev. B **63**, (2001).

Xu, H.H., Smith, D.T., Schumacher, G.E., Eichmiller, F.C. and Antonucci, J.M., "Indentation Modulus and Hardness of Whisker-Reinforced Heat-Cured Dental Resin Composites," Dental Materials 16 (2000) 248-254.

Xu, H.H., Quinn, J.B., Smith, D.T., Antonucci, J.M., Schumacher, G.E., and Eichmiller, F.C., "Dental Resin Composites Containing Silica-Fused Whiskers: Effects of Whisker-to-Silica Ratio on Fracture Toughness and Indentation Properties," Biomaterials (2001), in press.

Xu, H.H., Eichmiller, F., Smith, D.T., Schumacher, G., Giuseppetti, A., and Antonucci, J., "Effect of Thermal Cycling on Whisker-Reinforced Dental Resin Composites," Biomaterials, accepted.

Xu, H.H., Quinn, J.B., Smith, D T., Giuseppetti, A.A., and Eichmiller, F.C., "Effects of Different Whiskers on the Reinforcement of Dental Resin Composites," Dental Materials, accepted.

Yang, Y., Al-Brithen, H., Smith, A.R., Borchers, J., Vaudin, M. and Cappelletti, M., "Molecular Beam Epitaxial Growth of n-phase Manganese Nitride Films," Appl. Phys. Lett., accepted.

Zhang, X.H., Gates, R.S., Anders, S., and Hsu, S.M., "An Accelerated Wear Test Method to Evaluate Lubricant Thin Films on Magnetic Hard Disks," Tribology Letters 11, (1),15-21, July 2001.

Yin, L., Ives, L.K., and Jahanmir, S., "Machining Behavior of Glass-Infiltrated Alumina," Machining Science and Technology, 5(2001) 43-62.

Yoon, K.J. and Wiederhorn, S.M. and Luecke, W.E., "Comparison of Tensile and Compressive Creep Behavior in Silicon Nitride," J. Am. Ceram. Soc. 2000, 83, 8, 2017-2022.

Zimmerman, M.H., Baskin,D.M., Faber, K.T., Fuller, E.R., Allen, A.J., and Keane, D.T., "Fracture of Textured Iron Titanate," Acta Materialia, in press (2001).

Ceramics Division

Chief

Stephen W. Freiman
Phone: 301-975-6119
E-mail: stephen.freiman@nist.gov

Deputy Chief

S. J. Dapkunas
Phone: 301-975-6119
E-mail: stanley.dapkunas@nist.gov

Group Leaders

Ceramic Manufacturing
Said Jahanmir
Phone: 301-975-3671
E-mail: said.jahanmir@nist.gov

Phase Equilibria
Terrell Vanderah
Phone: 301-975-5785
E-mail: terrell.vanderah@nist.gov

Film Characterization and Properties
Debra Kaiser
Phone: 301-975-6759
E-mail: debra.kaiser@nist.gov

Materials Microstructural Characterization
Gabrielle Long
Phone: 301-975-5975
E-mail: gabrielle.longi@nist.gov

Surface Properties
Stephen Hsu
Phone: 301-975-6120
E-mail: stephen.hsu@nist.gov

Data Technologies
S. J. Dapkunas
Phone: 301-975-6119
E-mail: stanley.dapkunas@nist.gov

Research Staff

Allen, Andrew
andrew.allen@nist.gov
- Small angle x-ray scattering
- Ceramic microstructure analysis

Begley, Edwin
edwin.begley@nist.gov
- Materials informatics
- Database management methods
- Engineering database structures

Belsky, Alec
alec.belsky@nist.gov
- Crystallographic database

Black, David
david.black@nist.gov
- Defect microstructures
- Polycrystalline diffraction imaging
- X-ray imaging

Blendell, John
john.blendell@nist.gov
- Ceramic processing and clean-room processing
- Sintering and diffusion controlled processes

Bouldin, Charles
charles.bouldin@nist.gov
- X-ray absorption spectroscopy
- Diffraction anomalous fine structure
- GeSi heterojunction bipolar transistors

Burdette, Harold
harold.burdette@nist.gov
- X-ray optics
- X-ray diffraction imaging
- Crystal growth
- Instrumentation

Burton, Benjamin
benjamin.burton@nist.gov
- Calculated phase diagrams
- Dielectric ceramics

Cellarosi, Mario
mario.cellarosi@nist.gov
- Glass standards
- Forensic data

Chuang, Tze-Jer
tze-jer.chuang@nist.gov
- Creep/creep rupture
- Fracture mechanics
- Finite-element modeling
- Lifetime predictions

Cline, James
james.cline@nist.gov
- Standard reference materials
- High-temperature x-ray diffraction
- Microstructural effects in x-ray diffraction
- Rietveld refinement of x-ray diffraction data

Cook, Lawrence
lawrence.cook@nist.gov
- High-temperature chemistry
- Phase equilibria

Dapkunas, Stanley
stanley.dapkunase@nist.gov
- Databases
- Ceramic coatings

Fischer, Daniel
daniel.fischer@nist.gov
- X-ray absorption fine structure
- X-ray scattering
- Surface science

Freiman, Stephen
stephen.freiman@nist.gov
- Electronic ceramics
- Mechanical properties

Fuller, Edwin
edwin.fuller@nist.gov
- Influence of microstructure on fracture
- Toughening mechanisms
- Microstructural modeling and simulation

Gates, Richard
richard.gates@nist.gov
- Tribo-chemistry
- Surface chemical properties of ceramics

Hackley, Vincent
vince.hackley@nist.gov
- Electrokinetic and electroacoustic measurement
- Slurry rheology
- Surface chemistry of powders

Harne, Mary
mary.harne@nist.gov
- Phase equilibria data
- Computerized data

Harris, Joyce
joyce.harris@nist.gov
- Data acquisition
- Digitization and data entry

Hockey, Bernard
bernard.hockey@nist.gov
- Electron microscopy
- High-temperature creep

Hsu, Stephen
stephen.hsu@nist.gov
- Ceramic wear mechanisms
- Engineered ceramic surfaces
- Magnetic storage disk lubrication

Ives, Lewis
lewis.ives@nist.gov
- Wear of materials
- Transmission electron microscopy
- Machining of ceramics

Jahanmir, Said
said.jahanmir@nist.gov
- Ceramic manufacturing
- Mechanisms of material removal
- Mechanics of contacts
- Effects of machining on mechanical properties

Kaiser, Debra
debra.kaiser@nist.gov
- Ferroelectric oxide thin films
- Physical properties and structures of high-temperature superconductors

Karen, Vicky
vicky.karen@nist.gov
- Crystallographic databases
- Structural analysis

Kelly, James
james.kelly@nist.gov
- Quantitative scanning electron microscopy
- Image analysis
- Microstructure analysis
- Powder standards

Krause, Ralph
ralph.krause@nist.gov
- Creep in flexure and tension
- Fracture mechanics

Locatelli, Mark
mark.locatelli@nist.gov
- Microstructural Simulation Modeling
- Ceramic Coating
- Low temperature co-fired ceramics

Long, Gabrielle
gabrielle.long@nist.gov
- Small-angle x-ray and neutron scattering
- Ceramic microstructure evolution as a function of processing
- X-ray optics

Luecke, William
william.luecke@nist.gov
- Creep/creep rupture
- Mechanical test development
- Ceramic membranes

Lum, Lin-Sien
lin-sien.lum@nist.gov
- Powder characterization
- Instrumental analysis

Minor, Dennis
dennis.minor@nist.gov
- Analytical scanning electron microscopy of ceramics and particulates
- Powder characterization
- Standard Reference Materials

Munro, Ronald
ronald.munro@nist.gov
Materials properties of advanced ceramics
Data evaluation and validation
Analysis of data relations

Paul, Albert
albert.paul@nist.gov
Laser physics
Residual stress measurement

Pei, Patrick
patrick.pei@nist.gov
Spectroscopic and thermal characterization
Magnetic Disk lubrication storage

Quinn, George
george.quinn@nist.gov
Mechanical property test standards
Standard reference materials

Robins, Lawrence
lawrence.robins@nist.gov
Defect identification and distribution
Cathodoluminescence imaging and spectroscopy
Photoluminescence spectroscopy
Raman spectroscopy

Schenck, Peter
peter.schenck@nist.gov
Emission and laser spectroscopy
Thin-film deposition
Computer graphics and image analysis
Combinatorial materials analysis

Smith, Douglas
douglas.smith@nist.gov
Surface forces
Adhesion and friction
Instrumented Indentation

Spal, Richard
richard.spal@nist.gov
X-ray optics
Diffraction physics
X-ray scattering

Vanderah, Terrell
terrell.vanderah@nist.gov
Solid-state chemistry
Phase equilibria of microwave dielectrics

Vaudin, Mark
mark.vaudin@nist.gov
Electron microscopy
Microscopy and diffraction studies of interfaces
Computer modeling of grain-boundary phenomena
Dielectric films

Wallace, Jay
jay.wallace@nist.gov
Mechanical test development
Thermal analysis

Wang, Pu Sen
pu-wang@nist.gov
Solid-state nuclear magnetic resonance
Spectroscopic characterization

White, Grady
grady.white@nist.gov
Mechanical properties
Nondestructive evaluation
Stress measurements

Woicik, Joseph
joseph.woicik@nist.gov
UV photoemission
X-ray standing waves
Surface and interface science

Wong-Ng, Winnie
winnie.wong-ng@nist.gov
X-ray crystallography and reference patterns
Phase equilibria/crystal chemistry of high-Tc superconductors

GUEST SCIENTISTS AND GRADUATE STUDENTS

Armstrong, Nicholas
University of Technology, Sydney Australia

Attota, Ravikiran
National University of Singapore

Bai, Mingwur
Tohoku University

Bonnell, David
Consultant

Boukari, Hacene
University of Maryland

Bumrongjaroen, Walairat
Federal Highway Administration

Cedeno, Christina
American Ceramic Society

Cockayne, Eric

Coutts, Rachel
University of Maryland

Dillingham, Jeremy
University of Maryland

Early, James
Consultant

Evans, Howard
Smithsonian Institution

Fang, Hsu-Wei
University of Maryland

Farabaugh, Edward
American Ceramic Society

Feldman, Albert
Consultant

Fu, Zugen
State Univ. of N.Y. at Stony Brook

Haller, Wolfgang
Consultant

Hastie, John
Consultant

Hayward, Evans
American Ceramic Society

Hryniewicz, Piotr
University of Delaware

Ilavsky, Jan
University of Maryland

Jemian, Peter
University of Illinois at Urbana/Champaign

Jillavenkatesa, Ajitkumar
Alfred University

Kalin, Mitjan
University of Ljubljana

Kieffer, John
University of Illinois

Kulkarni, Anand
State University of New York

Kweon, Hyun-kyu
Tohoku University

Larsen-Basse, Jorn
National Science Foundation

Levin, Igor
University of Maryland

Li, Na
Beijing U. of Aeronautics & Astronautics

Lim, Dae-Soon
Korea University

Lindsey, Tammy
Appalachian State University

Ling, Yin
Tianjin University

McMurdie, Howard
Joint Center for Powder Diffraction Studies

Mighell, Alan
Consultant

Nuffer, Juergen
University of Tech. Darmstadt

Ondik, Helen
Consultant

Ozoon, Takuya
Tokyo Institute of Technology

Park, Youngsoo
University of Illinois

Peiris, Suhithi
Naval Research Laboratory

Research Staff

Piermarini, Gasper
University of Maryland

Prosandeev, Serguei
Rostov State University

Ritter, Joseph
Consultant

Roberts, Ellis
Consultant

Roth, Robert
Viper Group

Sambasivan, Sharadha
Brookhaven National Laboratory

Sun, Dah Chen
State University of New York at Birmington

Swanson, Nils
American Ceramic Society

Texter, John
National Science Foundation

Turchinskaya, Marina
Consultant

Wolfenstine, Jeffrey
U S. Army Research Laboratory

Yeager, Glenn
Trak Ceramics, Inc.

Yin, Zhanfeng
University of Maryland

Ying, Tony
U.S. Mint of the Treasury Department

Organizational Charts

Materials Science and Engineering Laboratory

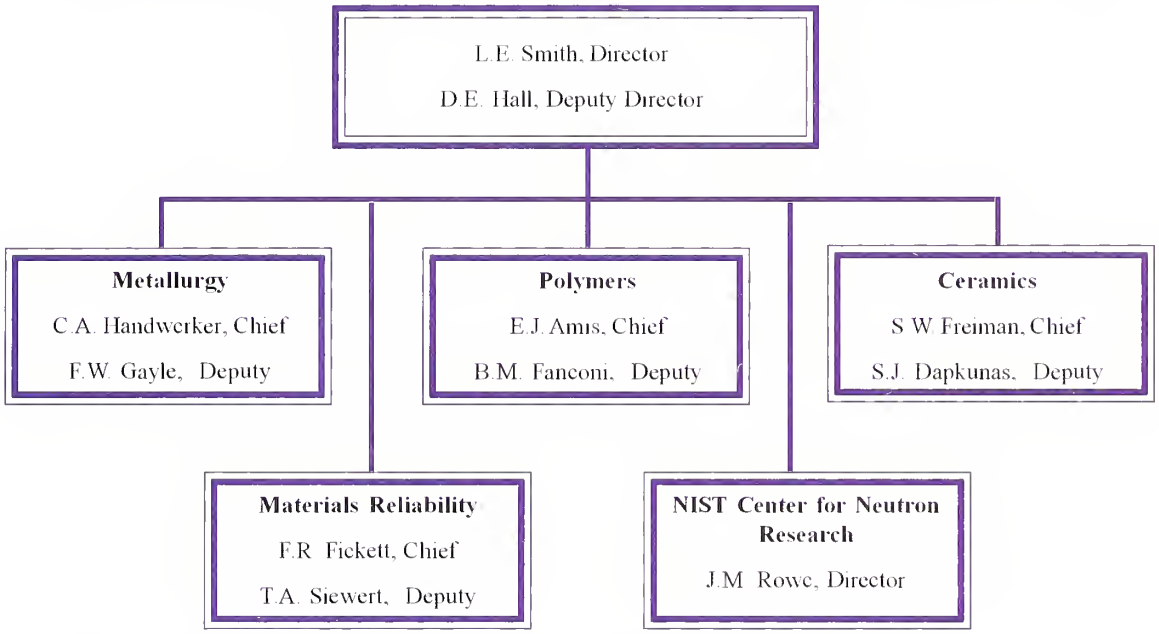

National Institute of Standards and Technology

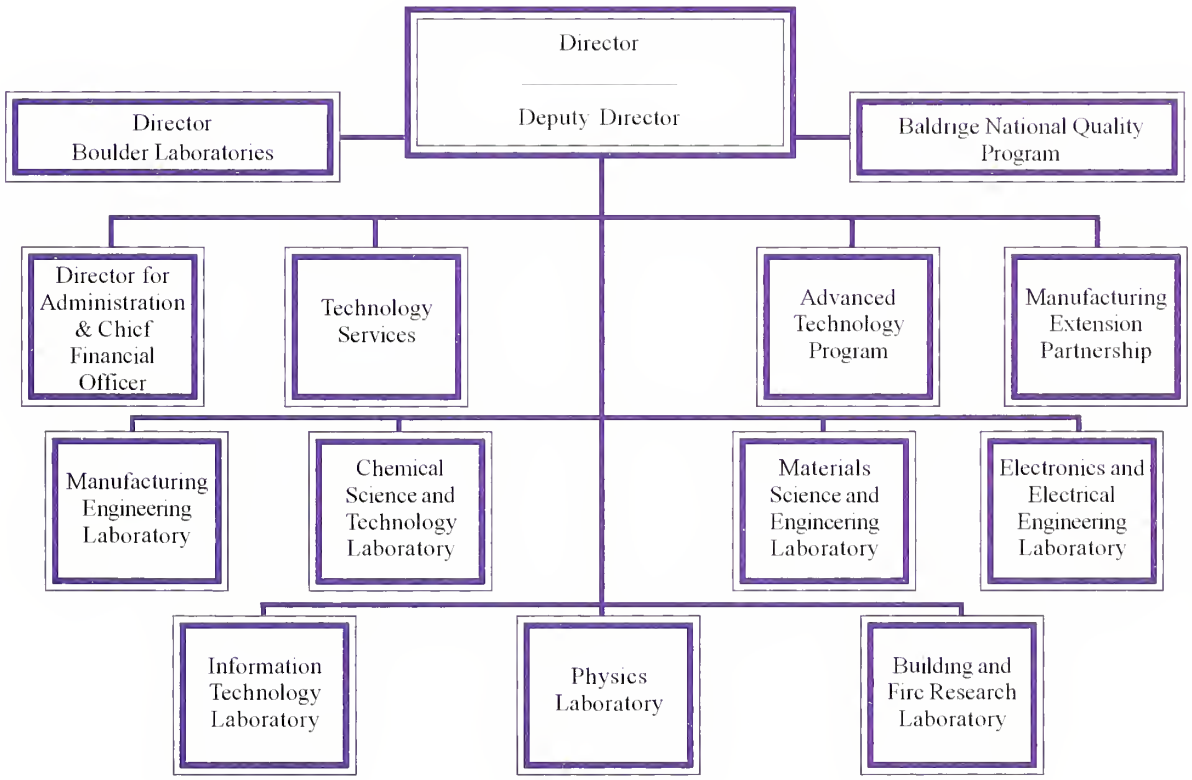

NISTIR 6780—CERAMICS DIVISION: FY 2001 PROGRAMS AND ACCOMPLISHMENTS

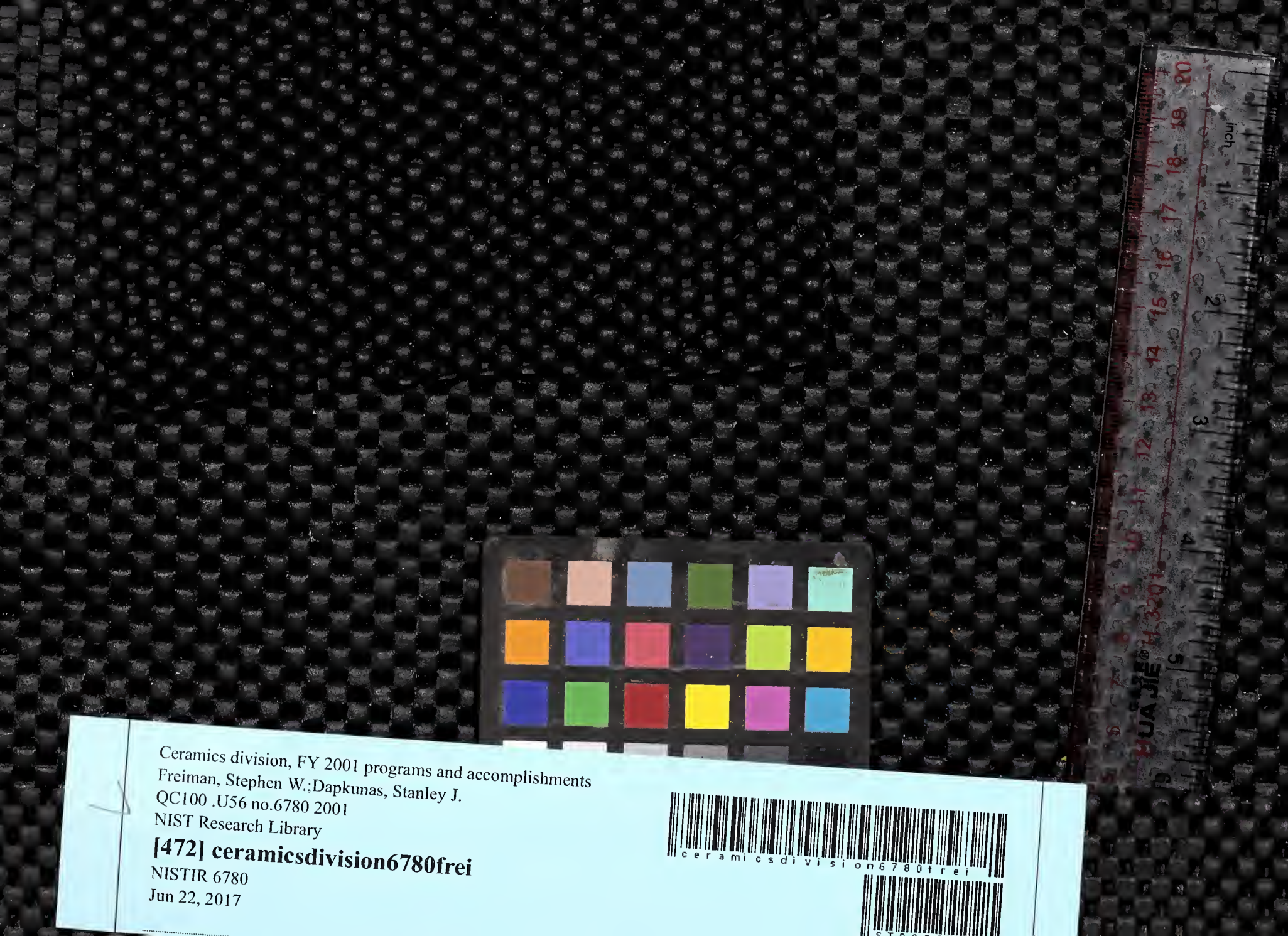
Ceramics division, FY 2001 programs and accomplishments
Freiman, Stephen W.;Dapkunas, Stanley J.
QC100 .U56 no.6780 2001
NIST Research Library
[472] ceramicsdivision6780frei
NISTIR 6780
Jun 22, 2017
ceramicsdivision6780frei